

# The ROSAT-ESO Flux Limited X-ray (REFLEX) Galaxy Cluster Survey. V. The cluster catalogue<sup>★</sup>

H. Böhringer<sup>1</sup>, P. Schuecker<sup>1</sup>, L. Guzzo<sup>2</sup>, C.A. Collins<sup>3</sup>, W. Voges<sup>1</sup>, R.G. Cruddace<sup>4</sup>, A. Ortiz-Gil<sup>5</sup>, G. Chincarini<sup>2,6</sup>, S. De Grandi<sup>2</sup>, A.C. Edge<sup>7</sup>, H.T. MacGillivray<sup>8</sup>, D.M. Neumann<sup>9</sup>, S. Schindler<sup>10</sup>, P. Shaver<sup>11</sup>

<sup>1</sup> Max-Planck-Institut für extraterrestrische Physik, D 85748 Garching, Germany

<sup>2</sup> Osservatorio Astronomico di Brera, via Bianchi 46, I-22055 Merate, Italy

<sup>3</sup> Astrophysics Research Institute, Liverpool John Moores University, Liverpool CH41 1LD, U.K.

<sup>4</sup> E. O. Hulburt Center for Space Research, Naval Research Laboratory, Washington, DC 20375., USA

<sup>5</sup> Observatorio Astronómico, Universidad de Valencia, 22085 Valencia, Spain

<sup>6</sup> Dipartimento di Fisica, Università degli Studi di Milano, Italy

<sup>7</sup> Physics Department, University of Durham, South Road, Durham DH1 3LE, U.K.

<sup>8</sup> Institute for Astronomy, University of Edinburgh, Blackford Hill, Edinburgh EH9 3HJ, U.K.

<sup>9</sup> CEA Saclay, Service d'Astrophysique, Gif-sur-Yvette, France

<sup>10</sup> Institute for Astrophysics, Universität Innsbruck, 6020 Innsbruck, Austria

<sup>11</sup> European Southern Observatory, D 85748 Garching, Germany

Received .... ; accepted ....

**Abstract.** We present the catalogue of the REFLEX Cluster Survey providing information on the X-ray properties, redshifts, and some identification details of the clusters in the REFLEX sample. The catalogue describes a statistically complete X-ray flux-limited sample of 447 galaxy clusters above an X-ray flux of  $3 \cdot 10^{-12} \text{ erg s}^{-1} \text{ cm}^{-2}$  (0.1 to 2.4 keV) in an area of 4.24 ster in the southern sky. The cluster candidates were first selected by their X-ray emission in the ROSAT-All Sky Survey and subsequently spectroscopically identified in the frame of an ESO key programme. Previously described tests have shown that the sample is more than 90% complete and there is a conservative upper limit of 9% on the fraction of clusters with a dominant X-ray contamination from AGN. In addition to the cluster catalogue we also describe the complete selection criteria as a function of the sky position and the conversion functions used to analyse the X-ray data. These are essential for the precise statistical analysis of the large-scale cluster distribution. This data set is at present the largest, statistically complete X-ray galaxy cluster sample. Together with these data set we also provide for the first time the full three-dimensional selection function. The sample forms the basis of several cosmological studies, one of the most important applications being the assessment of the statistics of the large-scale structure of the universe and the test of cosmological models. Part of these cosmological results have already been published. \*\*

## 1. Introduction

Clusters of galaxies are the largest building blocks of our Universe that can still reasonably well be characterized as unique objects. This makes them on one hand very important large-scale astrophysical laboratories in which a large variety of astrophysical processes can be studied in well

*Send offprint requests to:* H. Böhringer  
hxb@mpe.mpg.de

\* Based on observations at the European Southern Observatory La Silla, Chile

\*\* The full versions of Tables 2 through 9 will be available in electronic form at the CDS via anonymous ftp to cdsarc.u-strasbg.fr (130.79.128.5) or via <http://cdsweb.u-strasbg.fr/cgi-bin/qcat?J/A+A/> as well as on our home page <http://www.xray.mpe.mpg.de/theorie/REFLEX/DATA>

characterized environments. For these laboratories we can measure for example their total gravitational mass, their matter composition, the internal gas density, temperature, and pressure of the intergalactic medium, their distance, and other important properties. The best basis for such astrophysical studies is a well documented catalogue of galaxy clusters to choose the best suited objects for the prospective study (e.g. Böhringer et al. 2001b).

On the other hand X-ray selected galaxy clusters are very good tracers of the large-scale structure of the Universe. Since there is a quite well understood relation between the distribution of galaxy clusters with known mass and the dark matter distribution, the statistics of the large-scale matter distribution in the Universe can be derived from the distribution of clusters in a well selected, statistically complete sample. This study of the large-scale

structure was the main objective for the construction of the REFLEX sample. Several results on the construction of the sample (Böhringer et al. 2001a, Paper I), the assessment of the large-scale structure (Collins et al. 2000, Paper II; Schuecker et al. 2001a, Paper III; Böhringer et al. 2002, Paper IV; Schuecker et al. 2002, 2003a (Papers VI and VII), 2003b, Kerscher et al. 2001), on the statistics of substructure in REFLEX clusters Schuecker et al. (2001b), on the statistics of the cluster galaxy velocity dispersions (Ortiz-Gil et al. 2003), and on the X-ray temperatures of the most luminous, distant REFLEX clusters (Zhang et al. 2003) have already been published. Several further papers are in preparation.

Due to the close correlation of X-ray luminosity and mass for clusters of galaxies (e.g. Reiprich & Böhringer 2002) the detection and selection of the sample clusters is currently best performed through the cluster X-ray emission. The ROSAT All-Sky Survey (RASS), which is still the only all-sky or wide-angle X-ray survey performed with an imaging X-ray telescope, is by far the best basis for such cosmological studies. It has been used previously in several projects to construct statistical galaxy cluster samples (Pierre et al. 1994, Romer et al. 1994, Ebeling et al. 1996, 1998, 2000, Burns et al. 1996, De Grandi et al. 1999, Ledlow et al. 1999, Böhringer et al. 2000, Henry et al. 2001, Cruddace et al. 2002, 2003, Ebeling et al. 2001, 2002, Gioia et al. 2003). Part of these projects were studies connected to and profiting from the REFLEX survey program. None of the previous projects covers an area in the southern sky as large as REFLEX, except for the XBACS Abell cluster survey (Ebeling et al. 1996), which is shallower and restricted to those clusters previously identified by Abell (1958) and Abell, Corwin, and Olowin (1989).

The REFLEX catalogue of 447 clusters provides presently the largest statistically complete X-ray cluster sample. The volume of the Universe that is probed is larger than that covered by any present galaxy redshift survey except for the Sloan Digital Sky Survey, which goes to a slightly larger depth but will only cover about half the sky area of that covered by REFLEX, when completed.

The paper is organized as follows. In section 2 we describe the survey and the selection characteristics. Section 3 provides a brief description of the X-ray data reduction and section 4 describes the redshift determination and the cluster galaxy redshift statistics. The main catalogue is presented in section 5 and some of its properties are reviewed in section 6. In the latter section we also provide the numerical data and the recipe to construct the survey selection function in one and two dimensions for any flux limit equal to or above the nominal REFLEX flux limit. Section 7 gives some further information on the identification and the properties of some individual clusters. Section 8 lists close cluster pairs and clusters with double or multiple X-ray maxima found in the REFLEX catalogue, and we describe in more detail those clusters where multiple redshift clustering is observed in the line-of-sight of the X-ray source. In section 9 we compare the results with the previously derived survey samples and, finally, in section

**Table 1.** Overview on the data presented in this paper in tabular form

Table	Content
2	count rate to flux conversion (for $z = 0$ )
3	K – correction as a function of $z$ and $T_x$
4	Flux conversion from the 0.1 – 2.4 keV to the 0.5 to 2.0 keV band
5	Flux conversion from the 0.1 – 2.4 keV band to bolometric flux
6&10	REFLEX cluster catalogue for $h = 0.7$ and $\Lambda$ – cosmology
7	Further X – ray parameters of the REFLEX clusters
8	Sky coverage as a function of the flux limit
9	Angular modulation of the survey selection function
11	Close cluster pairs in the REFLEX sample
12	Clusters with multiple maxima in the REFLEX sample
13	Line – of – sight redshift clustering at the position of REFLEX clusters

10 we provide a summary and conclusions. Table 1 gives an overview of the information presented in this paper in tabular form.

The luminosities and other cluster parameters which depend on the distance scale are derived for a Hubble constant of  $H_0 = 70 \text{ km s}^{-1} \text{ Mpc}^{-1}$  and a cosmological model with  $\Omega_m = 0.3$  and  $\Omega_\Lambda = 0.7$  in the main tables of the paper. We also give in complementary tables provided only in electronic form the cluster properties for the previously most often used Einstein-de Sitter model with  $H_0 = 50 \text{ km s}^{-1} \text{ Mpc}^{-1}$ ,  $\Omega_m = 1.0$  and  $\Omega_\Lambda = 0$  for an easier comparison with previous literature results.

## 2. The REFLEX Survey

The construction of the REFLEX cluster sample is described in detail in paper I. The survey area covers the southern sky up to declination  $\delta = +2.5^\circ$ , avoiding the band of the Milky Way ( $|b_{ll}| \leq 20^\circ$ ) and the regions of the Magellanic clouds. The total survey area is  $13924 \text{ deg}^2$  or  $4.24 \text{ sr}$ . The regions that have been excised are defined in Table 2 in paper I.

The X-ray detection of the clusters is based on the second processing of the RASS (RASS II, Voges et al. 1999), providing 54076 sources in the REFLEX area. Note that the public RASS catalogue available through the internet (<http://www.xray.mpe.mpg.de/rosat/survey/rass-bsc/>; <http://www.xray.mpe.mpg.de/rosat/survey/rass-fsc/>) is based on the third processing of the RASS which has a more complete sky coverage. Since we have frozen the cluster candidate list in 1998 near the end of the optical follow-up program, the cluster selection of the present cluster catalogue is based on RASS II. We have, however, checked that the X-ray properties of the individual catalogued objects are still consistent with the results obtained with the new processing. We have in particular redetermined all cluster centers by applying our analysis

**Table 2.** Count rate to flux conversion factors for different temperatures (for  $Z = 0.3$  solar,  $z = 0$ ) as a function of column density. The values quoted give the 0.1 - 2.4 keV flux per counts in the 0.5 to 2 keV band (channel 52 to 201) in units of  $10^{-12}$  erg s $^{-1}$  cm $^{-2}$  counts $^{-1}$ . The last column gives the hardness ratio for an assumed temperature of 5 keV, defined as (counts(0.5 - 2.0keV)-counts(0.1-0.4 keV))/(counts(0.5-2keV)+counts(0.1-0.4 keV)).

$N_H$ 10 $^{20}$ cm $^{-2}$	temperature												HR (for 5 keV)
	0.5 keV	1.0 keV	1.5 keV	2.0 keV	3.0 keV	4.0 keV	5.0 keV	6.0 keV	7.0 keV	8.0 keV	9.0 keV	10.0 keV	
0.10	1.281	1.413	1.751	1.831	1.868	1.880	1.887	1.893	1.897	1.900	1.901	1.902	0.003
0.30	1.291	1.422	1.761	1.842	1.879	1.891	1.898	1.904	1.908	1.910	1.912	1.913	0.089
1.00	1.325	1.453	1.796	1.880	1.917	1.929	1.936	1.942	1.946	1.948	1.950	1.951	0.323
3.02	1.429	1.543	1.900	1.989	2.028	2.040	2.046	2.052	2.055	2.057	2.059	2.059	0.691
10.00	1.840	1.886	2.278	2.383	2.427	2.438	2.442	2.446	2.449	2.450	2.451	2.450	0.943
30.20	3.654	3.213	3.583	3.718	3.766	3.766	3.762	3.760	3.756	3.753	3.749	3.744	0.978

An extended version of this table is given in electronic form at CDS and our home page.

**Table 3.** K-correction table for different temperatures and redshifts. The given value is to be multiplied with the luminosity in the observed band to obtain the luminosity in the rest frame band.

redshift	temperature											
	0.5 keV	1.0 keV	1.5 keV	2.0 keV	3.0 keV	4.0 keV	5.0 keV	6.0 keV	7.0 keV	8.0 keV	9.0 keV	10.0 keV
0.0500	1.0026	0.9935	0.9867	0.9838	0.9800	0.9771	0.9750	0.9733	0.9720	0.9709	0.9700	0.9693
0.1000	1.0086	1.0253	0.9852	0.9700	0.9596	0.9540	0.9502	0.9472	0.9449	0.9431	0.9415	0.9402
0.1500	1.0126	1.0258	0.9806	0.9611	0.9450	0.9359	0.9299	0.9253	0.9217	0.9189	0.9166	0.9147
0.2000	1.0273	1.0416	0.9771	0.9528	0.9314	0.9192	0.9112	0.9050	0.9003	0.8966	0.8936	0.8911
0.2500	1.0452	1.0799	0.9880	0.9489	0.9197	0.9041	0.8940	0.8864	0.8806	0.8760	0.8724	0.8693
0.3000	1.0497	1.0820	0.9833	0.9401	0.9070	0.8891	0.8775	0.8686	0.8619	0.8566	0.8523	0.8488
0.4000	1.0584	1.0850	0.9768	0.9254	0.8837	0.8614	0.8469	0.8359	0.8276	0.8211	0.8159	0.8115

An extended version of this table is given in electronic form at CDS and our home page.

software to the RASS III data base (to ensure that the naming convention will be stable when finally basing all the analysis on RASS III). The positional changes were small in relation to the extent of the X-ray source. The second, enlarged version of the REFLEX sample with a lower flux limit will be based completely on RASS III.

All sources were reanalysed by means of the growth curve analysis (GCA) method (Böhringer et al. 2000) and the results are used to produce a flux-limited sample of RASS sources with a nominal flux of  $F_n \geq 3 \cdot 10^{-12}$  erg s $^{-1}$  cm $^{-2}$  (with  $F_n$  as defined below). This redetermination of the fluxes has been shown to be crucial for a precise measure of the fluxes of extended sources, as are the majority of the REFLEX clusters (Ebeling et al. 1996, De Grandi et al. 1997, Böhringer et al. 2000). Cluster candidates were found using a machine based correlation of these X-ray sources with galaxy density enhancements in the COSMOS optical data base (derived from digital scans of the UK Schmidt survey plates by COSMOS at the Royal Observatory Edinburgh (MacGillivray & Stobie 1984, Heydon-Dumbleton et al. 1989). The resulting candidate list was carefully screened based on X-ray and op-

tical information, literature data, and results from the optical follow-up observation program. The selection process was designed to provide a completeness in the final cluster catalogue in excess of 90% with respect to the flux-limited sample of GCA selected RASS sources. This high completeness of the cluster identification of the RASS sources ensures that the selection effects introduced by the optical identification process are minimized and negligible for our purpose (see also the statistics given in paper I). Further tests provide support that this value of  $> 90\%$  also describes the overall detection completeness of the flux-limited cluster sample in the survey area. For example an independent search for X-ray emission from the clusters catalogued by Abell, Corwin, & Olowin (1989) returns only one supplementary cluster, S567, with a flux above the flux-limit that has not been included in the REFLEX sample. In addition tests based on the Galactic latitude, redshift and photon count distribution, and on an independent screening of all significantly extended RASS X-ray sources in the survey region, are consistent with this claim (Böhringer et al. 2001, Schuecker et al. 2001). Based on the X-ray spectral properties of the REFLEX cluster

sources we can also estimate that at most 9% of the X-ray cluster sources may have a strong X-ray flux contribution from AGN (see paper I).

To test further the identification of cluster candidates prior to the follow-up observations in La Silla, we adopted a very conservative scheme, as described in more detail in paper I. To reject a source, we required it to have at least two (in some combinations three) properties which are incompatible with a cluster identification. The properties were drawn from the following list: X-ray source is point-like, X-ray source is too soft, no optical cluster visible on digitized optical images, known optical or radio AGN at the center of the X-ray emission. This conservative scheme made the follow-up observations somewhat more expensive, but ensured a high completeness of the final catalogue.

The final cluster sample comprises 447 objects. The distribution of these sources in the sky is shown in Figs. 1 and 2

### 3. Determination of the X-ray parameters

The X-ray count rates, fluxes, and luminosities of the REFLEX clusters are determined from the count rate measurements provided by the GCA (Böhringer et al. 2000). In the first step the source count rates are integrated out to the radius where an effectively flat plateau of the cumulative source count curve is reached. The radius at which the plateau is reached is documented.

To determine the cluster X-ray flux we convert the measured count rate into a unabsorbed “nominal” X-ray flux for the ROSAT band (0.1 to 2.4 keV),  $F_n$ , by assuming a Raymond-Smith type spectrum (Raymond & Smith 1977) for a temperature of 5 keV, a metallicity  $\alpha$  of 0.3 of the solar value (Anders & Grevesse 1989), a redshift of zero, and an interstellar hydrogen column density given for the line-of-sight in the compilation by Dickey & Lockman (1990), as provided within EXSAS (Zimmermann et al. 1994). The value of  $F_n$  is used to make the flux cut independent of any redshift information (since the redshift is not available for all objects at the start of the survey). With the redshift value at hand, the unabsorbed X-ray flux is redetermined ( $F_x$ ) with an improved spectral model, where the temperature is now estimated (iteratively) from the preliminarily derived X-ray luminosity and the luminosity-temperature relation (uncorrected for cooling flow effects) derived by Markevitch (1998). The estimated temperature of the cluster is now taken into account, by folding the appropriate thermal spectrum with the instrument response and the interstellar absorption, leading to a revised flux,  $F_x$  of the source (this correction is less than 5% for sources with an X-ray luminosity above  $4 \cdot 10^{43} \text{ erg s}^{-1}$ ). To obtain the cluster rest-frame luminosity from the flux,  $F_x$  we use the usual conversion with the cosmological luminosity distance and further scale the luminosity by the ratio of the luminosity integrated in the observed, redshifted and rest frame 0.1 - 2.4 keV band. The latter is equivalent to the K-correction. We note one

simplification made in the above transformation. In calculating the revised flux,  $F_x$ , we should have additionally taken the redshift effect into account by folding a redshifted source spectrum with the instrument response matrix and interstellar absorption effect to calculate the exact countrate-to-flux conversion factor. We found, however, that this correction is largest for the low temperature objects at high redshift and since we observe these objects only at closer distances, we established that this effect never becomes larger than 2% for any source in our catalogue and therefore we neglected this effect for the present analysis. In the various applications of our project we have used the results in Tables 2 and 3 for all the necessary conversion factors. Therefore in neglecting this effect we limit the necessary interpolations between observed and tabulated values to two-dimensional interpolations. This helps in the theoretical modeling when large parameter grids have to be evaluated.

Thus, luminosities are calculated for the rest frame energy band 0.1 to 2.4 keV. We also account for the X-ray flux missed outside the detection aperture by the following correction. We correct the fluxes and luminosities based on a self-similar cluster model as described in Böhringer et al. (2000): a  $\beta$ -model (Cavaliere & Fusco-Femiano 1976) with a  $\beta$ -value of 2/3, a core radius that scales with mass, and an assumed extent of the X-ray halo out to 12 times the core radius. The correction procedure has been successfully tested by simulations based on the same cluster model. The typical mean correction factor is about 8% with the largest corrections of up to 30% occurring for the nearby groups which are extended and have a low surface brightness (Böhringer et al. 2000). Note that in contrast to our convention of extrapolating the corrected total flux out to the estimated virial radius, Ebeling et al. (1996, 1998) and De Grandi et al. (1999) extrapolate their flux corrections to infinity. The difference between the two approaches - which uses the same  $\beta$ -model with a slope of 2/3 - is 8.3%. Nevertheless the agreement between the results of, for example, Ebeling et al. (1998) and the results of Böhringer et al. (2000) have been found to show a bias smaller than this difference. We attribute this to the fact that the GCA method is capturing slightly more of the cluster flux than the other methods.

To allow the reader to easily and fully reproduce our present results and the results on the cosmological implications of the REFLEX project published in other papers of this series, without having to resort to ROSAT instrument specific calculations, we provide here all the conversion tables used in the flux and luminosity determination described above. In the underlying calculations we were aiming for an accuracy of better than about 2-3% (e.g. in the energy dependent vignetting correction, the tested difference between calculations with different radiation codes), so that the errors from the conversion factors is in any case negligible compared to the measurement errors. Table 2 gives the conversion factor from the observed count rate in the ROSAT hard band (defined by the range from energy channel 52 to 201) to the flux in the ROSAT

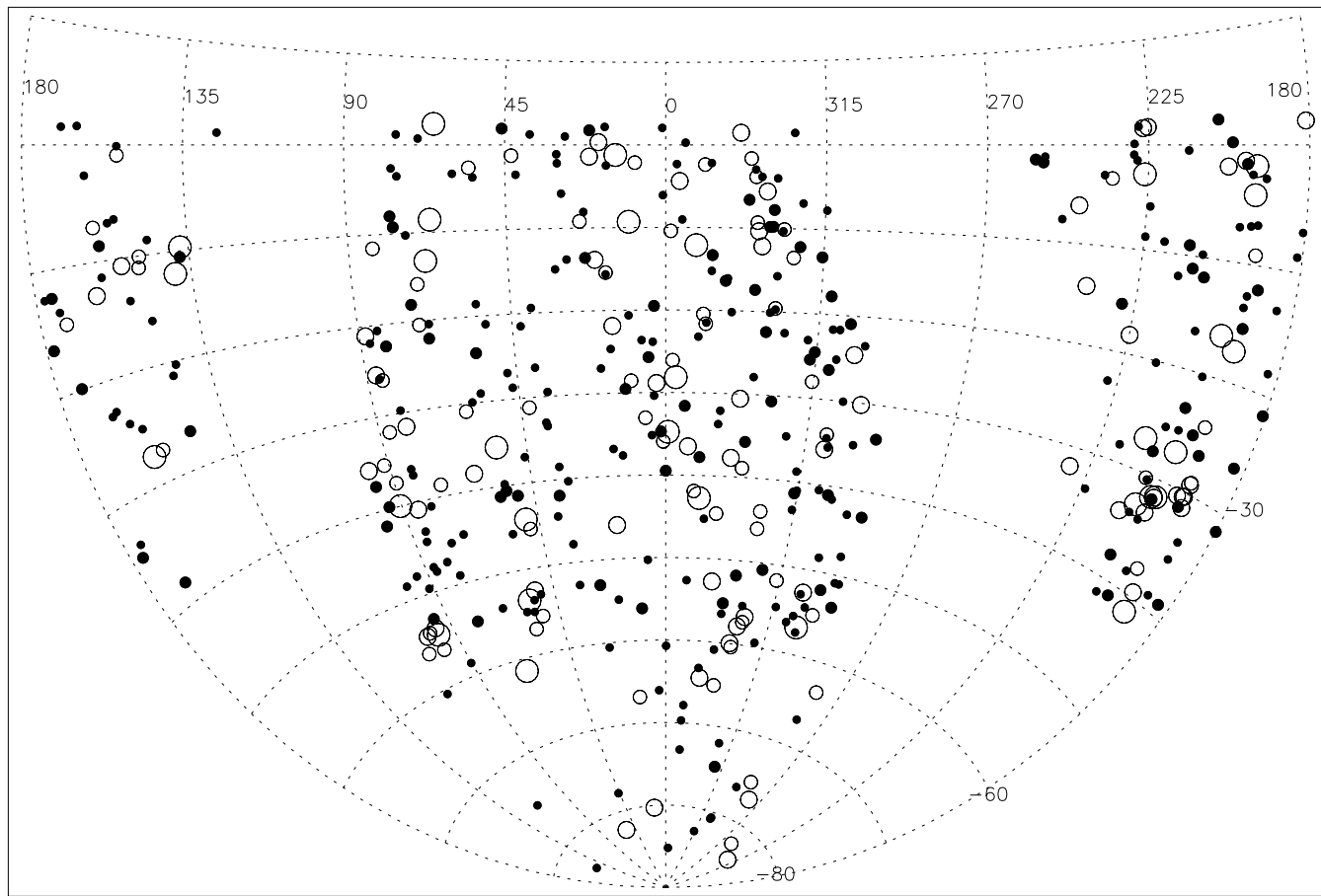


**Fig. 1.** Sky distribution in  $\alpha$  and  $\delta$  of the galaxy clusters in the REFLEX sample. The symbols give an indication of the cluster flux. The clusters are sorted into five flux bins:  $3 - 5 \cdot 10^{-12}$ ,  $5 - 7 \cdot 10^{-12}$ ,  $7 - 10 \cdot 10^{-12}$ ,  $1 - 2 \cdot 10^{-11}$ , and  $\geq 2 \cdot 10^{-11}$   $\text{erg s}^{-1} \text{cm}^{-2}$  and indicated by increasing symbol size, respectively. The three largest symbol classes are shown as open circles to avoid shading of other clusters.

band (0.1 - 2.4 keV) for various temperatures covering the relevant temperature range,  $\alpha = 0.3$  solar, and  $z = 0$ , as a function of the interstellar column density. A graphical representation of this function for three selected temperatures can be found in Böhringer et al. (2000, Fig. 8a) together with the column density dependence of the hardness ratio for the same temperatures (Fig. 8b). This table is used to interpolate the count rate conversion factor for the first step described above, where a fixed temperature of 5 keV is used. In the second step the calculation is improved by interpolating to the estimated temperature. Table 3 then provides the K-correction factors to convert the redshifted luminosity measure into rest-frame luminosity as a function of redshift and temperature of the cluster.

For an easy comparison of the catalogue with data given in other frequently used energy bands, we provide in Table 4 the conversion factor from the 0.1 - 2.4 keV to the 0.5 - 2.0 keV band as a function of temperature. Table 5 provides the conversion from the ROSAT band (0.1 - 2.4 keV) to the bolometric system. The print version of the

paper gives only a few example lines for Tables 2 through 5. The full tables can be obtained from the electronic version of the paper.

#### 4. Redshift determination

For cluster candidates with published redshifts we adopted the following procedure to obtain the final redshift. The search for redshift information in the literature was conducted with an aperture radius of 7 arcmin for more distant clusters and the search radius was increased to half the virial radius (half the virial radius was taken to be 5 times the core radius estimated from  $L_X$  as described in Böhringer et al. 2000) if this radius was larger than 7 arcmin. This is of course an iterative process in which a first redshift result was chosen for which the search radius was calculated and then a refined search for cluster galaxy members was performed in NED. This was found to be very important for the nearby clusters where an increasing number of redshifts becomes available from large redshift surveys which help greatly in improving the cluster red-

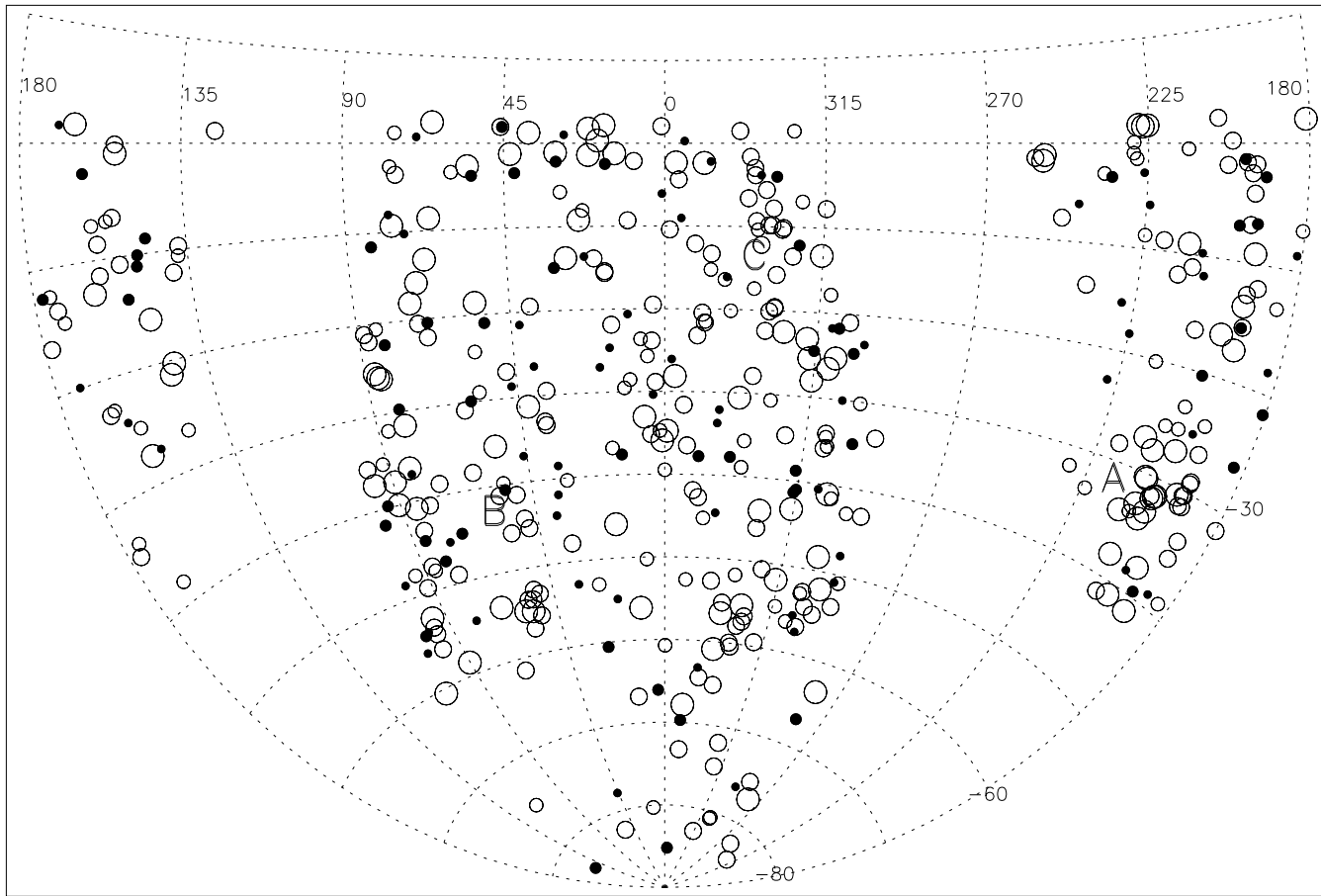


**Fig. 2.** The same sky distribution of REFLEX clusters as shown in Fig. 2, but now the symbols indicate the cluster distance. The clusters are sorted into five redshift classes:  $z = 0 - 0.05$ ,  $z = 0.05 - 0.1$ ,  $z = 0.1 - 0.15$ ,  $z = 0.15 - 0.2$ , and  $z \geq 0.2$  indicated by decreasing symbol size with increasing redshift. The three largest symbol classes are shown as open circles to avoid shading of other clusters. In this plot superstructures can be recognized. Three of the most prominent superclusters have been marked: A is the Shapley concentration partly overlapping with Hydra-Centaurus in the foreground, B is the Horlogium-Reticulum complex, and C refers to the Aquarius-Cetus and Aquarius-Capricornus superclusters. For more details on these superstructures see Einasto et al. (2001).

shifts. The final redshift taken was the cluster redshift that involved the largest number of galaxy redshifts. If no reliable cluster redshift was available, the cluster redshift was computed from the median of individual galaxy redshifts located within the aperture radius around the central target position after the rejection of obvious non-members of the cluster. The secondary line-of-sight clustering found for a number of REFLEX clusters is further described in section 8. The present literature redshift compilation is largely based on information requested from NED in July 2003.

Cluster candidates without published redshifts or reliable identification were observed from 1992 to 1999 within a large ESO key programme (Böhringer et al. 1998, Guzzo et al. 1999). For a detailed spectroscopic follow-up we used for the brighter objects the ESO 1.5m with the Boller & Chivens spectrograph and the ESO 2.2m with the EFOSC-2 instrument. For the more distant and thus fainter objects

the ESO 3.6m telescope with the EFOSC-1 (later EFOSC-2) instrument was used. This instrument was preferentially used in multi-object spectroscopic mode, but also long-slit spectra were taken with EFOSC for some of the clusters. If necessary we also performed CCD imaging in order to test for galaxy overdensities in the target direction. A detailed description of the observing strategy, the reduction of the spectra, redshift measurements, astrometry, and morphological classification is in preparation (Guzzo et al. 2003, in preparation). A brief summary is given below.

The main goal of the follow-up observations was to get for each X-ray cluster candidate at least five spectra, which we found was enough for a first identification of the X-ray source and for a good estimate of the cluster redshift. This comparatively small number of spectra results from the fact that the optical follow-up could be restricted to the location of the X-ray peak, that is, to the region

**Table 4.** Conversion factor to be multiplied to the flux in the 0.5 to 2.0 keV band to obtain the flux in the 0.1 to 2.4 keV band as a function of temperature.

temperature (keV)	flux ratio
0.5	1.387
1.0	1.496
1.5	1.615
2.0	1.623
3.0	1.618
4.0	1.611
5.0	1.607
6.0	1.605
7.0	1.603
8.0	1.599
9.0	1.598
10.0	1.597

**Table 5.** Conversion factor of the flux/luminosity in the 0.1 to 2.4 keV band to bolometric flux/luminosity as a function of temperature

temperature (keV)	flux ratio
0.30	1.443
0.51	1.187
1.02	1.269
1.98	1.448
3.00	1.660
5.10	2.122
8.08	2.743
10.17	3.152
15.04	4.053

An extended version of this table is given in electronic form at CDS and our home page.

of the expected deepest cluster potential well where contamination by background galaxies is minimal. In order to optimize the efficiency of cluster identification and redshift measurement, for clusters with a few bright (nearby) galaxies, spectra were observed in the single-slit mode, whereas for clusters with many faint galaxies the multi-slit mode was chosen. The multi-slit mode gives spectra for about 10-25 galaxies, so that for many clusters we also have information about the velocity dispersion (Ortiz-Gil et al. 2003).

Fig. 3 shows the cumulative distribution of the REFLEX clusters with a number of member galaxy redshifts greater than the given limit. Indeed about half of the clusters have 5 or more galaxy redshifts and the derived redshift is fairly secure. However, about 42 clusters feature only one galaxy redshift, mostly values coming from the literature. The available observation time budget for this project did not allow for a redetermination of all the

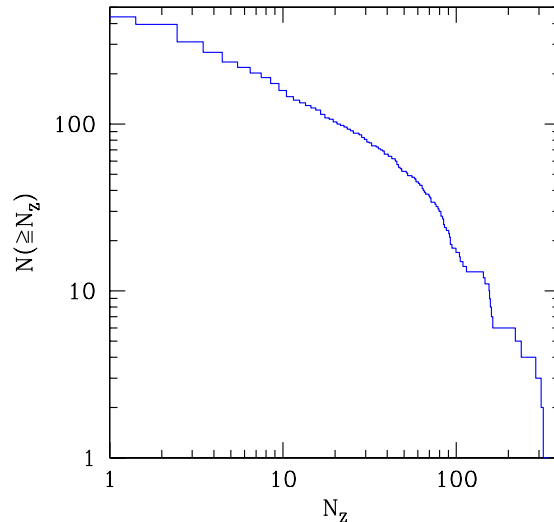


**Fig. 3.** Cumulative distribution,  $N_{cl}(\geq N_z)$ , of the number of galaxy redshifts known for the clusters in the REFLEX sample.

literature values. Still most of these data yield a reliable, as they refer to the central brightest cluster galaxy at the center of the X-ray emission. For 8 clusters in the catalogue we were so far not able to find the information in the literature on the number of galaxies from which the cluster redshift was determined.

The majority of spectra were reduced in a standard manner (bias and flat field correction, wavelength calibration) using procedures from the IRAF software package. Cosmics were rejected from the combination of at least two spectral exposures obtained for each spectral observation. All spectra were visually classified into the categories elliptical galaxy, spiral galaxy, Seyfert 1/2 galaxy, quasar, starforming galaxy (tentatively), and stellar. Heliocentric redshifts were determined from cross-correlation with a sample of 17 template spectra with spectral types covering the large range usually found in clusters of galaxies and in the field. In addition, redshifts were also determined from emission lines (if present), including a measurement of their equivalent widths. The final redshifts of the clusters were obtained from the median of the measured galaxy redshifts after the rejection of obvious non-members. The criterion for the assignment of the cluster membership was a maximum velocity deviation of 3000 km s<sup>-1</sup> from the median.

All optical and X-ray information is collected and organized in a data base which we are planing to make publicly available. A more detailed account of the optical data will be given in a forthcoming paper listing in particular the individual galaxy redshifts determined in this ESO key program (Guzzo et al.)

## 5. The catalogue

Table 6 and 10 list the X-ray properties and redshifts of the 447 galaxy clusters of the REFLEX sample (compared to the previously used sample of 449 clusters, 7 clusters have been removed as detailed in section 7, 4 clusters considered before as being contaminated by non-cluster emission have been added, and one double cluster has been split into two sources). *Please note that the table is artificially split here in two parts, as a result of memory limitation problems with the current A&A LATEX implementation. This should be corrected with the help of the editor before going into print.* The columns of the table provide: (1) the REFLEX name, (2) a previous catalogue name, where for some of the smaller galaxy groups the name refers to the central dominant galaxy in the group (e.g. the NGC name of this galaxy), (3) and (4) the right ascension and declination for the epoch J2000 in hours (degrees), minutes, and seconds, (5) the redshift, (6) the number of galaxies with which the redshift has been determined after the rejection of non-members (a zero means that no information is available about the number of galaxies used to determine the cluster redshift), (7) and (8) the measured, unabsorbed X-ray flux,  $F_x$ , in units of  $10^{-12}$  erg s $^{-1}$  cm $^{-2}$  for the 0.1 - 2.4 keV energy band and the fractional error in percent (note that this is not the nominal flux,  $F_n$ , used to define the flux limit of REFLEX;  $F_n$  is given in Table 7), (9) the X-ray luminosity uncorrected for missing flux in units of  $10^{44}$  erg/s in the rest frame 0.1 to 2.4 keV band, (10) the aperture radius in arcmin within which the X-ray count rate and flux were determined (the radius where the plateau value is reached in the cumulative count rate curve of the GCA), (11) the 0.1 - 2.4 keV luminosity corrected for the estimated flux lost outside the measurement aperture, (12) the interstellar column density in units of  $10^{20}$  cm $^{-2}$  as obtained from the 21 cm observations by Dickey & Lockman (1990) and Stark et al. (1992), (13) comment flags as described below, and (14) references to literature values for the cluster redshifts. The comment flags refer to: (L) clusters which are too extended for the standard GCA count rate determination in  $2 \times 2$  degree $^2$  fields, and therefore were analysed in  $4 \times 4$  or  $8 \times 8$  degree $^2$  fields, (B) clusters blended with point sources or double clusters which were deblended, (X) clusters where the details of the source identification are commented in Section 7, (P) parts of close cluster pairs or groups, and (D) double clusters discussed in section 8. For 12 objects marked with an astrisk in column (13) the cluster origin of the X-ray emission is not completely certain as detailed in section 7.

Further more detailed X-ray properties on the REFLEX clusters as determined with the GCA method are given in Table 7, where the following columns are listed: (1) name, (2) and (3) repeat the J2000 sky coordinates, but now in units of decimal degrees, (4) the count rate as measured with the GCA method for the aperture size given in column 10 in Table 6, (5) X-ray flux,  $F_n$ , determined in the first step for an assumed temperature of 5

keV used for the source selection, (6) the X-ray luminosity in the rest frame 0.1 to 2.4 keV band uncorrected for missing (unabsorbed) flux, (7) the number of source photons detected within the reference aperture (column 14), (8) the probability for the X-ray source to be a point source in values of  $-\log_{10}(P)$  (determined as described below), (9) and (10) the best fitted core radius for the  $\beta$ -model fit and a minimal core radius still consistent within  $2\sigma$  error limits, respectively. Note that the core radii determined here are only a qualitative measure for the source extent, since the errors are very large and the fitting grid was coarsely spaced. Therefore core radii and their lower limiting values can give a further qualitative feeling for the extent of the X-ray sources, but **we recommend not to use these results for  $r_c$  as a quantitative measure of cluster shapes at this point.** Columns (11) and (12) give the spectral hardness ratio defined by the equation given below and its Poisson error. Column (13) indicates the deviation of the measured hardness ratio from the expectation value calculated for given  $N_H$  and for an assumed temperature of 5 keV as factors of  $\sigma$ . The last column (14) repeats from Table 6 the aperture radius within which the source count rate was measured, but now in physical units of Mpc. This is the radius where the cumulative source count rate profile reaches the plateau value. The print version of this paper gives only a few example lines of this table. The full table as well as a second version of Table 6 for an Einstein-de Sitter Universe model is provided in the electronic version.

The probability of an X-ray source to be a point source, as given in column (5) was determined by means of a Kolmogorov-Smirnov test comparing the normalized radially cumulative photon distribution within an aperture radius of 6 arcmin with the expectations for a point source and background. In this test we consider a source to be significantly extended if the probability is less than 1%, corresponding to an entry value in Table 7 larger than 2. The source hardness ratio, as given in column (8), was determined from the source count rate in the soft (ROSAT PSPC channel 11 to 40) and hard (PSPC channel 52 to 201) band by the formula:

$$HR = \frac{H - S}{H + S}$$

where H is the hard band and S the soft band count rate.

Figure 1 shows the sky distribution of the REFLEX clusters with five different X-ray flux classes marked by different symbols. The empty region around RA = 75 deg (5 hr) and DEC = -70 deg is due to the excision of the regions of the Large and Small Magellanic Clouds. Fig. 2 shows the same sky distribution but now with the clusters sorted in five different redshift classes. This illustrates the large scale clustering of the clusters, and several known superclusters are marked.



**Table 6.** The REFLEX cluster catalogue

name (1)	alt.name (2)	RA(2000) (3)	DEC(2000) (4)	$z$ (5)	$N_{gal}$ (6)	$F_x$ (7)	Error (8)	$L_x$ (9)	$R_{ap}$ (10)	$L_x^*$ (11)	$N_H$ (12)	$Cm$ (13)	Ref. (14)
RXCJ0003.1 – 0605	A2697	00 03 11.8	–06 05 10	0.2320	0	4.497	12.4	6.395	7.5	6.876	3.1		139
RXCJ0003.2 – 3555	A2717	00 03 12.1	–35 55 38	0.0490	40	7.537	17.8	0.421	10.0	0.478	1.1		2
RXCJ0003.8 + 0203	A2700	00 03 50.6	+02 03 48	0.0924	9	4.155	18.8	0.855	8.5	0.929	3.0		S, 10
RXCJ0006.0 – 3443	A2721	00 06 03.0	–34 43 27	0.1147	75	5.832	13.6	1.875	10.0	1.995	1.2		1
RXCJ0011.3 – 2851	A2734	00 11 20.7	–28 51 18	0.0620	83	12.014	9.0	1.089	12.5	1.197	1.8		2
RXCJ0013.6 – 1930	A0013	00 13 38.3	–19 30 08	0.0940	37	6.071	11.3	1.285	11.5	1.353	2.0		S, 2, 140, 141
RXCJ0014.3 – 6604	A2746	00 14 18.4	–66 04 39	0.1599	5	4.485	13.8	2.907	7.5	3.160	2.8	X	E
RXCJ0014.3 – 3023	A2744	00 14 18.8	–30 23 00	0.3066	65	4.964	18.7	12.787	12.0	12.916	1.6		142, 143
RXCJ0015.4 – 2350		00 15 24.0	–23 50 42	0.0645	4	3.426	18.3	0.336	11.5	0.354	2.5	X	33
RXCJ0017.5 – 3509	A2755	00 17 33.7	–35 09 54	0.0968	23	3.211	20.0	0.729	11.5	0.752	1.3		E, 3, 33, 140, 141
RXCJ0020.7 – 2542	A0022	00 20 42.8	–25 42 37	0.1410	3	5.910	12.1	2.909	7.5	3.232	2.3		1
RXCJ0025.5 – 3302	S0041	00 25 32.4	–33 02 50	0.0491	3	8.818	9.7	0.494	13.0	0.537	1.7		26, 144
RXCJ0027.3 – 5015	A2777	00 27 21.3	–50 15 04	0.1448	1	4.286	17.1	2.247	8.5	2.390	1.7		E, 145
RXCJ0028.6 – 2338	A0042	00 28 39.3	–23 38 14	0.1120	5	4.836	13.3	1.491	13.0	1.521	1.8		33
RXCJ0034.6 – 0208		00 34 36.0	–02 08 24	0.0812	2	8.629	7.9	1.360	28.0	1.388	2.8	DL	S, 139
RXCJ0040.1 – 5607	A2806	00 40 06.5	–56 07 00	0.0277	20	4.068	19.3	0.071	13.5	0.077	2.2		12, 18, 146
RXCJ0041.8 – 0918	A0085	00 41 50.1	–09 18 07	0.0555	308	74.215	3.2	5.293	25.0	5.631	3.6	L	130, 148, 149
RXCJ0042.1 – 2832	A2811	00 42 08.7	–28 32 09	0.1082	29	9.774	9.8	2.788	10.0	3.030	1.5		E, 33, 96
RXCJ0043.4 – 2037	A2813	00 43 24.4	–20 37 17	0.2924	7	3.186	15.6	7.387	8.5	7.615	1.5		E
RXCJ0049.4 – 2931	S0084	00 49 24.0	–29 31 28	0.1084	18	5.228	16.0	1.503	11.0	1.566	1.8		33, 150
RXCJ0052.7 – 8015	A2837	00 52 44.9	–80 15 59	0.1141	7	11.264	21.2	3.547	12.5	3.734	6.6		E
RXCJ0055.9 – 3732	C10053 <sup>a</sup>	00 55 59.2	–37 32 51	0.1653	21	3.985	17.3	2.764	13.0	2.792	2.6	B	E, 1
RXCJ0056.3 – 0112	A0119	00 56 18.3	–01 12 60	0.0442	104	33.613	5.3	1.505	26.5	1.568	3.1	L	2
RXCJ0057.8 – 6648	S0112	00 57 48.1	–66 48 44	0.0661	8	7.225	36.0	0.743	11.5	0.799	2.6		30, 151
RXCJ0102.7 – 2152	A0133	01 02 42.1	–21 52 25	0.0569	9	19.031	6.7	1.439	13.0	1.617	1.6		5, 24, 152, 153
RXCJ0105.5 – 2439	A0141	01 05 34.8	–24 39 17	0.2300	0	3.884	15.7	5.416	7.5	5.762	1.6		1
RXCJ0106.8 – 0229	A0145	01 06 52.4	–02 29 24	0.1909	1	3.209	21.1	3.010	14.0	3.040	4.1		19, 154
RXCJ0107.8 – 3643	A2871	01 07 49.1	–36 43 38	0.1186	19	3.557	13.6	1.229	12.0	1.254	1.9		E, 2, 3, 33
RXCJ0108.1 + 0210	A0147	01 08 11.5	+02 10 34	0.0436	8	4.369	16.0	0.192	12.0	0.206	3.0		120, 123, 156, 157
RXCJ0108.8 – 1524	A0151N	01 08 50.1	–15 24 36	0.0533	63	6.862	9.8	0.456	8.5	0.530	1.7	B	1, 2
RXCJ0108.9 – 1537	A0151S	01 08 55.2	–15 37 44	0.0970	13	3.703	15.3	0.845	10.0	0.889	1.8	B	3
RXCJ0110.0 – 4555	A2877	01 10 00.4	–45 55 22	0.0238	58	14.005	8.0	0.179	20.0	0.195	2.1	L	12, 130, 131, 146
RXCJ0115.2 + 0019	A0168	01 15 12.0	+00 19 48	0.0450	76	10.429	9.3	0.488	20.0	0.503	3.3	L	S, 2
RXCJ0117.8 – 5455		01 17 50.5	–54 55 26	0.2510	6	3.054	33.4	5.155	6.5	5.543	2.7	X*	E
RXCJ0118.1 – 2658	A2895	01 18 11.1	–26 58 23	0.2275	4	3.822	14.0	5.225	7.5	5.559	1.6		S, 96
RXCJ0120.9 – 1351	CAN010 <sup>b</sup>	01 20 58.9	–13 51 31	0.0519	7	12.430	7.9	0.778	15.5	0.828	1.9	B	S, 120
RXCJ0125.5 + 0145	NGC533	01 25 30.2	+01 45 44	0.0174	19	4.712	15.9	0.032	15.0	0.036	3.1		E, 120
RXCJ0125.6 – 0124	A0194	01 25 40.8	–01 24 26	0.0180	146	9.713	14.1	0.070	24.0	0.074	4.1	L	158
RXCJ0131.8 – 1336	A0209	01 31 53.0	–13 36 34	0.2060	2	5.481	10.4	6.037	9.5	6.289	1.6		1
RXCJ0132.6 – 0804		01 32 40.9	–08 04 20	0.1489	3	3.784	11.9	2.108	10.0	2.173	3.4	X*	E
RXCJ0137.2 – 0912		01 37 15.4	–09 12 10	0.0409	5	7.090	8.4	0.272	9.5	0.316	2.8		S, 120
RXCJ0145.0 – 5300	A2941	01 45 02.3	–53 00 50	0.1168	4	6.028	16.0	2.005	7.5	2.253	2.3		E
RXCJ0145.2 – 6033	RBS0238 <sup>c</sup>	01 45 16.7	–60 33 54	0.1805	11	4.811	13.4	4.010	4.5	4.890	3.4		E
RXCJ0152.7 + 0100	A0267	01 52 42.3	+01 00 45	0.2300	1	3.090	14.6	4.329	5.0	4.919	2.8	DB	55, 147, 159
RXCJ0152.9 – 1345	NGC0720	01 52 59.0	–13 45 12	0.0050	3	2.284	16.4	0.001	10.5	0.001	1.7		12, 160, 161
RXCJ0157.4 – 0550	A0281	01 57 24.3	–05 50 24	0.1289	4	3.277	14.7	1.355	10.0	1.397	2.2	D	E, 1
RXCJ0201.7 – 0212	A0291	02 01 44.2	–02 12 03	0.1960	2	4.244	11.5	4.199	5.0	4.883	2.6		S, 53, 54
RXCJ0202.3 – 0107	A0295	02 02 19.9	–01 07 13	0.0427	47	3.586	13.7	0.151	14.0	0.157	2.6		2, 148, 162
RXCJ0206.4 – 1453	A0305	02 06 30.0	–14 53 38	0.1529	2	2.993	17.9	1.778	6.0	1.976	2.5		S
RXCJ0211.4 – 4017	A2984	02 11 25.5	–40 17 12	0.1008	6	3.222	11.5	0.798	8.0	0.858	1.4		33
RXCJ0216.7 – 4749	S0239	02 16 42.3	–47 49 24	0.0640	1	3.574	16.9	0.346	11.5	0.364	3.0		5, 9, 29
RXCJ0217.2 – 5244		02 17 12.6	–52 44 49	0.3432	2	3.641	15.4	11.914	11.5	12.034	3.2		E
RXCJ0220.9 – 3829		02 20 56.6	–38 29 05	0.2280	5	3.406	11.8	4.679	7.0	5.031	1.9		E
RXCJ0225.1 – 2928		02 25 10.5	–29 28 26	0.0604	17	4.736	23.4	0.408	12.0	0.434	1.7		S, 96
RXCJ0225.9 – 4154	A3016	02 25 54.6	–41 54 35	0.2195	1	5.185	11.2	6.507	11.0	6.640	2.1		S
RXCJ0229.3 – 3332		02 29 22.3	–33 32 16	0.0792	17	3.912	12.9	0.588	12.5	0.606	2.1	P	S, 33
RXCJ0230.7 – 3305	A3027	02 30 43.5	–33 05 55	0.0760	22	3.207	15.7	0.445	15.0	0.449	2.0	PB	33
RXCJ0231.9 + 0114	RCS145 <sup>d</sup>	02 31 57.1	+01 14 40	0.0221	10	2.618	21.1	0.029	14.5	0.031	2.9		55, 64, 110
RXCJ0232.2 – 4420		02 32 16.8	–44 20 51	0.2836	2	4.074	17.7	8.875	6.5	9.647	2.6	B	S
RXCJ0236.6 – 1923	A0367	02 36 40.2	–19 23 13	0.0907	27	3.434	14.6	0.679	8.5	0.730	2.7		140, 141

name (1)	alt.name (2)	<i>R.A.</i> (3)	<i>Decl.</i> (4)	<i>z</i> (5)	<i>N<sub>gal</sub></i> (6)	<i>F<sub>x</sub></i> (7)	<i>Error</i> (8)	<i>L<sub>x</sub></i> (9)	<i>R<sub>ap</sub></i> (10)	<i>L<sub>x</sub><sup>*</sup></i> (11)	<i>N<sub>H</sub></i> (12)	<i>C<sub>m</sub></i> (13)	<i>Ref.</i> (14)
RXCJ0237.4 – 2630	A0368	02 37 29.2	–26 30 17	0.2216	10	3.082	15.4	3.971	6.5	4.270	1.6		<i>E</i>
RXCJ0248.0 – 0332	A0383	02 48 02.0	–03 32 15	0.1883	1	4.837	18.3	4.377	10.0	4.559	4.1		<i>S</i> , 7, 147
RXCJ0249.6 – 3111	S0301	02 49 36.9	–31 11 19	0.0230	28	6.979	8.6	0.083	17.0	0.089	1.8	<i>L</i>	14, 28, 72, 96
RXCJ0250.2 – 2129		02 50 17.2	–21 29 56	0.2070	2	3.526	16.5	3.942	6.5	4.285	2.5	<i>X*</i>	<i>E</i>
RXCJ0252.8 – 0116	NGC1132	02 52 49.4	–01 16 27	0.0235	6	6.028	16.2	0.075	9.5	0.091	5.2		55, 163
RXCJ0301.6 + 0155	Zw0258.9 <sup>e</sup>	03 01 37.2	+01 55 11	0.1712	14	4.973	15.8	3.704	6.0	4.209	7.7	<i>X</i>	<i>E</i>
RXCJ0303.3 + 0155	A0409	03 03 21.1	+01 55 35	0.1530	1	5.082	15.1	2.990	6.0	3.437	7.8		53
RXCJ0303.7 – 7752		03 03 46.4	–77 52 09	0.2742	8	3.243	20.2	6.593	6.0	7.166	8.9		<i>E</i>
RXCJ0304.1 – 3656	A3084	03 04 07.2	–36 56 36	0.2192	2	3.010	15.5	3.806	7.0	4.049	2.0		<i>E</i>
RXCJ0307.0 – 2840	A3088	03 07 04.1	–28 40 14	0.2537	10	3.877	17.3	6.675	9.0	6.953	1.4		<i>E</i>
RXCJ0311.4 – 2653	A3094	03 11 25.0	–26 53 59	0.0685	23	2.942	50.4	0.329	8.0	0.362	1.6		3, 17, 33, 96
RXCJ0314.3 – 4525	A3104	03 14 19.8	–45 25 27	0.0718	4	8.255	9.5	1.009	9.5	1.134	3.6		<i>E</i>
RXCJ0317.9 – 4414	A3112	03 17 58.5	–44 14 20	0.0752	38	29.301	3.9	3.904	15.5	4.243	2.5		<i>S</i> , 3, 31
RXCJ0322.2 – 5310	APMCC391 <sup>f</sup>	03 22 12.7	–53 10 41	0.0797	6	3.099	10.9	0.476	12.0	0.491	2.3		<i>E</i>
RXCJ0322.3 – 4121	A3122	03 22 18.6	–41 21 34	0.0643	87	6.355	9.7	0.616	14.0	0.642	2.1		3, 140, 141
RXCJ0328.6 – 5542	A3126	03 28 37.5	–55 42 46	0.0853	42	8.441	7.6	1.476	10.0	1.622	3.1		38, 164
RXCJ0330.0 – 5235	A3128	03 30 00.7	–52 35 46	0.0624	40	12.786	5.5	1.171	22.0	1.195	1.5	<i>DL</i>	3, 38, 131, 165
RXCJ0331.1 – 2100		03 31 07.3	–21 00 12	0.1880	9	4.044	24.5	3.662	4.5	4.360	2.5	<i>X*</i>	<i>E</i>
RXCJ0334.9 – 5342	APMCC421 <sup>f</sup>	03 34 56.2	–53 42 08	0.0619	4	3.323	11.9	0.301	14.0	0.307	1.2		24, 17, 164
RXCJ0336.3 – 4037	A3140	03 36 18.7	–40 37 20	0.1729	9	5.631	15.4	4.267	8.0	4.588	1.4		<i>E</i>
RXCJ0336.3 – 0347		03 36 22.9	–03 47 29	0.1595	3	3.745	15.9	2.426	9.5	2.527	4.9	<i>X*</i>	<i>E</i>
RXCJ0337.0 – 3949	A3142	03 36 60.0	–39 49 12	0.1030	21	3.298	23.6	0.855	10.0	0.891	1.8		2
RXCJ0338.4 – 3526	FORNAX	03 38 27.9	–35 26 54	0.0051	32	21.272	11.1	0.012	19.0	0.016	1.5	<i>B</i>	166, 167, 168, 170, 171
RXCJ0340.1 – 5503	IC1987	03 40 08.6	–55 03 14	0.0464	1	3.803	12.0	0.190	17.0	0.194	2.2	<i>L</i>	17, 164
RXCJ0340.1 – 1835	NGC1407 <sup>g</sup>	03 40 11.4	–18 35 15	0.0056	4	3.443	14.0	0.002	14.5	0.002	5.2		172
RXCJ0340.6 – 0239		03 40 41.8	–02 39 57	0.0352	2	7.923	10.6	0.225	17.5	0.237	7.3		<i>E</i>
RXCJ0340.8 – 4542	RBS0459 <sup>c</sup>	03 40 49.3	–45 42 19	0.0698	9	3.981	14.0	0.461	10.5	0.490	1.6		<i>E</i>
RXCJ0342.8 – 5338	A3158	03 42 53.9	–53 38 07	0.0590	105	36.344	3.3	2.951	30.0	3.011	1.1	<i>L</i>	2
RXCJ0345.7 – 4112	S0384	03 45 45.7	–41 12 27	0.0603	1	5.763	18.9	0.495	11.5	0.532	1.9		<i>E</i> , 29, 30
RXCJ0345.9 – 2416	A0458	03 45 56.0	–24 16 49	0.1057	30	5.510	10.0	1.501	9.5	1.614	1.6		1
RXCJ0346.1 – 5702	A3164	03 46 09.6	–57 02 60	0.0570	3	7.465	12.7	0.570	20.0	0.576	2.6	<i>L</i>	146
RXCJ0347.0 – 2900	A3165	03 47 00.2	–29 00 13	0.1419	3	4.054	22.0	2.033	8.0	2.186	0.9		19, 173
RXCJ0351.1 – 8212	S0405	03 51 08.9	–82 12 60	0.0613	2	14.078	8.0	1.243	16.5	1.308	7.7	<i>L</i>	<i>E</i> , 27
RXCJ0352.3 – 5453	RBS0485 <sup>c</sup>	03 52 20.7	–54 53 09	0.0447	2	3.798	25.9	0.176	13.0	0.185	3.0		<i>E</i>
RXCJ0358.8 – 2955	A3192	03 58 50.5	–29 55 18	0.1681	13	3.060	13.3	2.202	7.5	2.343	1.0		<i>E</i>
RXCJ0359.1 – 0320		03 59 09.2	–03 20 28	0.1220	4	3.546	17.1	1.302	8.5	1.385	8.2		<i>E</i>
RXCJ0408.2 – 3053	A3223	04 08 16.2	–30 53 40	0.0600	81	8.186	8.8	0.693	16.0	0.722	1.8		<i>E</i> , 2
RXCJ0413.9 – 3805		04 13 57.1	–38 05 60	0.0501	22	12.608	7.7	0.734	15.0	0.789	1.4	<i>B</i>	<i>E</i> , 31, 96, 144
RXCJ0419.6 + 0224	NGC1550	04 19 37.8	+02 24 50	0.0131	7	40.095	6.1	0.153	22.0	0.182	11.6	<i>L</i>	11, 64, 123, 174
RXCJ0425.8 – 0833	RBS0540 <sup>c</sup>	04 25 51.4	–08 33 33	0.0397	2	28.011	5.8	1.008	13.5	1.186	6.4	<i>X</i>	<i>E</i> , 175, 176
RXCJ0429.1 – 5350	S0463	04 29 07.8	–53 50 51	0.0400	28	4.018	16.5	0.148	10.0	0.164	0.8		19, 72, 74, 177
RXCJ0431.4 – 6126	A3266	04 31 24.1	–61 26 38	0.0589	317	49.741	1.8	4.019	18.0	4.416	1.5		155
RXCJ0433.6 – 1315	A0496	04 33 38.4	–13 15 33	0.0326	143	72.075	3.7	1.746	19.0	2.054	5.7		120, 130, 152, 178, 179
RXCJ0437.1 – 2027	A0499	04 37 07.2	–20 27 26	0.1550	2	3.442	56.5	2.094	13.0	2.094	2.6	<i>X</i>	<i>E</i>
RXCJ0437.1 + 0043		04 37 10.1	+00 43 38	0.2842	5	3.942	13.0	8.629	8.5	8.989	8.2		<i>E</i>
RXCJ0438.9 – 2206	A0500	04 38 54.7	–22 06 49	0.0670	3	6.168	16.1	0.652	10.0	0.716	2.8		29
RXCJ0445.1 – 1551	NGC1650	04 45 10.0	–15 51 01	0.0360	3	8.634	10.3	0.255	16.0	0.274	4.8		120
RXCJ0448.2 – 2028	A0514	04 48 12.2	–20 28 11	0.0720	90	8.583	8.8	1.052	15.5	1.096	3.2		2
RXCJ0449.9 – 4440	A3292	04 49 55.2	–44 40 41	0.1501	2	4.418	13.7	2.501	6.0	2.842	1.5		<i>E</i>
RXCJ0454.1 – 1014	A0521	04 54 09.1	–10 14 19	0.2475	42	4.944	16.6	8.014	11.5	8.178	5.4		<i>E</i> , 180
RXCJ0454.8 – 1806	CID28 <sup>b</sup>	04 54 50.3	–18 06 33	0.0335	17	5.539	11.8	0.142	12.5	0.156	4.2		<i>E</i> , 120
RXCJ0500.7 – 3840	A3301	05 00 46.5	–38 40 41	0.0536	5	7.370	10.0	0.495	13.5	0.527	3.1		40
RXCJ0501.3 – 0332	A0531	05 01 19.4	–03 32 33	0.0913	10	3.994	23.4	0.801	10.0	0.843	6.0		<i>E</i>
RXCJ0501.6 + 0110		05 01 39.1	+01 10 30	0.1248	15	4.398	16.3	1.696	10.0	1.785	7.9	<i>B</i>	<i>E</i>
RXCJ0507.6 – 0238	A0535	05 07 36.0	–02 38 24	0.1241	2	3.341	21.7	1.273	13.0	1.286	9.7	<i>B</i>	<i>E</i>
RXCJ0507.7 – 0915	A0536	05 07 45.7	–09 15 16	0.0398	1	5.056	13.7	0.184	14.0	0.196	7.9		1
RXCJ0510.2 – 4519	A3322	05 10 13.9	–45 19 16	0.2000	1	4.792	14.3	4.960	6.5	5.511	3.4		181
RXCJ0510.7 – 0801		05 10 44.7	–08 01 06	0.2195	14	6.565	10.7	8.209	10.0	8.551	8.3		<i>E</i>
RXCJ0514.6 – 4903	A3330	05 14 36.3	–49 03 18	0.0912	2	4.130	17.9	0.826	14.0	0.843	2.4		17, 32, 182
RXCJ0516.6 – 5430	S0520	05 16 38.0	–54 30 51	0.2952	8	5.816	21.5	13.727	16.5	13.866	6.2		<i>E</i>

name (1)	alt.name (2)	R.A. (3)	Decl. (4)	$z$ (5)	$N_{gal}$ (6)	$F_x$ (7)	Error (8)	$L_x$ (9)	$R_{ap}$ (10)	$L_x^*$ (11)	$N_H$ (12)	$Cm$ (13)	Ref. (14)
RXCJ0521.4 – 4049	A3336	05 21 29.6	–40 49 29	0.0756	2	4.899	19.4	0.667	15.0	0.681	3.3		17, 69
RXCJ0525.5 – 3135	A3341	05 25 32.8	–31 35 44	0.0380	64	11.350	7.3	0.375	16.5	0.403	1.8		2
RXCJ0525.8 – 4715	A3343	05 25 51.6	–47 15 02	0.1913	5	3.814	11.1	3.594	7.5	3.865	4.0		<i>E</i>
RXCJ0528.2 – 2942		05 28 15.4	–29 42 57	0.1582	2	3.864	37.6	2.458	12.0	2.483	1.8	<i>B</i>	<i>E</i>
RXCJ0528.9 – 3927	RBS0653	05 28 56.3	–39 27 46	0.2839	4	5.888	8.6	12.856	11.0	13.118	2.1		<i>E</i>
RXCJ0530.6 – 2226	A0543	05 30 38.4	–22 26 54	0.1706	11	5.828	11.2	4.288	14.0	4.331	2.6		<i>E</i> , 1
RXCJ0532.3 – 1131	A0545	05 32 23.1	–11 31 50	0.1540	2	8.490	8.7	5.047	7.5	5.671	11.2		1
RXCJ0532.9 – 3701		05 32 55.5	–37 01 28	0.2708	9	3.302	11.7	6.525	7.0	6.941	2.7		<i>E</i>
RXCJ0533.3 – 3619	S0535	05 33 18.5	–36 19 32	0.0479	4	3.734	11.9	0.199	13.0	0.209	2.9		<i>E</i>
RXCJ0538.2 – 2037	A3358	05 38 16.3	–20 37 23	0.0915	0	4.601	10.4	0.927	6.5	1.066	4.0		106
RXCJ0540.1 – 4050	S0540	05 40 06.3	–40 50 32	0.0358	1	14.881	5.2	0.438	15.5	0.481	3.5		5, 9
RXCJ0540.1 – 4322	A3360	05 40 10.0	–43 22 56	0.0850	36	4.759	9.6	0.830	11.0	0.874	3.8	<i>B</i>	38, 140, 141
RXCJ0542.1 – 2607	CID36 <sup>b</sup>	05 42 09.3	–26 07 25	0.0390	4	7.375	8.9	0.257	18.0	0.268	1.9	<i>P</i>	<i>E</i> , 120
RXCJ0543.4 – 4430		05 43 24.4	–44 30 19	0.1637	3	4.174	9.4	2.816	12.0	2.873	4.6		<i>E</i>
RXCJ0545.4 – 2556	A0548W	05 45 27.2	–25 56 20	0.0424	155	2.440	13.5	0.102	9.5	0.111	1.8	<i>P</i>	2, 72
RXCJ0545.5 – 4756	A3363	05 45 30.6	–47 56 26	0.1254	2	4.522	9.4	1.762	10.0	1.855	6.2	<i>B</i>	<i>E</i>
RXCJ0547.6 – 3152	A3364	05 47 38.2	–31 52 31	0.1483	10	8.526	7.5	4.667	17.5	4.667	2.0		<i>E</i>
RXCJ0547.7 – 4723	S0547	05 47 45.6	–47 23 24	0.0515	2	2.876	29.6	0.178	15.0	0.182	6.5		<i>E</i>
RXCJ0548.6 – 2527	A0548E	05 48 39.5	–25 27 30	0.0420	237	14.109	6.2	0.573	21.0	0.597	1.9	<i>PL</i>	3
RXCJ0548.8 – 2154		05 48 50.4	–21 54 43	0.0928	9	3.977	12.3	0.825	11.5	0.859	3.0		<i>E</i> , 3
RXCJ0552.8 – 2103	A0550	05 52 52.4	–21 03 25	0.0989	25	10.319	6.8	2.429	13.5	2.557	4.3		<i>E</i>
RXCJ0557.2 – 3727	S0555	05 57 13.2	–37 27 58	0.0442	4	7.141	10.9	0.322	17.5	0.335	4.0		<i>E</i>
RXCJ0600.8 – 5835	S0560	06 00 48.3	–58 35 14	0.0369	2	2.600	7.6	0.082	12.5	0.086	4.6		<i>E</i>
RXCJ0601.7 – 3959	A3376	06 01 45.7	–39 59 34	0.0468	32	20.492	4.8	1.036	21.5	1.079	5.0	<i>L</i>	72
RXCJ0605.8 – 3518	A3378	06 05 52.8	–35 18 02	0.1392	2	9.393	6.2	4.478	12.5	4.665	4.3		<i>E</i>
RXCJ0607.0 – 4928	A3380	06 07 01.4	–49 28 60	0.0553	3	3.592	14.4	0.258	14.0	0.266	4.6	<i>B</i>	<i>E</i>
RXCJ0616.5 – 3948	S0579	06 16 31.4	–39 48 01	0.1520	7	5.180	9.7	3.004	11.0	3.097	8.2		<i>E</i>
RXCJ0616.8 – 4748		06 16 53.6	–47 48 18	0.1164	1	4.813	9.8	1.597	14.0	1.613	4.8		<i>E</i>
RXCJ0621.7 – 5242		06 21 43.6	–52 42 11	0.0511	2	5.058	8.8	0.308	14.0	0.324	5.2		70, 71
RXCJ0624.6 – 3720	A3390	06 24 36.7	–37 20 09	0.0333	15	5.608	11.3	0.142	17.5	0.148	7.1	<i>D</i>	146
RXCJ0626.3 – 5341	A3391	06 26 22.8	–53 41 44	0.0514	85	19.583	3.8	1.198	19.0	1.261	5.4		1
RXCJ0627.1 – 3529	A3392	06 27 08.2	–35 29 20	0.0554	9	9.969	6.3	0.715	9.0	0.841	7.1		146
RXCJ0627.2 – 5428	A3395	06 27 14.4	–54 28 12	0.0506	159	23.679	3.2	1.403	18.0	1.509	8.5	<i>PL</i>	1
RXCJ0628.8 – 4143	A3396	06 28 49.8	–41 43 42	0.1759	10	5.743	9.2	4.521	12.0	4.613	6.3		<i>E</i>
RXCJ0631.3 – 5610		06 31 20.7	–56 10 20	0.0540	3	7.695	9.0	0.525	20.0	0.536	7.9	<i>L</i>	<i>E</i>
RXCJ0637.3 – 4828	A3399	06 37 18.9	–48 28 42	0.2026	11	3.400	10.2	3.641	6.5	3.958	6.9		<i>E</i>
RXCJ0638.7 – 5358	S0592	06 38 46.5	–53 58 18	0.2266	11	7.531	8.1	10.085	9.5	10.616	6.6		<i>E</i>
RXCJ0645.4 – 5413	A3404	06 45 29.3	–54 13 08	0.1644	2	10.597	7.9	7.139	13.0	7.360	6.6		<i>E</i>
RXCJ0658.5 – 5556	1ES0657 <sup>h</sup>	06 58 31.1	–55 56 49	0.2965	78	9.079	7.9	21.646	9.0	23.028	6.3		<i>E</i> , 73, 79
RXCJ0712.0 – 6030	AM0711 <sup>i</sup>	07 12 05.4	–60 30 06	0.0322	2	3.515	17.7	0.083	15.0	0.087	9.7		<i>E</i>
RXCJ0738.1 – 7506		07 38 09.0	–75 06 24	0.1110	3	3.083	15.9	0.938	8.5	0.998	17.4		<i>E</i>
RXCJ0821.8 + 0112	A0653	08 21 51.7	+01 12 42	0.0822	6	4.142	19.2	0.673	12.0	0.701	4.2	<i>B</i>	<i>E</i>
RXCJ0909.1 – 0939	A0754	09 09 08.4	–09 39 58	0.0542	92	57.001	3.3	3.879	19.0	4.310	4.6		146
RXCJ0910.6 – 1034	A0761	09 10 36.3	–10 34 52	0.0916	2	5.161	11.5	1.042	7.5	1.171	4.6		53, 81
RXCJ0918.1 – 1205	A0780	09 18 06.5	–12 05 36	0.0539	4	39.461	9.1	2.659	15.0	3.022	4.9	<i>BX</i>	1
RXCJ0937.9 – 2020	S0617	09 37 59.7	–20 20 45	0.0344	11	3.592	11.5	0.098	12.0	0.105	4.0		25
RXCJ0944.1 – 2116		09 44 10.3	–21 16 40	0.0077	1	2.480	43.5	0.003	11.5	0.004	4.4		<i>E</i> , 12, 84
RXCJ0944.6 – 2633		09 44 36.6	–26 33 56	0.1421	3	6.032	10.0	3.019	6.0	3.510	6.0		<i>E</i>
RXCJ0945.4 – 0839	A0868	09 45 24.4	–08 39 15	0.1535	2	4.726	10.8	2.814	8.5	2.994	4.2		1, 56
RXCJ0948.6 – 8327		09 48 39.4	–83 27 56	0.1982	1	3.025	25.9	3.085	7.5	3.282	9.2	<i>D</i>	<i>E</i>
RXCJ0953.2 – 1558		09 53 12.1	–15 58 52	0.0302	2	3.675	13.9	0.077	15.0	0.081	5.3		<i>E</i>
RXCJ0956.4 – 1004	A0901	09 56 26.4	–10 04 12	0.1634	9	9.115	9.6	6.077	17.0	6.077	5.1	<i>D</i>	<i>E</i>
RXCJ0958.3 – 1103	A0907	09 58 22.1	–11 03 35	0.1669	2	7.833	8.3	5.472	8.5	5.948	5.1		<i>E</i>
RXCJ1013.5 – 1350		10 13 36.0	–13 50 33	0.1517	5	3.776	14.6	2.191	6.5	2.434	7.6		<i>H</i>
RXCJ1013.6 – 0054	A0957	10 13 40.3	–00 54 52	0.0445	48	9.014	12.8	0.412	16.5	0.434	3.8		3, 41, 55, 96
RXCJ1013.7 – 0006	A0954	10 13 44.8	–00 06 31	0.0927	19	3.393	14.9	0.703	8.0	0.764	3.8		55, 119
RXCJ1017.3 – 1040	A0970	10 17 23.4	–10 40 39	0.0586	51	11.231	8.8	0.905	12.5	0.995	5.1		85
RXCJ1020.4 – 0631	A0978	10 20 28.8	–06 31 11	0.0540	63	3.704	13.2	0.253	11.0	0.269	4.7		2
RXCJ1023.8 – 2715	A3444	10 23 50.8	–27 15 31	0.2542	7	7.055	9.7	12.109	6.0	13.760	5.6		<i>H</i>
RXCJ1027.9 – 0647	A1023	10 27 59.6	–06 47 46	0.1176	6	3.146	15.6	1.075	6.0	1.208	4.5	<i>X*</i>	<i>H</i>

name (1)	alt.name (2)	<i>R.A.</i> (3)	<i>Decl.</i> (4)	<i>z</i> (5)	<i>N<sub>gal</sub></i> (6)	<i>F<sub>x</sub></i> (7)	<i>Error</i> (8)	<i>L<sub>x</sub></i> (9)	<i>R<sub>ap</sub></i> (10)	<i>L<sub>x</sub><sup>*</sup></i> (11)	<i>N<sub>H</sub></i> (12)	<i>C<sub>m</sub></i> (13)	<i>Ref.</i> (14)
RXCJ1036.6 – 2731	A1060	10 36 41.8	–27 31 28	0.0126	154	84.353	6.5	0.297	35.5	0.334	4.9	<i>L</i>	146
RXCJ1038.4 – 2454		10 38 24.1	–24 54 10	0.1230	10	4.134	13.5	1.545	8.5	1.661	5.5	<i>H</i>	
RXCJ1039.7 – 0841	A1069	10 39 44.5	–08 41 01	0.0650	35	6.444	15.2	0.639	13.0	0.673	3.9		2
RXCJ1041.5 – 1123		10 41 34.2	–11 23 19	0.0839	7	3.178	15.3	0.544	10.0	0.573	4.1	<i>H</i>	
RXCJ1044.5 – 0704	A1084	10 44 33.0	–07 04 22	0.1342	6	9.451	12.2	4.213	7.0	4.899	3.4	<i>H</i>	
RXCJ1050.4 – 1250	USGCS152 <sup>j</sup>	10 50 25.5	–12 50 47	0.0155	6	10.929	6.8	0.059	13.0	0.072	5.0		<i>E</i> , 20, 31
RXCJ1050.5 – 0236	A1111	10 50 35.5	–02 36 00	0.1651	9	3.636	15.0	2.512	7.0	2.730	4.0	<i>BX</i>	<i>H</i>
RXCJ1050.6 – 2405		10 50 36.3	–24 05 46	0.2037	1	3.601	18.4	3.904	8.5	4.067	5.9	<i>X*</i>	<i>E</i>
RXCJ1058.1 + 0135	A1139	10 58 10.4	+01 35 11	0.0398	27	2.379	20.0	0.087	15.0	0.089	4.0	<i>B</i>	146
RXCJ1101.2 – 2243	A1146	11 01 16.8	–22 43 41	0.1416	58	3.464	15.4	1.740	7.0	1.891	6.2		1, 86
RXCJ1107.3 – 2300	S0651	11 07 19.0	–23 00 08	0.0639	2	4.570	16.2	0.441	15.0	0.450	5.2	<i>H</i>	
RXCJ1114.1 – 3811	MS1111.8 <sup>k</sup>	11 14 12.0	–38 11 21	0.1306	9	6.979	10.9	2.942	12.0	3.065	9.9	<i>E</i>	
RXCJ1115.8 + 0129		11 15 54.0	+01 29 44	0.3499	3	3.848	22.2	13.172	9.0	13.579	4.4	<i>B</i>	<i>E</i>
RXCJ1130.3 – 1434	A1285	11 30 19.5	–14 34 59	0.1068	8	9.929	13.1	2.754	14.5	2.839	4.1	<i>H</i>	
RXCJ1131.9 – 1955	A1300	11 31 56.3	–19 55 37	0.3075	60	5.117	14.7	13.270	8.5	13.968	4.5		87, 88
RXCJ1135.2 – 1331	A1317	11 35 17.2	–13 31 08	0.0722	6	4.046	17.6	0.505	11.0	0.532	3.8		19, 89
RXCJ1139.4 – 3327		11 39 27.3	–33 27 14	0.1076	5	4.313	55.2	1.220	7.5	1.341	6.9	<i>H</i>	
RXCJ1141.4 – 1216	A1348	11 41 24.3	–12 16 20	0.1195	6	5.344	12.3	1.877	7.0	2.109	3.3	<i>X</i>	<i>H</i> , 16
RXCJ1145.3 – 3425	A3490	11 45 19.1	–34 25 43	0.0697	7	6.414	15.6	0.737	9.0	0.828	6.4	<i>H</i>	
RXCJ1149.7 – 1219	A1391	11 49 47.8	–12 19 04	0.1557	6	4.792	15.2	2.930	11.0	3.021	3.1	<i>X</i>	19, 31
RXCJ1151.6 – 1619		11 51 38.1	–16 19 14	0.0722	4	5.182	12.3	0.641	7.0	0.745	3.5	<i>H</i>	
RXCJ1200.0 – 3124	A3497	12 00 05.0	–31 24 21	0.0685	2	6.467	32.4	0.716	12.5	0.762	5.7	<i>H</i>	
RXCJ1202.9 – 0650	A1448	12 02 54.3	–06 50 07	0.1268	6	3.890	14.1	1.552	12.0	1.584	3.0		16, 31, 80
RXCJ1203.2 – 2131	A1451	12 03 17.0	–21 31 22	0.1992	16	6.271	21.4	6.408	5.0	7.629	4.5	<i>H</i>	
RXCJ1204.4 + 0154	MKW4	12 04 25.2	+01 54 02	0.0199	25	17.188	6.0	0.153	17.0	0.176	1.9		64, 94, 95, 97
RXCJ1206.2 – 0848		12 06 12.5	–08 48 22	0.4414	1	3.231	15.8	18.325	5.0	20.590	4.2	<i>E</i>	
RXCJ1212.3 – 1816		12 12 18.9	–18 16 43	0.2690	2	3.121	45.6	6.073	10.0	6.197	4.5	<i>X</i>	<i>E</i>
RXCJ1215.4 – 3900		12 15 29.0	–39 00 55	0.1190	6	5.534	35.5	1.916	10.5	2.017	6.3	<i>H</i>	
RXCJ1219.3 – 1315	A1520	12 19 19.8	–13 15 36	0.0688	5	4.081	35.0	0.460	2.5	0.821	4.0	<i>E</i>	
RXCJ1234.2 – 3856		12 34 17.0	–38 56 34	0.2373	2	3.995	14.0	5.979	4.0	7.291	6.2	<i>X*</i>	<i>E</i>
RXCJ1236.7 – 3354	S0700	12 36 44.7	–33 54 10	0.0796	4	4.932	19.8	0.749	8.5	0.832	5.6	<i>H</i>	
RXCJ1236.7 – 3531	S0701	12 36 46.5	–35 31 58	0.0736	2	3.913	16.4	0.508	8.5	0.558	5.3	<i>H</i>	
RXCJ1244.6 – 1159	A1606	12 44 38.0	–11 59 07	0.0963	9	6.344	13.1	1.416	10.5	1.506	3.7		31
RXCJ1247.7 – 0247	A1612	12 47 43.2	–02 47 32	0.1797	2	3.111	34.0	2.595	11.5	2.621	1.8	<i>E</i>	
RXCJ1248.7 – 4118	A3526	12 48 47.9	–41 18 28	0.0114	287	250.983	2.4	0.721	80.0	0.751	8.2	<i>L</i>	158
RXCJ1252.5 – 3116		12 52 34.1	–31 16 04	0.0535	3	12.910	7.8	0.861	9.5	1.013	5.5	<i>H</i>	
RXCJ1253.0 – 0912	HCG62	12 53 05.5	–09 12 01	0.0146	45	6.538	13.2	0.031	13.0	0.037	2.9		48
RXCJ1253.2 – 1522	A1631	12 53 14.4	–15 22 48	0.0462	71	6.720	14.9	0.332	18.5	0.342	4.0		1, 148
RXCJ1253.6 – 3931		12 53 40.9	–39 31 55	0.1794	1	11.009	8.3	8.971	6.0	10.680	7.9	<i>X*</i>	<i>E</i>
RXCJ1254.0 – 0642	A1634	12 54 02.7	–06 42 04	0.1962	2	4.049	22.5	4.016	12.5	4.057	2.5	<i>B</i>	<i>E</i>
RXCJ1254.3 – 2901	A3528N	12 54 23.5	–29 01 22	0.0542	69	8.801	20.0	0.603	8.0	0.727	6.1	<i>PB</i>	2
RXCJ1254.6 – 2913	A3528S	12 54 41.4	–29 13 24	0.0544	52	15.402	16.0	1.064	12.0	1.196	6.1	<i>PB</i>	<i>H</i> , 3, 64, 75, 98
RXCJ1254.7 – 1526		12 54 46.9	–15 26 40	0.1506	14	3.737	18.9	2.134	10.5	2.200	4.0	<i>H</i>	
RXCJ1255.5 – 3019	A3530	12 55 34.5	–30 19 50	0.0541	46	10.314	10.4	0.704	16.5	0.741	6.0	<i>B</i>	75, 77, 76, 98
RXCJ1255.7 – 1239		12 55 42.1	–12 39 18	0.0585	13	2.989	22.2	0.241	10.5	0.256	3.6		16, 31, 99
RXCJ1256.9 – 3119		12 56 59.8	–31 19 19	0.0561	16	5.378	16.0	0.397	12.5	0.422	6.0		12, 75
RXCJ1257.1 – 1724	A1644	12 57 09.8	–17 24 01	0.0473	92	37.967	10.0	1.952	22.0	2.077	5.3	<i>L</i>	1
RXCJ1257.1 – 1339		12 57 10.1	–13 39 20	0.0151	2	2.302	18.0	0.012	6.5	0.016	3.5		20
RXCJ1257.2 – 3022	A3532	12 57 16.9	–30 22 37	0.0554	44	18.733	24.0	1.340	15.5	1.457	6.0	<i>B</i>	1, 104
RXCJ1258.6 – 0145	A1650	12 58 41.1	–01 45 25	0.0845	2	20.909	6.1	3.563	14.0	3.873	1.5		1
RXCJ1258.8 – 2640	A1648	12 58 49.8	–26 40 03	0.0767	2	5.119	31.2	0.719	8.5	0.799	6.9	<i>H</i>	
RXCJ1259.3 – 0411	A1651	12 59 21.5	–04 11 41	0.0845	34	23.207	6.0	3.946	14.0	4.289	1.7		78, 105
RXCJ1301.6 – 0650		13 01 36.3	–06 50 00	0.0898	4	4.008	76.4	0.776	14.0	0.792	2.6		31
RXCJ1302.8 – 0230	A1663	13 02 50.7	–02 30 22	0.0847	3	4.460	21.9	0.772	12.0	0.804	1.7		<i>E</i> , 19, 31
RXCJ1303.7 – 2415	A3541	13 03 44.0	–24 15 03	0.1288	8	8.656	12.5	3.541	7.5	4.024	9.2	<i>H</i>	
RXCJ1304.2 – 3030		13 04 16.7	–30 30 55	0.0117	8	8.280	13.6	0.025	20.0	0.028	6.2	<i>L</i>	5, 82, 83, 98
RXCJ1305.9 – 3739	S0721	13 05 54.5	–37 39 41	0.0497	25	8.181	23.9	0.470	16.0	0.495	5.6	<i>DB</i>	14
RXCJ1309.2 – 0136	MS1306.7 <sup>l</sup>	13 09 17.0	–01 36 45	0.0880	0	5.334	15.1	0.989	12.5	1.030	1.8		39
RXCJ1311.4 – 0120	A1689	13 11 30.0	–01 20 07	0.1832	66	15.332	8.0	13.088	10.5	14.073	1.8		1
RXCJ1314.2 – 0659	A1698	13 14 13.5	–06 59 36	0.1892	7	3.942	19.9	3.624	11.0	3.698	2.8	<i>E</i>	

name (1)	alt.name (2)	<i>R.A.</i> (3)	<i>Decl.</i> (4)	<i>z</i> (5)	<i>N<sub>gal</sub></i> (6)	<i>F<sub>x</sub></i> (7)	<i>Error</i> (8)	<i>L<sub>x</sub></i> (9)	<i>R<sub>ap</sub></i> (10)	<i>L<sub>x</sub><sup>*</sup></i> (11)	<i>N<sub>H</sub></i> (12)	<i>Cm</i> (13)	<i>Ref.</i> (14)
RXCJ1314.4 – 2515		13 14 28.0	–25 15 41	0.2439	9	6.794	16.5	10.615	11.5	10.943	6.7		<i>H</i>
RXCJ1315.3 – 1623	NGC5044	13 15 24.0	–16 23 23	0.0087	16	58.129	4.0	0.097	36.0	0.110	4.9	<i>L</i>	15, 20, 64, 74, 90, 91, 92, 93
RXCJ1317.1 – 3821		13 17 09.6	–38 21 42	0.2553	2	4.062	14.8	7.059	4.5	8.305	4.7		<i>E</i>
RXCJ1320.7 – 4102	S0727	13 20 42.7	–41 02 23	0.0495	7	4.906	17.8	0.280	13.0	0.298	7.3		<i>E</i>
RXCJ1325.1 – 2014	A1732	13 25 06.8	–20 14 11	0.1926	10	4.160	14.8	3.959	9.0	4.124	7.8		<i>H</i>
RXCJ1326.2 + 0013		13 26 17.8	+00 13 32	0.0826	16	5.548	11.7	0.911	9.0	1.001	1.8	<i>X</i>	<i>E</i> , 55, 96, 55, 96
RXCJ1326.9 – 2710	A1736	13 26 54.0	–27 10 60	0.0458	109	36.893	6.5	1.778	34.0	1.796	5.4	<i>L</i>	146
RXCJ1327.9 – 3130	A3558	13 27 57.5	–31 30 09	0.0480	341	58.526	3.9	3.096	18.0	3.518	3.6	<i>P</i>	1, 14, 44, 102, 141, 148
RXCJ1329.7 – 3136	A3558(B)	13 29 42.9	–31 36 09	0.0488	57	14.434	30.0	0.796	14.5	0.865	3.6	<i>PB</i>	3, 14, 44, 63, 101, 102
RXCJ1330.8 – 0152	A1750	13 30 49.9	–01 52 22	0.0852	46	13.211	11.6	2.291	24.0	2.291	2.5	<i>DL</i>	1, 41, 96
RXCJ1331.5 – 3148	A3558(C)	13 31 32.4	–31 48 55	0.0448	55	4.901	32.0	0.226	9.0	0.257	4.0	<i>PB</i>	<i>H</i> , 3, 14, 74, 76, 100, 101, 102
RXCJ1332.3 – 3308	A3560	13 32 22.6	–33 08 22	0.0487	29	14.129	9.3	0.775	15.5	0.833	3.9		<i>H</i> , 76, 87, 103, 108
RXCJ1332.9 – 2519		13 32 55.8	–25 19 26	0.1199	3	3.427	27.0	1.212	12.0	1.237	6.1	<i>X</i>	<i>E</i>
RXCJ1333.6 – 3139	A3562	13 33 36.3	–31 39 40	0.0490	114	24.485	6.6	1.357	17.0	1.475	3.9	<i>P</i>	1, 141
RXCJ1333.6 – 2317	A1757	13 33 42.0	–23 17 02	0.1264	4	6.442	15.0	2.540	12.0	2.646	7.1		<i>H</i>
RXCJ1336.6 – 3357	A3565	13 36 38.8	–33 57 30	0.0123	45	2.348	18.0	0.008	9.5	0.010	4.1		146
RXCJ1337.4 – 4120		13 37 28.1	–41 20 01	0.0519	2	4.813	16.3	0.303	8.5	0.344	6.3		<i>E</i>
RXCJ1342.0 + 0213	A1773	13 42 05.5	+02 13 39	0.0765	14	5.788	12.9	0.808	11.5	0.860	1.8		1, 10
RXCJ1346.2 – 1632		13 46 13.6	–16 32 42	0.0557	1	3.064	16.8	0.223	6.0	0.265	7.5		<i>E</i>
RXCJ1346.8 – 3752	A3570	13 46 52.5	–37 52 28	0.0377	8	5.527	33.8	0.180	14.0	0.191	4.4		4, 12, 113
RXCJ1347.2 – 3025	A3574W	13 47 12.3	–30 25 10	0.0145	5	2.479	50.6	0.012	10.0	0.014	4.4	<i>PX</i>	12, 64, 74, 103, 107, 112, 113
RXCJ1347.4 – 3250	A3571	13 47 28.4	–32 50 59	0.0391	84	115.471	10.0	3.996	36.0	4.206	3.9	<i>L</i>	146
RXCJ1347.5 – 1144		13 47 30.0	–11 44 56	0.4516	2	6.468	10.4	38.732	5.5	44.520	4.9		<i>E</i>
RXCJ1348.9 – 2526	A1791	13 48 55.8	–25 26 31	0.1269	8	3.842	28.8	1.536	11.0	1.584	5.8		<i>E</i>
RXCJ1349.3 – 3018	A3574E	13 49 19.3	–30 18 34	0.0160	55	7.549	25.0	0.043	20.0	0.047	4.4	<i>PX</i>	146
RXCJ1350.7 – 3343		13 50 43.9	–33 43 17	0.1142	1	4.021	17.3	1.280	7.0	1.422	4.8		<i>E</i>
RXCJ1352.2 – 0945	A1807	13 52 14.0	–09 45 33	0.2021	2	3.031	16.6	3.225	10.0	3.291	3.5		<i>E</i>
RXCJ1353.4 – 2753		13 53 29.3	–27 53 19	0.0468	3	4.993	20.8	0.253	10.0	0.281	4.7	<i>B</i>	<i>E</i>
RXCJ1401.6 – 1107	A1837	14 01 36.7	–11 07 28	0.0698	38	5.517	13.4	0.634	9.5	0.697	4.7		1
RXCJ1403.5 – 3359	S0753	14 03 35.9	–33 59 16	0.0132	12	8.081	14.4	0.032	17.0	0.036	5.6		5, 91, 98, 109, 114
RXCJ1407.4 – 2700	A3581	14 07 28.1	–27 00 55	0.0230	24	26.535	5.8	0.316	15.0	0.381	4.3		<i>E</i> , 146
RXCJ1408.1 – 0904	CAN40 <sup>b</sup>	14 08 07.0	–09 04 16	0.0354	4	4.781	13.9	0.137	11.5	0.151	3.7		<i>E</i> , 120
RXCJ1415.2 – 0030	A1882	14 15 14.2	–00 30 04	0.1403	20	4.217	20.0	2.063	15.5	2.063	3.2	<i>X</i>	55
RXCJ1416.8 – 1158		14 16 51.5	–11 58 34	0.0982	10	3.976	17.7	0.931	5.5	1.108	6.0	<i>X</i>	16, 31
RXCJ1421.9 – 2009		14 21 57.3	–20 09 36	0.1208	4	3.078	25.7	1.115	10.0	1.149	7.5		<i>H</i>
RXCJ1435.0 – 2821	A3605	14 35 00.6	–28 21 56	0.0689	2	4.358	50.3	0.491	17.5	0.496	6.4		<i>E</i>
RXCJ1436.8 – 0900		14 36 53.5	–09 00 13	0.0842	2	3.776	30.3	0.646	5.0	0.798	6.2		<i>E</i>
RXCJ1455.2 – 3325		14 55 13.9	–33 25 36	0.1158	1	3.815	16.7	1.252	6.0	1.423	7.1		<i>E</i>
RXCJ1456.3 – 0549	A1994	14 56 19.6	–05 49 39	0.2200	5	3.059	16.1	3.900	5.5	4.333	6.3		<i>E</i>
RXCJ1459.0 – 0843		14 59 03.5	–08 43 30	0.1043	3	3.837	16.0	1.022	8.5	1.099	7.1		<i>E</i>
RXCJ1459.4 – 1811	S0780	14 59 29.3	–18 11 13	0.2357	2	10.187	18.0	14.910	11.5	15.531	7.8		<i>E</i>
RXCJ1501.1 + 0141	NGC5813	15 01 11.9	+01 41 53	0.0050	6	12.324	6.3	0.007	8.5	0.014	4.2		12, 15
RXCJ1504.1 – 0248		15 04 07.7	–02 48 18	0.2153	6	22.111	5.3	26.389	12.0	28.073	6.0	<i>X</i>	<i>E</i>
RXCJ1506.4 + 0136	NGC5846	15 06 29.7	+01 36 08	0.0066	8	8.028	13.8	0.008	13.0	0.011	4.2		48, 64, 123, 125, 126
RXCJ1511.5 + 0145		15 11 33.5	+01 45 51	0.0384	2	2.459	58.5	0.084	17.0	0.085	4.0	<i>B</i>	<i>E</i> , 123
RXCJ1512.8 – 2254		15 12 12.6	–22 54 59	0.3152	1	3.452	17.3	9.371	6.0	10.186	8.5		<i>E</i>
RXCJ1512.8 – 0128		15 12 51.0	–01 28 47	0.1223	2	3.354	18.5	1.238	5.5	1.423	5.2		<i>E</i>
RXCJ1514.9 – 1523		15 14 58.0	–15 23 10	0.2226	3	5.270	16.7	6.802	9.0	7.160	8.5		<i>E</i>
RXCJ1516.3 + 0005	A2050	15 16 19.2	+00 05 52	0.1181	17	4.956	13.8	1.697	7.5	1.886	4.6		<i>E</i> , 55
RXCJ1516.5 – 0056	A2051	15 16 34.0	–00 56 56	0.1198	7	3.918	61.7	1.383	13.0	1.397	5.5		55
RXCJ1524.2 – 3154		15 24 12.8	–31 54 14	0.1028	6	11.346	15.4	2.891	11.0	3.142	8.3		<i>E</i>
RXCJ1539.5 – 8335		15 39 33.9	–83 35 32	0.0728	2	16.844	8.5	2.102	9.0	2.502	8.5		<i>E</i>
RXCJ1540.1 – 0318	A2104	15 40 07.5	–03 18 29	0.1533	52	7.434	10.1	4.375	9.0	4.704	9.2		128
RXCJ1548.7 – 0259	A2128	15 48 45.9	–02 59 47	0.1010	2	3.943	16.6	0.980	11.0	1.021	8.4	<i>B</i>	111, 116
RXCJ1558.3 – 1410		15 58 23.2	–14 10 04	0.0970	1	14.131	7.5	3.181	10.0	3.574	11.1	<i>B</i>	117
RXCJ1615.7 – 0608	A2163	16 15 46.9	–06 08 45	0.2030	1	19.686	6.4	20.853	9.5	23.170	12.3		118
RXCJ1633.8 – 0738		16 33 53.9	–07 38 42	0.0974	10	3.445	15.0	0.793	11.0	0.818	11.8		<i>E</i>
RXCJ1655.9 – 0113		16 55 56.2	–01 13 45	0.0408	1	3.792	33.0	0.145	15.0	0.151	8.0		93
RXCJ1657.7 – 0149		16 57 45.4	–01 49 54	0.0313	3	4.194	16.0	0.094	17.5	0.097	8.8		<i>E</i>
RXCJ1705.1 – 8210	S0792	17 05 10.3	–82 10 26	0.0737	4	7.092	17.7	0.916	12.0	0.974	7.6		<i>E</i>

This catalogue is continued in Table 10 where also all the references for the reference codes in this table are given.

**Table 7.** X-ray properties of the REFLEX clusters

name	<i>RA</i> (2000)	<i>DEC</i> (2000)	count rate $s^{-1}$	$F_n$ $10^{-12} \text{erg}$ $s^{-1} \text{cm}^{-2}$	$L_x$ $10^{44}$ $\text{ergs}^{-1}$	$N_{ph}$	$P_{ext}$	$r_c$	$r_c(\text{min})$	<i>HR</i>	<i>HR<sub>err</sub></i>	$\Delta HR$ ( $\sigma$ )	$R_{ap}$ Mpc
(1)	(2)	(3)	(4)	(5)	(6)	(7)	(8)	(9)	(10)	(11)	(12)	(13)	(14)
RXCJ0003.1 – 0605	0.7991	–0.0860	0.218	4.473	6.395	76.3	3.8	1.5	1.0	0.7	0.1	0.06	1.664
RXCJ0003.2 – 3555	0.8006	–35.9271	0.400	7.762	0.421	56.8	7.5	1.5	0.5	0.5	0.2	0.70	0.575
RXCJ0003.8 + 0203	0.9607	+2.0634	0.205	4.192	0.855	74.2	3.3	1.0	0.5	0.8	0.1	1.18	0.877
RXCJ0006.0 – 3443	1.5126	–34.7241	0.301	5.853	1.875	68.0	5.4	1.5	1.0	0.2	0.1	–1.05	1.248
RXCJ0011.3 – 2851	2.8364	–28.8551	0.612	12.129	1.089	155.4	13.9	1.5	1.5	0.4	0.1	–1.53	0.896
RXCJ0013.6 – 1930	3.4094	–19.5021	0.306	6.089	1.285	95.8	6.1	1.5	1.5	0.5	0.1	–0.61	1.203
RXCJ0014.3 – 6604	3.5768	–66.0775	0.220	4.474	2.907	60.9	0.4	0.0	0.0	0.6	0.1	–0.80	1.240
RXCJ0014.3 – 3023	3.5783	–30.3834	0.250	4.929	12.787	30.5	1.3	0.5	0.0	0.2	0.2	–1.67	3.255
RXCJ0015.4 – 2350	3.8500	–23.8450	0.175	3.526	0.336	48.5	1.8	6.0	2.0	0.4	0.2	–1.36	0.854
RXCJ0017.5 – 3509	4.3904	–35.1650	0.166	3.241	0.729	58.8	6.7	3.0	2.0	0.3	0.2	–0.73	1.236

The complete table is given in electronic form at CDS and our home page.

## 6. Selection properties of the cluster sample

A number of tests in papers I through III demonstrate the quality of the catalogue, in particular the completeness and homogeneity. For example through the LogN-logS distribution, a  $V/V_{max}$ -test, and the photon number distribution, do not indicate a significant deficiency at faint fluxes or low source photon numbers. The sample shows a large scale density homogeneity at least out to  $z = 0.15$  with pronounced traces of large scale structure on scales smaller than the sample size (paper III). The two-point correlation function (paper II) shows a good overall isotropy (except for possibly small dynamical redshift distortion effects which are expected and currently investigated) and the number count distribution on large scales ( $\geq 50h^{-1}$  Mpc) is approximately Gaussian (paper IV). We do not see any significant bias in the cluster density as a function of Galactic latitude or longitude (papers II and III). Here we provide another test, showing the cluster density as a function of interstellar absorption. Fig. 4 shows the surface density of clusters averaged over  $0.5 \cdot 10^{20} \text{ cm}^{-2}$  column density intervals and compares it to the distribution of  $N_H$  over the sky. The density is almost constant within the formal Poissonian errors (which do not include fluctuations from large-scale structure and cosmic variance) up to the region where the statistics becomes too poor and the expectation value drops below one or two. Since the column density as well as the stellar density, which hampers the cluster identification, increases with decreasing  $|b|$ , we are also testing here the bias in the optical cluster identification due to crowding of the sky fields near the Galactic plane and find no major effect. These plots have to be compared with similar tests conducted with the optically identified clusters in the Abell catalogue (e.g. Ebeling et al. 1996).

Another mark of quality of the REFLEX cluster identification is the fact that the vast majority of the clusters, 79.5%, have been identified as extended sources. Fig. 5

**Table 8.** Statistics of the sky coverage as a function of the sensitivity. A graphical representation of this table can be found in Böhringer et al. 2001, Fig. 23

sensitivity limit $10^{-13} \text{erg s}^{-1} \text{cm}^{-2} \text{count}^{-1}$	fraction of the survey area
0.102	$8.6 \cdot 10^{-4}$
0.300	0.032
0.500	0.192
0.700	0.574
1.000	0.780
2.000	0.940
3.002	0.970
5.000	0.984

The complete table is given in electronic form at CDS and our home page.

shows the LogN-logS distribution of the subsample of clusters detected as significantly extended in the GCA.

To reproduce the observational results described here in theoretical modeling the precise selection function of the REFLEX survey has to be known. Two major factors modify the depth of our survey as a function of sky position: the RASS exposure time and the interstellar column density in the line-of-sight. We model the sensitivity function which depends on these two parameters in the following way: we calculate the flux limit reached per number of photons specified to be required for secure source detection. In this sense Table 8 gives the sky area in the REFLEX survey for a given flux limit for the detection of one photon. This sky coverage table is for example used in the calculation of the luminosity function in paper IV, where we assume conservatively that at least 30 photons are detected for the cluster. The flux limit as listed in the first column of Table 8 has therefore to be multiplied by 30 and we note for example that 78% of the survey area

**Table 9.** Sensitivity as a function of the sky position used to produce the sensitivity map shown in Böhringer et al. 2001, Fig.22. Also given are the sky distribution of the RASS 2 exposure (shown in Böhringer et al. 2001, Fig.2) and the interstellar column density distribution in the REFLEX area.

RA (J2000)	DEC (J2000)	exposure (sec)	$N_H$ $10^{20} * \text{cm}^{-2}$	sensitivity limit $10^{-13} \text{erg s}^{-1} \text{cm}^{-2}$ count $^{-1}$
0.0000	2.0000	401.09	3.300	0.514
1.0006	2.0000	360.85	3.000	0.567
2.0012	2.0000	250.08	3.000	0.818
3.0018	2.0000	332.16	3.040	0.616
4.0024	2.0000	398.57	3.070	0.514
5.0030	2.0000	404.37	3.150	0.508
6.0037	2.0000	442.88	3.150	0.464
7.0043	2.0000	662.26	3.040	0.309
8.0049	2.0000	464.21	2.730	0.438
9.0055	2.0000	291.09	2.660	0.696
10.0061	2.0000	323.05	2.320	0.622

The complete table is given in electronic form at CDS and our home page.

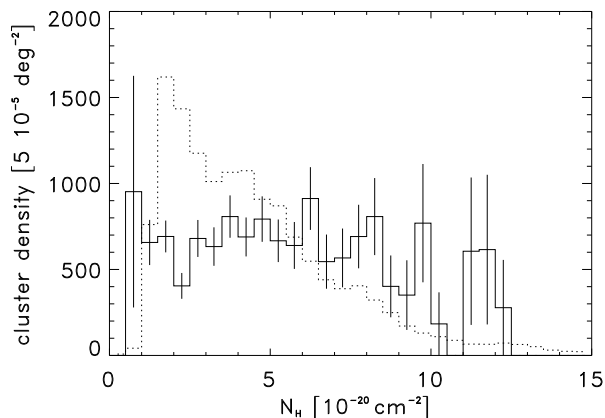


**Fig. 4.** Sky density of the REFLEX clusters as a function of the Galactic hydrogen column density (solid line) in units of  $\text{deg}^2$  multiplied by a factor of 20000. The dotted line gives the sky area distribution of  $N_H$  values in units of  $\text{deg}^2$  for  $0.5 \cdot 10^{20} \text{cm}^{-2}$  bins.

reaches the nominal flux limit of the REFLEX survey of  $3 \cdot 10^{-12} \text{erg s}^{-1} \text{cm}^{-2}$ . Note also, that this excludes some clusters in the catalogue with less than 30 source photon counts from the analysis. For the large-scale structure analysis in paper III we have included more clusters for a better three-dimensional coverage and relaxed the detection requirement to 10 source photons. In this case the REFLEX survey reaches the nominal flux limit in 97% of the survey area, which corresponds to a more simple survey window function in k-space for the determination of the density fluctuation power spectrum.

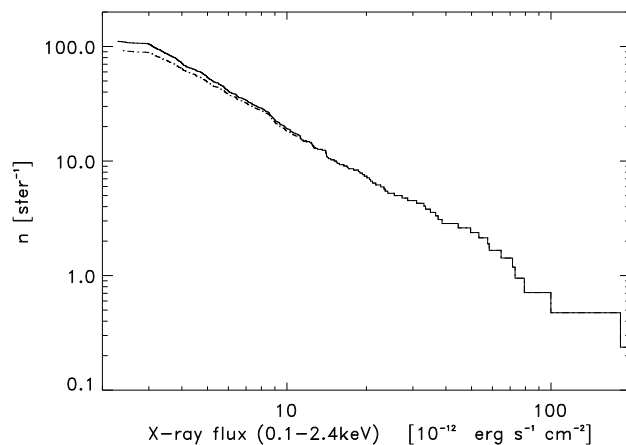


**Fig. 5.** LogN-LogS distribution of the REFLEX clusters. The upper curve shows all the clusters while the lower, dashed curve shows the 79.5% fraction of significantly extended sources as measured with the KS test for the survey point spread function.

For the large-scale structure modeling, e.g. for the construction of the comparison Poisson sample used in the evaluation of the two-point correlation function or the density distribution power spectrum, the sensitivity limit as a function of the sky position has to be known. This has been constructed from the exposure map of the RASS2 product and the 21 cm maps from Dickey & Lockman (1990) and Stark et al. (1992), and is given in a similar way in Table 9. In fact Table 8 is only a cumulative account of Table 9. The table gives the sensitivity distribution on a roughly one square degree grid. It lists also the exposure and interstellar column density distribution used in the calculation. For both tables only a few example lines are given in the print version of the paper, but the full tables (which in case of Table 9 consists of 13902 lines) are provided in the electronic version of the paper and on our home page given above.

## 7. Information on individual Objects

The REFLEX data base used for the cosmology work in the REFLEX papers up to number VIII is based on the catalogue version of 1999. As we have collected more information since, we went through a further critical inspection of all the catalogue entries prior to the release of this catalogue, in addition to the revision of redshifts as described above. A major route of approach was to carefully assess the nature of those objects for which the X-ray criteria left us with a not very satisfactory means of identification. Thus we inspected especially all those X-ray sources again which appeared point-like in the RASS. The fact that an X-ray source appears point-like at the resolution of the All-Sky Survey is not yet a criterion to reject a source. An illustrative example for this is the massive, and optically very impressive cluster RXCJ1206.2-0848 at redshift  $z = 0.4414$  which appears in the RASS as a point

**Table 10.** The REFLEX cluster catalogue - continued

name (1)	alt.name (2)	<i>R.A.</i> (3)	<i>Decl.</i> (4)	<i>z</i> (5)	<i>N<sub>gal</sub></i> (6)	<i>F<sub>x</sub></i> (7)	<i>Error</i> (8)	<i>L<sub>x</sub></i> (9)	<i>R<sub>ap</sub></i> (10)	<i>L<sub>x</sub><sup>*</sup></i> (11)	<i>N<sub>H</sub></i> (12)	<i>Cm</i> (13)	<i>Ref.</i> (14)
RXCJ1706.4 – 0132	Zw1703.8 <sup>m</sup>	17 06 26.6	–01 32 23	0.0912	4	6.081	19.5	1.209	9.5	1.314	10.2	<i>E</i>	
RXCJ1840.6 – 7709		18 40 37.2	–77 09 20	0.0194	1	10.295	10.4	0.087	10.0	0.112	8.1		34
RXCJ1847.3 – 6320	S0805	18 47 20.0	–63 20 13	0.0146	24	5.968	26.1	0.029	13.0	0.034	6.0		12
RXCJ1855.8 – 6654		18 55 53.2	–66 54 48	0.1797	2	3.444	25.2	2.856	8.5	3.006	6.1		<i>E</i>
RXCJ1912.6 – 7517	S0810	19 12 40.3	–75 17 30	0.0726	13	9.451	18.1	1.177	10.5	1.293	6.7	<i>B</i>	<i>E</i>
RXCJ1925.4 – 4256	A3638	19 25 29.6	–42 56 57	0.0774	1	6.550	21.5	0.938	10.0	1.020	6.6		<i>E, 1, 121</i>
RXCJ1926.9 – 5342		19 26 58.3	–53 42 11	0.0570	2	5.504	26.6	0.420	4.0	0.618	3.9		<i>E</i>
RXCJ1928.2 – 5055	A3639	19 28 14.0	–50 55 48	0.1496	10	3.675	19.7	2.069	6.5	2.299	5.3		133
RXCJ1931.6 – 3354		19 31 38.7	–33 54 47	0.0972	2	6.392	16.8	1.456	9.5	1.583	7.6		<i>E</i>
RXCJ1934.7 – 5053	S0821	19 34 47.3	–50 53 49	0.2371	2	4.040	21.1	6.035	9.0	6.286	5.5		<i>E</i>
RXCJ1938.3 – 4748		19 38 19.5	–47 48 16	0.2665	1	3.143	20.6	5.987	8.0	6.236	6.1		<i>E</i>
RXCJ1946.5 – 4256	S0827	19 46 34.3	–42 56 32	0.1128	4	3.219	20.8	1.006	9.0	1.059	5.9		<i>E</i>
RXCJ1947.3 – 7623		19 47 19.3	–76 23 32	0.2170	3	3.527	20.3	4.335	4.0	5.287	7.0		<i>E</i>
RXCJ1952.2 – 5503	A3651	19 52 16.5	–55 03 42	0.0600	79	7.498	17.0	0.635	12.5	0.683	4.9		2
RXCJ1953.0 – 5201	A3653	19 53 00.9	–52 01 51	0.1069	11	5.838	14.3	1.629	10.5	1.733	4.8		<i>E</i>
RXCJ1958.2 – 3011		19 58 14.8	–30 11 22	0.1171	4	11.271	9.5	3.753	12.0	3.993	8.4	<i>X*</i>	<i>E</i>
RXCJ1959.1 – 3454	A3654	19 59 10.7	–34 54 36	0.1728	12	3.103	22.2	2.373	5.5	2.666	7.5	<i>B</i>	<i>E</i>
RXCJ2003.5 – 2323		20 03 30.4	–23 23 05	0.3171	4	3.124	18.2	8.601	6.5	9.248	8.6		<i>E</i>
RXCJ2009.0 – 5421	S0849	20 09 04.0	–54 21 28	0.0516	2	3.140	20.1	0.196	7.0	0.228	5.4		<i>E</i>
RXCJ2009.9 – 4823	S0851	20 09 54.1	–48 23 35	0.0097	4	3.390	21.4	0.007	8.5	0.010	5.0		74, 135, 136
RXCJ2011.3 – 5725		20 11 23.1	–57 25 39	0.2786	5	3.153	23.0	6.649	6.0	7.227	3.3		<i>E</i>
RXCJ2012.0 – 4129	A3668	20 12 03.0	–41 29 30	0.1496	4	4.181	16.0	2.353	8.5	2.503	5.0		<i>E</i>
RXCJ2012.5 – 5649	A3667	20 12 30.5	–56 49 55	0.0556	162	70.892	5.3	5.081	26.0	5.405	4.6	<i>L</i>	2, 3, 138, 140, 141
RXCJ2014.2 – 8038	A3664	20 14 13.4	–80 38 30	0.1380	8	3.525	19.9	1.674	7.0	1.820	9.9	<i>P</i>	<i>E</i>
RXCJ2014.8 – 2430		20 14 49.7	–24 30 30	0.1612	2	14.040	13.4	9.157	6.5	11.033	7.4		<i>E</i>
RXCJ2016.2 – 8047	A3666	20 16 14.0	–80 47 57	0.1309	2	3.184	20.3	1.362	6.5	1.497	9.9	<i>P</i>	<i>E</i>
RXCJ2018.4 – 4102	IC4992	20 18 25.6	–41 02 48	0.0192	2	3.871	16.6	0.032	9.5	0.039	4.7		5, 15
RXCJ2018.7 – 5242	S0861	20 18 45.7	–52 42 22	0.0505	13	11.735	9.6	0.694	14.0	0.754	4.7		<i>E</i>
RXCJ2020.8 – 3002	A3674	20 20 49.9	–30 02 01	0.2073	5	3.132	28.4	3.531	9.5	3.640	6.7		<i>E</i>
RXCJ2021.9 – 5256	A3675	20 21 54.7	–52 56 52	0.1383	3	3.359	16.5	1.603	11.5	1.636	4.3		<i>E</i>
RXCJ2023.0 – 2056	S0868	20 23 01.6	–20 56 55	0.0564	2	5.497	17.8	0.411	8.5	0.467	5.6		<i>E</i>
RXCJ2023.4 – 5535		20 23 24.5	–55 35 32	0.2320	3	3.351	18.6	4.788	6.5	5.204	5.2		<i>E</i>
RXCJ2030.7 – 3532		20 30 47.9	–35 32 40	0.1398	2	3.220	20.4	1.573	7.0	1.710	3.9		<i>E</i>
RXCJ2031.8 – 4037		20 31 51.5	–40 37 14	0.3416	2	3.310	21.8	10.715	5.0	12.039	3.9		<i>E</i>
RXCJ2032.1 – 5627	A3685	20 32 08.8	–56 27 09	0.1380	5	3.668	17.7	1.742	7.5	1.893	5.1		<i>E</i>
RXCJ2034.3 – 3429	A3693	20 34 19.5	–34 29 15	0.1240	9	4.385	22.0	1.668	10.0	1.756	3.9		<i>E, 3</i>
RXCJ2034.7 – 3404	A3694	20 34 42.1	–34 04 26	0.0936	2	8.730	14.2	1.835	10.5	1.995	3.9		40
RXCJ2034.7 – 3548	A3695	20 34 47.9	–35 48 48	0.0894	81	16.940	12.4	3.206	28.0	3.238	3.6	<i>L</i>	2, 140, 141
RXCJ2034.9 – 2143		20 34 55.8	–21 43 02	0.1947	2	3.310	42.3	3.244	11.0	3.277	4.1		<i>E</i>
RXCJ2035.7 – 2513	A3698	20 35 44.3	–25 13 04	0.0200	7	2.388	28.1	0.022	12.5	0.024	4.5	<i>X</i>	146
RXCJ2043.2 – 2144		20 43 12.6	–21 44 06	0.2041	3	3.628	16.4	3.930	5.5	4.416	4.2		<i>E</i>
RXCJ2043.2 – 2629	S0894	20 43 14.4	–26 29 24	0.0408	1	4.647	31.6	0.178	13.0	0.189	5.3		9, 28
RXCJ2048.1 – 1750	A2328	20 48 10.6	–17 50 38	0.1475	3	5.930	15.2	3.215	10.5	3.349	4.8		<i>E</i>
RXCJ2055.8 – 5455	A3718	20 55 51.5	–54 55 12	0.1390	8	4.087	44.9	1.960	4.0	2.481	4.5		<i>E</i>
RXCJ2058.2 – 0745	A2331	20 58 15.2	–07 45 41	0.0793	16	3.486	19.3	0.530	13.5	0.541	5.3		10
RXCJ2101.4 – 4100	S0915	21 01 28.1	–41 00 06	0.1694	4	3.112	16.2	2.278	6.0	2.531	3.5		<i>E</i>
RXCJ2101.5 – 1317		21 01 34.7	–13 17 31	0.0282	2	4.250	20.7	0.077	10.0	0.089	4.1		<i>E</i>
RXCJ2101.8 – 2802	A3733	21 01 48.7	–28 02 06	0.0382	91	8.842	11.5	0.294	20.0	0.303	6.9	<i>L</i>	13, 14, 146
RXCJ2102.1 – 2431	RBS1712 <sup>c</sup>	21 02 09.9	–24 31 53	0.1880	1	5.238	10.9	4.718	8.0	5.073	5.3		19, 27, 169
RXCJ2103.4 – 4319	A3736	21 03 26.0	–43 19 46	0.0487	4	4.599	50.1	0.253	15.0	0.264	3.2		132
RXCJ2104.3 – 4120	A3739	21 04 20.1	–41 20 58	0.1651	3	5.988	15.3	4.093	13.5	4.134	3.6		<i>E</i>
RXCJ2104.9 – 5149		21 04 54.7	–51 49 35	0.0491	1	8.926	12.3	0.500	11.0	0.562	3.1		5, 145
RXCJ2104.9 – 8243	A3728	21 04 58.7	–82 43 22	0.0969	4	2.997	20.1	0.682	6.0	0.775	8.2		<i>E</i>
RXCJ2106.0 – 3846	A3740	21 06 04.3	–38 46 21	0.1521	2	4.360	14.1	2.545	9.0	2.679	3.8	<i>DB</i>	182
RXCJ2107.2 – 2526	A3744	21 07 12.3	–25 26 17	0.0381	71	4.854	11.8	0.162	10.5	0.180	5.5		2
RXCJ2111.6 – 2308	AM2108 <sup>n</sup>	21 11 39.9	–23 08 59	0.0333	15	2.472	20.7	0.063	13.5	0.066	4.4		17
RXCJ2116.8 – 5929	S0927	21 16 48.5	–59 29 53	0.0602	0	4.534	17.3	0.388	10.5	0.417	4.0		9
RXCJ2124.3 – 7446		21 24 22.8	–74 46 25	0.0586	2	5.009	19.8	0.405	8.0	0.466	5.8		<i>E</i>
RXCJ2125.2 – 0657		21 25 12.4	–06 57 56	0.1153	2	3.285	36.7	1.076	11.0	1.109	5.9		<i>E</i>
RXCJ2125.9 – 3443	A3764	21 25 55.0	–34 43 28	0.0757	38	2.931	53.7	0.404	14.0	0.408	4.9		140, 141



name (1)	alt.name (2)	<i>R.A.</i> (3)	<i>Decl.</i> (4)	<i>z</i> (5)	<i>N<sub>gal</sub></i> (6)	<i>F<sub>x</sub></i> (7)	<i>Error</i> (8)	<i>L<sub>x</sub></i> (9)	<i>R<sub>ap</sub></i> (10)	<i>L<sub>x</sub><sup>*</sup></i> (11)	<i>N<sub>H</sub></i> (12)	<i>Cm</i> (13)	<i>Ref.</i> (14)
RXCJ2127.1 – 1209	A2345	21 27 11.0	–12 09 33	0.1760	1	5.271	13.6	4.154	11.0	4.282	4.8		81
RXCJ2129.8 – 5048	A3771	21 29 51.0	–50 48 04	0.0796	2	5.051	66.2	0.767	11.5	0.807	2.2		181, 121
RXCJ2133.4 – 7156		21 33 24.3	–71 56 09	0.0559	2	2.998	23.1	0.220	8.5	0.242	2.0		<i>E</i>
RXCJ2134.2 – 1328	A2351	21 34 16.5	–13 28 48	0.0897	2	8.918	13.8	1.712	7.5	1.991	5.2		<i>B E</i>
RXCJ2135.2 + 0125	A2355	21 35 17.2	+01 25 54	0.1244	2	4.493	26.0	1.721	13.5	1.738	4.8		1
RXCJ2139.8 – 2228	S0963	21 39 51.8	–22 28 24	0.0328	16	3.154	20.8	0.078	10.0	0.087	3.4		<i>B E</i> , 25
RXCJ2143.9 – 5637	APMCC699 <sup>f</sup>	21 43 58.3	–56 37 35	0.0824	2	10.658	10.2	1.733	13.0	1.844	3.4		<i>E</i>
RXCJ2145.9 – 1006	A2377	21 45 54.8	–10 06 16	0.0808	1	7.190	41.6	1.124	12.5	1.183	4.0		<i>P</i> 1, 1
RXCJ2146.3 – 5717	A3806	21 46 20.9	–57 17 19	0.0760	99	7.072	34.6	0.974	17.5	0.994	2.6		<i>B</i> 2
RXCJ2146.9 – 4354	A3809	21 46 57.8	–43 54 36	0.0620	94	9.190	11.0	0.833	14.0	0.886	1.8		<i>B</i> 2
RXCJ2147.0 – 1019		21 47 00.5	–10 19 04	0.0780	2	2.959	18.1	0.434	5.5	0.517	4.0		<i>PX E</i>
RXCJ2147.9 – 4600	S0974	21 47 55.5	–46 00 19	0.0593	4	6.906	11.9	0.573	13.5	0.603	2.7		24, 30, 32
RXCJ2149.1 – 3041	A3814	21 49 07.4	–30 41 55	0.1184	19	6.182	12.9	2.117	9.5	2.276	2.3		33, 96
RXCJ2151.3 – 5521		21 51 22.7	–55 21 12	0.0385	31	3.137	19.4	0.107	13.0	0.113	2.9		<i>B E</i> , 129
RXCJ2151.8 – 1543	A2382	21 51 52.9	–15 43 02	0.0614	4	4.028	17.8	0.359	9.0	0.395	4.0		27, 81
RXCJ2152.2 – 1942	A2384(B)	21 52 14.2	–19 42 20	0.0963	4	4.059	30.0	0.912	6.0	1.060	3.0		<i>PB E</i>
RXCJ2152.4 – 1933	A2384(A)	21 52 24.0	–19 33 54	0.0943	1	7.717	20.0	1.648	8.5	1.852	3.0		<i>PB</i> 1
RXCJ2154.1 – 5751	A3822	21 54 09.2	–57 51 19	0.0760	84	15.994	6.8	2.185	16.0	2.300	2.1		2
RXCJ2154.2 – 0400	A2389	21 54 12.1	–04 00 19	0.1509	3	3.540	34.5	2.031	13.0	2.052	5.0		<i>E</i>
RXCJ2157.4 – 0747	A2399	21 57 25.8	–07 47 41	0.0579	8	5.851	19.0	0.462	14.0	0.481	3.5		<i>DB E</i> , 10, 122
RXCJ2158.3 – 2006	A2401	21 58 20.1	–20 06 16	0.0570	23	3.662	19.0	0.280	11.0	0.298	2.6		2, 3
RXCJ2158.4 – 6023	A3825	21 58 27.2	–60 23 58	0.0750	61	8.097	10.3	1.085	13.0	1.142	2.8		3
RXCJ2158.5 – 0948	A2402	21 58 30.5	–09 48 28	0.0809	1	5.663	12.2	0.890	10.0	0.957	4.0		111, 157, 181
RXCJ2201.8 – 2226	S0987	22 01 50.9	–22 26 40	0.0691	10	5.737	15.0	0.647	14.0	0.674	2.6		<i>S</i> , 24, 33
RXCJ2201.9 – 5956	A3827	22 01 56.0	–59 56 58	0.0980	20	18.577	6.3	4.264	11.5	4.686	2.8		3
RXCJ2202.0 – 0949	A2410	22 02 05.9	–09 49 28	0.0809	10	5.863	13.6	0.921	13.5	0.959	4.2		<i>D E</i> , 10
RXCJ2205.6 – 0535	A2415	22 05 40.5	–05 35 36	0.0582	3	14.289	16.2	1.135	15.5	1.207	4.7		<i>B E</i>
RXCJ2209.3 – 5148	A3836	22 09 23.3	–51 48 54	0.1065	2	5.942	15.6	1.645	13.5	1.696	2.1		<i>E</i> , 29
RXCJ2210.3 – 1210	A2420	22 10 19.7	–12 10 34	0.0846	9	15.613	7.5	2.674	11.0	2.971	3.9		<i>S</i> , 10
RXCJ2211.7 – 0350		22 11 43.4	–03 50 07	0.2700 <sup>est</sup>	0	3.326	16.7	6.528	5.0	7.418	5.9		–
RXCJ2213.0 – 2753		22 13 05.2	–27 53 59	0.0610	6	3.346	26.8	0.294	10.0	0.316	1.4		<i>S</i> , 96
RXCJ2214.5 – 1022	A2426	22 14 32.6	–10 22 18	0.0980	15	12.458	8.7	2.867	12.5	3.050	3.9		<i>S</i> , 2
RXCJ2216.2 – 0920	A2428	22 16 15.5	–09 20 24	0.0825	2	8.593	10.1	1.400	8.5	1.591	4.5		<i>S</i>
RXCJ2216.9 – 1725	RBS1842 <sup>c</sup>	22 16 56.4	–17 25 34	0.1301	2	5.515	14.5	2.315	11.0	2.411	2.3		<i>X*</i> <i>S</i>
RXCJ2217.7 – 3543	A3854	22 17 43.3	–35 43 34	0.1486	44	6.406	10.7	3.535	8.5	3.842	1.1		33, 37, 38
RXCJ2218.0 – 6511	RBS1847 <sup>c</sup>	22 18 05.6	–65 11 06	0.0951	5	9.021	8.9	1.953	14.0	2.034	2.8		<i>E</i>
RXCJ2218.2 – 0350	MS2215 <sup>o</sup>	22 18 17.1	–03 50 03	0.0901	3	9.355	11.1	1.813	14.5	1.889	5.7		<i>D S</i>
RXCJ2218.6 – 3853	A3856	22 18 40.2	–38 53 51	0.1411	10	7.132	10.2	3.516	9.0	3.781	1.3		16, 31, 33
RXCJ2218.8 – 0258		22 18 49.1	–02 58 07	0.0902	8	4.044	32.4	0.790	10.0	0.840	5.8		<i>B E</i>
RXCJ2220.5 – 3509	A3866	00.0	00	0.1544	1	9.489	8.8	5.656	8.5	6.215	1.1		<i>X</i> 146
RXCJ2223.8 – 0138	A2440	22 23 53.0	–01 38 16	0.0906	48	9.875	10.9	1.929	10.5	2.097	5.3		<i>S</i> , 42
RXCJ2224.4 – 5515	APMCC772 <sup>f</sup>	22 24 27.5	–55 15 22	0.0791	2	5.965	15.6	0.894	12.0	0.941	3.5		<i>E</i>
RXCJ2224.7 – 5632	S1020	22 24 43.6	–56 32 05	0.0355	0	3.057	16.2	0.089	7.5	0.105	4.1		9
RXCJ2225.8 – 0636	A2442	22 25 51.0	–06 36 12	0.0897	12	5.129	14.3	0.991	8.5	1.089	5.1		<i>E</i>
RXCJ2227.8 – 3034	A3880	22 27 52.4	–30 34 12	0.0579	28	10.035	8.2	0.789	8.5	0.939	1.1		14, 33
RXCJ2228.8 – 6053		22 28 51.3	–60 53 56	0.0423	2	3.829	15.5	0.158	13.0	0.166	2.2		<i>E</i>
RXCJ2234.5 – 3744	A3888	22 34 31.0	–37 44 06	0.1510	70	11.225	8.9	6.363	7.5	7.314	1.2		<i>X</i> 1, 44
RXCJ2235.6 + 0128	A2457	22 35 40.6	+01 28 18	0.0594	18	11.139	15.7	0.924	18.0	0.953	5.8		<i>B</i> 10
RXCJ2243.0 – 2009	A2474	22 43 04.6	–20 09 59	0.1359	3	4.977	40.0	2.297	14.5	2.320	2.6		<i>E</i>
RXCJ2246.3 – 5243	A3911	22 46 18.6	–52 43 46	0.0965	2	12.436	9.7	2.778	26.0	2.806	1.5		<i>L</i> 132
RXCJ2248.5 – 1606	A2485	22 48 32.9	–16 06 23	0.2472	1	3.063	31.4	4.998	9.5	5.100	3.3		<i>E</i>
RXCJ2248.7 – 4431	S1063	22 48 43.5	–44 31 44	0.3475	3	8.590	10.9	28.939	9.0	30.786	1.8		<i>E</i>
RXCJ2249.9 – 6425	A3921	22 49 57.0	–64 25 46	0.0940	32	14.033	8.5	2.948	14.0	3.103	2.8		<i>E</i> , 3
RXCJ2251.0 – 1624	A2496	22 51 00.6	–16 24 24	0.1221	3	5.238	20.4	1.917	5.5	2.282	3.2		<i>S</i>
RXCJ2251.7 – 3206		22 51 47.6	–32 06 12	0.2460	1	3.562	18.8	5.718	6.5	6.215	1.4		<i>X*</i> <i>E</i>
RXCJ2253.5 – 3343	A3934	22 53 34.2	–33 43 27	0.2240	1	3.036	18.7	4.008	3.5	5.010	1.2		7, 124
RXCJ2254.0 – 6315	AM2250 <sup>P</sup>	22 54 03.2	–63 15 15	0.2112	7	4.714	11.7	5.490	11.5	5.602	2.2		<i>E</i>
RXCJ2305.5 – 4513	A3970	23 05 34.6	–45 13 14	0.1253	3	4.327	42.8	1.683	11.0	1.735	1.7		<i>S</i>
RXCJ2306.6 – 1319		23 06 36.0	–13 19 12	0.0659	2	5.890	34.4	0.601	15.0	0.620	3.1		<i>E</i>
RXCJ2307.2 – 1513	A2533	23 07 15.3	–15 13 42	0.1110	1	4.904	26.1	1.484	6.0	1.726	2.8		19

<sup>est</sup> this redshift is highly uncertain due to the currently very poor spectra. The observation will be repeated This table is also available in electronic form at CDS and at our home page (see footnote to abstract).

name (1)	alt.name (2)	<i>R.A.</i> (3)	<i>Decl.</i> (4)	<i>z</i> (5)	<i>N<sub>gal</sub></i> (6)	<i>F<sub>x</sub></i> (7)	<i>Error</i> (8)	<i>L<sub>x</sub></i> (9)	<i>R<sub>ap</sub></i> (10)	<i>L<sub>x</sub><sup>*</sup></i> (11)	<i>N<sub>H</sub></i> (12)	<i>Cm</i> (13)	<i>Ref.</i> (14)
RXCJ2308.3 – 0211	A2537	23 08 23.2	–02 11 31	0.2966	2	4.264	14.3	10.174	13.5	10.174	4.3		<i>S</i>
RXCJ2312.3 – 2130	A2554	23 12 20.7	–21 30 02	0.1108	35	4.209	24.1	1.268	4.5	1.585	2.0		38, 127
RXCJ2313.0 – 2137	A2556	23 13 00.9	–21 37 55	0.0871	9	7.764	18.0	1.419	7.0	1.669	2.0		<i>S</i> , 127
RXCJ2313.9 – 4244	S1101	23 13 58.6	–42 44 02	0.0564	4	23.412	7.2	1.738	12.0	1.998	1.9		<i>S</i>
RXCJ2315.7 – 3746	A3984	23 15 44.2	–37 46 56	0.1786	3	5.819	20.5	4.738	8.0	5.150	1.5		<i>S</i>
RXCJ2315.7 – 0222		23 15 45.2	–02 22 37	0.0267	3	8.332	10.6	0.134	20.0	0.141	4.2	<i>L</i>	<i>S</i> , 27, 51
RXCJ2316.1 – 2027	A2566	23 16 07.5	–20 27 19	0.0822	11	7.415	18.2	1.199	9.0	1.332	2.1		<i>S</i> , 127
RXCJ2319.2 – 6750	A3990	23 19 12.0	–67 50 24	0.0286	0	2.434	14.5	0.045	10.5	0.049	2.8	<i>D</i>	47
RXCJ2319.6 – 7313	A3992	23 19 41.8	–73 13 51	0.0984	3	3.993	17.9	0.937	7.5	1.030	1.9		<i>E</i>
RXCJ2321.4 – 2312	A2580	23 21 24.3	–23 12 20	0.0890	17	3.270	25.6	0.621	7.0	0.690	2.0		<i>S</i> , 127
RXCJ2321.5 – 4153	A3998	23 21 33.4	–41 53 56	0.0894	16	8.720	13.3	1.662	11.0	1.787	2.0		<i>S</i> , 16, 31, 33, 48
RXCJ2321.8 – 6941	A3995	23 21 48.6	–69 41 55	0.1846	14	4.334	10.5	3.815	5.5	4.385	3.4		<i>E</i>
RXCJ2325.3 – 1207	A2597	23 25 20.0	–12 07 38	0.0852	3	20.558	5.8	3.556	11.5	3.996	2.5		<i>S</i> , 1
RXCJ2326.7 – 5242		23 26 46.9	–52 42 36	0.1074	3	3.370	20.3	0.955	11.0	0.985	1.6		<i>E</i>
RXCJ2331.2 – 3630	A4010	23 31 12.7	–36 30 24	0.0957	30	11.013	22.1	2.417	9.5	2.686	1.4		<i>E</i> , 140, 141
RXCJ2336.2 – 3136	S1136	23 36 17.0	–31 36 37	0.0643	2	5.273	20.5	0.516	12.0	0.549	1.2		15, 52, 26
RXCJ2337.6 + 0016	A2631	23 37 40.6	+00 16 36	0.2779	5	3.555	19.8	7.420	10.0	7.571	3.8		55
RXCJ2340.1 – 8510	A4023	23 40 10.3	–85 10 42	0.1934	3	3.176	18.9	3.066	8.5	3.194	7.5		<i>E</i>
RXCJ2341.2 – 0901	A2645	23 41 16.8	–09 01 39	0.2510	5	3.414	26.1	5.731	11.5	5.789	2.5		1
RXCJ2344.2 – 0422		23 44 16.0	–04 22 03	0.0786	2	12.638	7.4	1.855	11.0	2.061	3.5		<i>S</i>
RXCJ2347.4 – 0218	HCG97	23 47 24.4	–02 18 52	0.0223	10	2.629	38.8	0.030	12.5	0.033	3.6		58, 59
RXCJ2347.7 – 2808	A4038	23 47 43.2	–28 08 29	0.0300	157	49.578	3.8	1.014	22.5	1.127	1.5	<i>L</i>	146
RXCJ2351.6 – 2605	A2667	23 51 40.7	–26 05 01	0.2264	1	9.295	10.1	12.422	8.0	13.651	1.7	<i>X</i>	<i>S</i> , 65, 129
RXCJ2354.2 – 1024	A2670	23 54 13.4	–10 24 46	0.0765	219	9.622	12.1	1.337	10.5	1.469	2.9	<i>B</i>	66, 86, 105
RXCJ2357.0 – 3445	A4059	23 57 02.3	–34 45 38	0.0475	45	32.663	5.5	1.698	24.0	1.787	1.1	<i>L</i>	146
RXCJ2359.3 – 6042	A4067	23 59 19.2	–60 42 00	0.0989	30	4.544	20.5	1.080	9.5	1.149	2.4		141
RXCJ2359.9 – 3928	A4068	23 59 55.7	–39 28 47	0.1024	12	5.024	18.4	1.279	11.0	1.346	1.3		16, 31, 67

<sup>a</sup> Cl0053-37, <sup>b</sup> cluster from the catalogue of Wegner et al. (1996, 1999), <sup>c</sup> from the ROSAT Bright Source Catalogue (Fischer et al. 1998, Schwobe et al. 2000), <sup>d</sup> RASSCAL145, <sup>e</sup> ZwCl0258.9+0142, <sup>f</sup> cluster from the catalogue by Dalton et al. (1994, 1997), <sup>g</sup> Eridanus group, <sup>h</sup> ES0657-558, <sup>i</sup> AM 0711-602, <sup>j</sup> USZ-SSRS2-group from the catalogue of Ramella et al. (2002), <sup>k</sup> MS1111.8-3754, <sup>l</sup> MS1306.7-0121, <sup>m</sup> ZwCl1703.8-0129, <sup>n</sup> AM 2108-232, <sup>o</sup> MS 2215.7-0404, <sup>p</sup> AM 2250-633

key to the redshift references: (E,H) ESO-Key Programme, (S) South Galactic Pole Project (part of Ph.D. thesis K.A. Romer), (1) Struble & Rood (1999), (2) Katgert et al. (1996), (3) Katgert et al. (1998), (4) Postman & Lauer (1995), (5) Lauberts & Valentijn (1989), (6) Ebeling et al. (1996), (7) Bauer et al. (2000), (8) Kapahi et al. (1998), (9) Abell et al. (1989), (10) Slingsland et al. (1998), (11) Müller et al. (1999), (12) Smith et al. (2000), (13) Solanes & Stein (1998), (14) Stein (1996), (15) NED information prior to 1992 without reference, (16) Tucker et al. (2000), (17) Dalton et al. (1994), (18) Dale et al. (1998), (19) Quintana & Ramirez (1994), (20) Da Costa et al. (1998), (21) Patten et al. (2000), (22) Barton et al. (1996), (23) Mahdavi et al. (2000), (24) Loveday et al. (1996), (25) Garilli et al. (1993), (26) Ratcliffe et al. (1998), (27) De Grandi et al. (1999), (28) Green et al. (1998), (29) Dalton et al. (1997), (30) Muriel et al. (1995), (31) Shectman et al. (1996), (32) Fairall (1984), (33) Collins et al. (1995), (34) Mould et al. (1991), (35) Ledlow & Owen (1995), (36) Slingsland et al. (1998), (37) West & Frandsen (1981), (38) Colless & Hewett (1987), (39) Stocke et al. (1991), (40) Muriel et al. (1991), (41) Beers et al. (1991), (42) Mohr et al. (1996), (43) Olowin et al. (1988), (44) Teague et al. (1990), (45) Reimers et al. (1996), (46) Maurogordato et al. (1997), (47) Huchra priv. com, (48) Zabludoff & Mulchaey (1998), (49) Andernach (2002), (50) Batuski et al. (1999), (51) Huchra et al. (1993), (52) Di Nella et al. (1996), (53) Crawford et al. (1995), (54) Crawford et al. (1999), (55) NED information based on SDSS, York et al. (2001), (56) Kristian et al. (1978), (57) Owen et al. (1999), (58) Hickson et al. (1992), (59) De Carvalho et al. (1997), (60) Jorgensen et al. (1995), (61) Ettori et al. (1995), (62) Green et al. (1990), (63) Dantas et al. (1997), AJ, 118, 1468, (64) de Vaucouleurs et al. (1991), (65) Caccianiga et al. (2000), (66) Sharples et al. (1998), (67) Vettolani et al. (1998), (68) Andernach & Tago (1998), (69) Vettolani et al. (1989), (70) Tritton (1972), (71) Tittley & Henriksen (2001), (72) Dressler & Shectman (1988), (73) Barrena et al. (2002), (74) Mathewson & Ford (1996), (75) Bardelli et al. (2001), (76) Quintana et al. (1995), (77) Vettolani et al. (1990), (78) Zabludoff et al. (1990), (79) Tucker et al. (1998), (80) Mamon et al. (2001), (81) Owen et al. (1995), (82) Huchmeier (1994), (83) da Costa et al. (1987), (84) Matthews & van Driel (2000), (85) Sodre et al. (2001), (86) den Hartog & Katgert (1996), (87) Pierre et al. (1997), (88) Lemonon et al. (1997), (89) Bade et al. (1995), (90) Jones & Forman (1999), (91) Fairall et al. (1992), (92) Mulchaey et al. (1996), (93) Strauss et al. (1992), (94) Beers et al. (1995), (95) Koranyi & Geller (2002), (96) NED information based on 2dF Survey, Colless et al. (2001), (97) Ramella et al. (2002), (98) Kaldare et al. (2003), (99) Quintana et al. (1996), (100) Richter (1987), (101) Bardelli et al. (1998), (102) Bardelli et al. (1994), (103) Drinkwater et al. (1999), (104) Christiani et al. (1987), (105) Oegerle & Hill (2001), (106) Henry & Mullis (1997) (priv. com.), (107) Willmer et al. (1999), (108) Heckman et al. (1994), (109) Bernardi et al. (2002), (110) Goto et al. (2002), (111) Huchra et al. (1991), (112) Quintana & de Souza (1993), (113) Schindler (2000), (114) Willmer et al. (1991), (115) Pena et al. (1991), (116) Thompson et al. (1992), (117) Peterson et al. (1997), (118) Arnaud et al. (1992), (119) Batuski et al. (1991), (120) Wegner et al. (1999), (121) Peacock & West (1992), (122) Blakeslee & Tonry (1992), (123) Falco et al. (1999), (124) Beers et al. (1992), (125) Trager et al. (2000), (126) Davoust et al. (1995), (127) Caretta et al. (2002), (128) Liang et al. (2000), (129) Rizza et al. (1998), (130) Malamuth et al. (1992), (131) Caldwell & Rose (1997), (132) Lauer & Postman (1994), (133) Garilli et al. (1991), (134) Whiteoak (1972), (135) Ramella et al. (1996), (136) Mathewson et al. (1992), (137) Melnick & Quintana (1981), (138) Sodre et al. (1992), (139) Cruddace et al. (2002), (140) den Hartog (1995), (141) Mazure et al. (1996), (142) Couch et al. (1998), (143) Couch & Sharples (1987), (144) da Costa et al. (1991), (145) Schwobe et al. (2000), (146) Chen et al. (1998), (147) Crawford et al. (1993), (148) Fadda et al. (1996), (149) Durret et al. (1998), (150) Lumsden et al. (1992), (151) Alonso et al. (1999), (152) Merrifield & Kent (1991), (153) Way et al. (1998), (154) Fetisova et al. (1993), (155) Quintana et al. (1996), (156) Trasarti-Battistoni (1998), (157) Postman et al. (1992), (158) Ramirez & de Souza (1998), (159) Böhlinger et al. (2000), (160) Dressler et al. (1986), (161) Ebeling et al. (2002), (162) Zabludoff et al. (1993), (163) Huchra et al. (1983), (164) Lucey et al. (1983), (165) Rose et al. (2002), (166) Drinkwater et al. (2001), (167) Mieske et al. (2002), (168) Minniti et al. (1998), (169) Edge & Stewart (1991), (170) Hilker et al. (1999), (171) Carter & Malin (1983), (172) Quintana et al. (1994),

source. But we use the point-like appearance here as a flag for sources to be doubly checked. On the other hand, if an X-ray source is clearly well extended, we can be sure that most of the X-ray emission is diffuse and the contribution to the X-ray flux from AGNs or radio galaxies found at other wavelength can at most be a minor fraction. In addition to the X-ray based reinspection we have also screened again the literature for any information that could cast doubts on the cluster identification, with a special eye on contaminating AGN. One source of further observational information that was used for some clusters are pointed observations with the ROSAT PSPC and HRI detector as well as new observations with XMM-Newton and CHANDRA.

As a result of this screening procedure we could improve our identification and discarded 6 objects from the REFLEX list as described in the subsection below. We should also point out that most of the critical cases commented below were known as problematic targets to our observing team at the time of the observation. One of the observational requirements was therefore to take a spectrum of suspicious objects in the center of the X-ray emission (often bright galaxies) to critically check for the presence of an AGN. More details about the spectra of these objects will be given in Guzzo et al. (in preparation). Thus for some of the objects where the identification is still not completely certain the standard optical means have already been used and a final decision can only come from a high angular resolution X-ray observation or for example from optical polarimetric measurements. In total we are left with 14 cases where the identification is not definitive. Following our previous philosophy to keep the objects in our working list until we can positively rule them out as cluster identifications, we have conservatively kept them in our catalogue but we have marked them in the table. We realistically expect that less than 10 are non-cluster objects. The effect this small fraction (less than 2.3 %) has on any of the cosmological applications of REFLEX is completely negligible.

In the following we provide notes on the results of our inspection including the critical cases mentioned as well as positive confirmations. These remarks should be of help for any further identification or follow-up work that may be conducted on these REFLEX objects. The comments given for each object illustrate some aspects of the manual screening process.

**RXCJ0014.3-6604**, A2746 (also included in XBACS) is a typical example of a point-like X-ray source which was inspected in more detail. The X-ray spectral hardness ratio is not outside the acceptable limit for cluster emission. The source appears very compact with a core radius  $2\sigma$  upper limit of about  $120h_{50}^{-1}$  kpc at a redshift of  $z = 0.156$ . This does not rule out that the X-ray emission comes from a cluster. We have five concordant redshifts including the cD galaxy, with no spectrum indicating an AGN and the optical image is clearly showing a galaxy cluster. Therefore, even though

we cannot establish the extent of the X-ray source, we conclude that the source is most likely a cluster.

**RXCJ0015.4-2350**, A14, has an X-ray emission which is very faint and diffuse: about 48 source photons spread in a clumpy distribution over a region with a radius of about 12 arcmin. The cluster position was not taken as the center of the large-scale distribution but at a local maximum. The cD galaxy, ESO 473-G 005 at the position 00 15 10.6, -23 52 57.0 is located at this highest local maximum. This is surely a good example of a dynamically young cluster with a size slightly smaller than the Virgo cluster. Even though there is a slight probability that the X-ray emission originates from a collection of point sources, by far the most likely interpretation is that of a poor galaxy cluster. This is supported by the finding of four coincident galaxy redshift in the optical follow-up.

**RXCJ0117.8-5455** is another source with X-ray emission consistent with a point source origin. The source is also detected as a bright radio source in the SUMSS survey (Mauch et al. 2003). Since the cluster is found to be at a redshift of  $z = 0.2510$  as determined from 6 galaxy velocities (where none of the spectra indicate an AGN), an upper limit on the X-ray core radius of about  $270 h_{50}^{-1}$  kpc is consistent with a cluster source and also the spectral hardness ratio is within the limits expected for cluster emission. Therefore this point-like X-ray source is kept in the catalogue until we have better data for a more secure identification.

**RXCJ0132.6-0804** is classified as Seyfert 1.5 in the cross correlation work of the ROSAT All-Sky Survey and the NVSS sources by Bauer et al. (2000). We find narrow emission lines in the central galaxy, PKS 0130-083, of this cluster at  $z = 0.1485$ . The OIII lines are more prominent than the  $H\beta$  lines which makes the AGN identification more likely than that of the typical emission lines often found in central cluster galaxies in cooling core clusters (e.g. Crawford et al. 1999). The X-ray luminosity of the object is about  $3.6 \cdot 10^{44}$  erg  $s^{-1}$  which is quite high for a Seyfert galaxy. The Digital Sky Survey image shows clearly a central dominant galaxy surrounded by a collection of galaxies and we recorded three coincident galaxy redshifts. The spectral hardness ratio is within the limits expected for thermal emission from a cluster. Therefore the identification of this X-ray source is uncertain at this stage. The X-ray emission could come from the cluster or the AGN. A high resolution X-ray observation is required for a definitive decision.

**RXCJ0250.2-2129** has been classified as a BL Lac ( $z = 0.4980$ , off-set 0.4 arcmin) in the ROSAT Bright Source Catalogue by Schwobe et al. (2000) and is listed as a radio source in Bauer et al. (2000). The BL Lac is not at the same redshift as the cluster. The X-ray source shows a marginal extent and is too soft by about  $1.3\sigma$  compared to the expectation. Our deeper CCD image clearly shows an optical cluster and we found two coincident galaxy redshifts. We therefore take the cluster identification as more likely, but cannot rule out a contribution to the X-ray emission by the AGN. The cluster is also covered by a

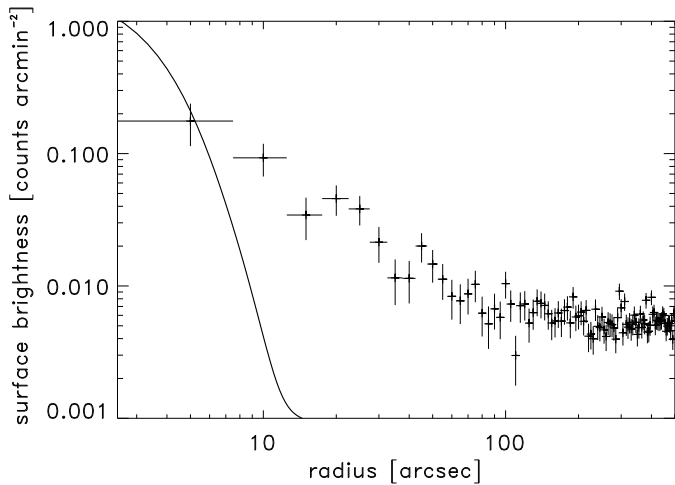


**Fig. 6.** Surface brightness profile of the REFLEX cluster RXCJ0301.6+0155 as observed in a pointed observation with the ROSAT HRI (data points and Poissonian errors). The profile is compared to the point spread function of the ROSAT HRI (solid line).

ROSAT PSPC archive observation. But the offset from the pointing center is so large that the possibility to better resolve a point source is not improved over the survey data.

**RXCJ0301.6+0155** This source, which has previously been identified as a cluster in the NORAS Survey (Böhringer et al. 2000) and which is coinciding with a Zwicky cluster (ZwC10258.9+01), appears point-like. A ROSAT HRI observation in the archive showed that the source is very compact but definitely not a point source. Therefore the cluster identification is well justified. The comparison between the surface brightness profile and the point spread function of the ROSAT HRI is shown in Fig. 6.

**RXCJ0331.1-2100** is coincident within 0.5 arcmin with a Seyfert 1.9 galaxy identified by Bauer et al. (2000). The source is listed in Schwope et al. (2000) as RBS 0436. The X-ray emission is only marginally extended, but the spectral hardness ratio is consistent with thermal intra-cluster medium emission. We have nine coincident galaxy redshifts for this cluster. Therefore it is possible that the AGN is contaminating the X-ray radiation, but there is also definitely a cluster at this position.

**RXCJ0336.3-0347** This is a compact X-ray source with a peaked center and a weak extent. The central galaxy is listed as an AGN, as 2MASS and radio source, probably a BL Lac at  $z = 0.1595$  (Bauer et al. 2000, Veron-Cetty & Veron 2001). It appears to have a bright central spot in sky images, but our spectra also easily show the underlying galaxy continuum with the Balmer break. The optical image also shows an optical cluster for which we have three concordant redshifts at the same redshift as the AGN. The most likely interpretation of this source is that it is indeed a galaxy cluster with some (less than half) contamination of the X-ray emission by the AGN.

The hardness ratio of the X-ray emission is consistent with a cluster, also.

**RXCJ0425.8-0833** is coincident within 1.3 arcmin with a Seyfert 2 galaxy identified by Hewitt & Burbidge (1991). The source is listed in Schwope et al. (2000) as RBS 0540. The central dominant galaxy has the spectrum of a passive elliptical galaxy without emission lines as found in our follow-up observations. The X-ray emission is very extended and the dominant part of the X-ray emission must come from the cluster, for which we have two concordant redshifts.

**RXCJ0437.1-2027**, A499, is detected with only 26 photons and the result for the extent is not completely convincing. A ROSAT HRI observation from the archive shows that the source is quite compact but clearly extended. Two coincident galaxy redshifts are available for this cluster.

**RXCJ0528.9-3927** also identified as RBS0653 (Schwope et al. 2000) is listed in NED as a QSO. The X-ray emission is slightly extended but the spectral hardness ratio deviates by  $5.2\sigma$  from the value expected for thermal cluster emission. A deeper X-ray observation with XMM-Newton shows this object to be an X-ray luminous cluster with a less than 20% contamination (in the ROSAT hard band) by a bright, soft AGN point source.

**RXCJ0918.1-1205**, A780 or Hydra A, is a well known X-ray cluster. Thus even though one finds a coincidence within 0.2 arcmin with a Seyfert galaxy listed by de Vaucouleurs et al. (1991), there is no doubt about the clear dominance of the thermal cluster emission.

**RXCJ1027.9-0647**, A1023, is coincident within 0.2 arcmin with an AGN at  $z = 0.1165$  identified by Grazian et al. (2002). The X-ray emission is marginally extended and the spectral hardness ratio is consistent with thermal cluster emission. There is a residual possibility that the X-ray emission of this source is contaminated by an AGN. Six coincident galaxy redshifts support the existence of a galaxy cluster at this position.

**RXCJ1050.5-0236**, A1111, is coincident within 0.6 arcmin with a Seyfert 2 galaxy identified by Machalski & Condon (1999). The X-ray emission is found to be extended and the dominant part of the X-ray emission comes from the cluster. There is an X-ray emitting star in the south of the cluster whose X-ray emission was deblended. Nine coincident galaxy redshifts leave no doubt about the existence of a cluster at this position (see also the ASCA study of Matsumoto et al. 2001).

**RXCJ1050.6-2405** features a point source and an extended fainter halo in the RASS. About one third of the flux seems to come from the central compact emission. The hardness ratio gives no indication for two source components, however, and is perfectly consistent with thermal emission from a cluster. At the cluster redshift of  $z = 0.2037$  the compact center could still be a bright compact cluster cooling core as well as a contaminating central AGN. Near the center (0.4 arcmin offset) is a radio source, PKS B1048-238 (MRC1048-238), at a redshift of  $z = 0.2060$  (McCarthy et al. 1996) and identified with

a broad line radio galaxy Kapahi et al. (1998). We expect that most of the X-ray emission is due to the cluster. But so far we have made no effort to subtracted the possible AGN contribution.

**RXCJ1141.4-1216**, A1348, is coincident within 0.2 arcmin with a Seyfert 1.8 galaxy listed by Machalski & Condon (1999). The X-ray emission shows a small extent and the X-ray emission is slightly softer ( $\sim 2.9\sigma$ ) than expected. From the extended X-ray emission we still conclude that most of the emission comes from the cluster. The X-ray luminosity of the object is  $3.3 \cdot 10^{44}$  erg s<sup>-1</sup> which would be towards the upper end of the luminosity distribution of Seyfert galaxies. Six coincident galaxy redshifts confirm the existence of a cluster at this position.

**RXCJ1149.7-1219**, A1391, is coincident within 0.9 arcmin with an AGN listed by Machalski & Condon (1999). The X-ray emission is found to be clearly extended and the dominant part of the X-ray emission must come from the cluster. Six coincident galaxy redshifts confirm the existence of a cluster at this position.

**RXCJ1212.3-1816** was detected with only 12.5 source photons with a significance of just about  $3\sigma$ . This signal is detected in an aperture significantly larger than the point spread function and the significance decreases for a smaller detection cell. Therefore, if the detection is accepted, the source has to be extended. We have two coincident cluster galaxy redshifts.

**RXCJ1234.2-3856** appears as a point source in RASS with a spectral hardness ratio consistent with thermal cluster emission. It is also listed as a radio source without classification by Bauer et al. (2000). Two coincident galaxy redshifts give some further support for the cluster identification.

**RXCJ1253.6-3931** appears as point-like source in the RASS with a cluster like hardness ratio and coincides within 0.5 arcmin with the unclassified radio source PMN J1253-3932 (see also Bauer et al. 2000). We have a spectrum as well as a redshift from the central galaxy which does not show an AGN or BL Lac signature. A CCD image shows a galaxy cluster. Therefore we keep this source in our list as a likely cluster candidate.

**RXCJ1326.2+0013** is coincident within 0.2 arcmin with a BL Lac found in the 2dF survey. The X-ray emission is clearly extended and the emission from the intracluster medium certainly dominates. The spectral hardness ratio is as expected and there are 16 coincident galaxy redshift. Therefore there is no doubt about the cluster identification of this source.

**RXCJ1332.9-2519** is detected in the RASS with very low surface brightness, but with 50 counts and an about  $4\sigma$  detection. An archival PSPC observation, with an exposure of only 982 sec shows a similar very low surface brightness structure providing a good confirmation of this very diffuse structure. We have three coincident galaxy redshifts from the follow-up observations confirming the existence of a cluster at this position.

**RXCJ1347.2-3025 & RXCJ1349.3-3018**, A 3574 or Klemola 27 at a redshifts of 0.0145 and 0.0160, re-

spectively, is a cluster with two components. It presents a particular problem to its detection and identification. The central galaxy is the X-ray luminous Seyfert 1 galaxy, IC 4329, and two further AGNs contribute to the X-ray emission from the cluster region. While the central detection could easily have been dismissed because of its almost point-like appearance in the RASS and its identification with a known X-ray AGN, the additional detection of fragments of the diffuse outer emission in the RASS analysis triggered a further inspection of this cluster. A pointed observation shows clearly the diffuse X-ray halo of the cluster in addition to the three cluster AGN point sources. We have used this pointed observation to subtract the contribution of the three AGN from the total emission. The central AGN IC4329A carries about 75% of the flux, the two other AGNs contribute about 4 to 5% each and the cluster emission amounts to 15 - 20%. Therefore, with a net flux of  $\sim 1.35 \cdot 10^{-11}$  erg s<sup>-1</sup> cm<sup>-2</sup> in the ROSAT band, the cluster is well above the flux limit of the REFLEX and the XBACS survey. Fig. 7 shows the surface brightness distribution of this cluster. In the catalogue we have listed the central cluster region and the western concentration (about 25 arcmin,  $\sim 0.6$  Mpc distance) as separate sources identified with A3574E and A3574W, respectively, recognizing that they are two separate virializing clumps. Also the diffuse Western component is, with a nominal flux,  $F_n \sim 3.5 \cdot 10^{-12}$  erg s<sup>-1</sup> cm<sup>-2</sup>, above the REFLEX flux limit.

The cluster properties were determined also with the help of the pointed observation, which allows a better contamination subtraction. The cluster was dismissed in XBACS as an AGN. At a larger distance it would probably have escaped its identification as a cluster in REFLEX. This shows that there is probably not only a small fraction of clusters which are erroneously included in the sample because of an AGN contribution to the X-ray flux, but also a small fraction of clusters which are erroneously discarded because the cluster X-ray emission is not easily visible if it is blended by a bright AGN.

**RXCJ1350.7-3343** has a central galaxy with a Seyfert 1 spectrum but the X-ray emission in RASS is extended and therefore indicates a galaxy cluster.

**RXCJ1415.2-0030**, tentatively identified with A1882 (offset 13.3 arcmin), is coincident within 1.6 arcmin with a QSO identified in the Sloan Digital Sky Survey. The X-ray emission is very extended and diffuse, however, and we do not detect a contribution by a point source. 20 concordant redshifts confirm the existence of a cluster.

**RXCJ1416.8-1158** appears as a point source in RASS and has a spectrum that is  $1.7\sigma$  too soft. 10 coincident galaxy redshift give good support for the existence of a cluster at this position.

**RXCJ1504.1-0248** is a very peculiar object. We have obtained a spectrum of the central galaxy (with an offset of 0.3 arcmin from our reference position of the cluster) which shows Liner like emission lines. It was identified as an AGN by Shectman et al. (1996). The X-ray source is

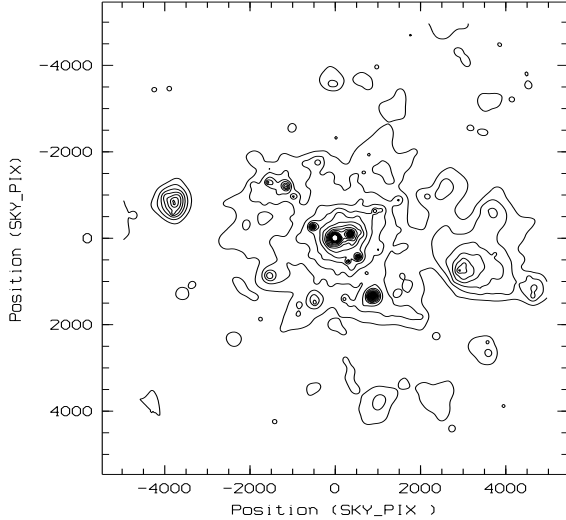


**Fig. 7.** ROSAT PSPC image of Abell 3574 (RXCJ1347.2-3025 & RXCJ1349.3-3018) from a pointed PSPC observation with an exposure of 8.3 ksec. The image is exposure and vignetting corrected. It has been treated with a variable Gaussian filter. The contours are logarithmically spaced. We can see two bright point sources in the center and another one to the south which carry most of the flux received from this object. The diffuse emission of the cluster shows some clumpiness and amounts to about 20% of the total emission. The central part and the Western subcluster are tabulated as two different catalogue entries. One sky pixel is 0.5 arcsec, thus the image size is  $42 \times 42$  arcmin<sup>2</sup>. The image is centered on the sky coordinate 13 49 19.2, -30 18 36 (J2000).

very compact but significantly extended (the probability that the emission comes from a point source is estimated to be 0.0016). The X-ray luminosity is extremely high with  $L_x \sim 4.3 \cdot 10^{45}$  erg s<sup>-1</sup> in the 0.1 - 2.4 keV band and not typical for a narrow line AGN.

A short CHANDRA observation that was finally performed early 2004 shows a perfect galaxy cluster image without any significant AGN contamination. This is in our sample the most spectacular example of an object which was for long time marked as very suspicious for its unusual compactness for given brightness and distance but was finally revealed to be a prominent X-ray cluster. The Liner-like spectrum observed for the central galaxy is also typical for cooling flow clusters (e.g. Crawford et al. 1999 and references therein).

**RXCJ1958.2-3011** is an X-ray source that appears point-like in RASS with a hardness ratio consistent with cluster emission. It is listed as an unclassified radio source in Bauer et al. (2000). The optical image shows a galaxy with a bright nucleus and our ESO spectrum indicates an enhanced blue continuum. There is clearly a cluster visible with a likely Bright Cluster Galaxy (BCG) that is about 1 arcmin offset to the NEE from the radio source and the center of the cluster emission. The cluster detection is further supported by four concordant redshifts. Therefore, we

classify this object as a cluster-AGN combination whose fluxes must be determined by a higher angular resolution X-ray image. Since low X-ray luminosity AGN appear very frequently in clusters, with an X-ray luminosity well below that of the cluster emission, we keep this object in the REFLEX catalogue at present.

**RXCJ2035.7-2513** shows diffuse X-ray emission around a large early type galaxy with a luminosity of about  $4 \cdot 10^{42}$  erg s<sup>-1</sup>. An archival PSPC image also shows the diffuse emission but also some contamination of 10-20% by point sources, which is within the error of the flux determination in the catalogue and no correction has been made. The object is probably associated with A3698 whose center has an offset of 4.6 arcmin assumed to coincide with NGC 6936. Seven coincident galaxy redshifts confirm the existence of a cluster at the X-ray source position.

**RXCJ2147.0-1019** contains a BL Lac identified by Bauer et al. (2000) within 0.2 arcmin of our reference position. The X-ray source is marginally extended (probability 97%) and has a hardness ratio well consistent with thermal cluster emission. We cannot rule out that the BL Lac could substantially contribute to the cluster emission, however.

**RXCJ2216.9-1725** contains a Seyfert galaxy identified by Schwöpe et al. (2000) within 0.2 arcmin of our reference position. The X-ray source is marginally extended (probability 90%) and the X-ray hardness ratio shows that the source is about  $2\sigma$  too soft. Therefore, it is not impossible that the Seyfert galaxy contributes to the X-ray emission. The cluster is with an X-ray luminosity of  $L_x \sim 4 \cdot 10^{44}$  erg s<sup>-1</sup> so luminous that the Seyfert galaxy has to be relatively bright to affect the total flux.

**RXCJ2220.5-3509**, A3866, has an AGN found in our spectroscopic follow-up 40 arcsec from the X-ray center at  $z = 0.0754$ . The X-ray emission shows a small but significant extent, but the core of the emission looks like a point source. The cluster redshift is measured as  $z = 0.1544$  and the optical image shows a nice cluster with a dominant giant galaxy close to the X-ray maximum. We expect that the X-ray emission from the cluster is partly contaminated by the AGN.

**RXCJ2234.5-3744**, A3888, is a cluster in which we also detected a Seyfert 1 galaxy within 2 arcmin from the center (A. K. Romer, Ph.D. Thesis). Therefore, there was some concern about the X-ray contamination from the AGN in this source. An XMM-Newton observation (P.I. A.C. Edge) allows us to distinguish the cluster and AGN X-ray emission. We find that the AGN contribution is about 10% of the total emission in the 0.5 - 2.0 keV band. 70 coincident galaxy redshifts confirm the existence of a cluster at this position.

**RXCJ2251.7-3206** is an X-ray source that appears point-like in RASS with a hardness ratio which is too soft by about  $2.9\sigma$  compared to the expectation for cluster emission. It has been found to be a radio source (Bauer et al. 2000) classified as a BL Lac (Schwöpe et al. 2000). We have one galaxy redshift for this cluster. The question

if it is an X-ray BL Lac or an X-ray cluster is undecided. This is to be clarified by further observations.

**RXCJ2351.6-2605** contains an AGN within 0.2 arcmin of our reference position identified by Caccianiga et al. (2000). The X-ray source is, however, extended with high significance, and the X-ray hardness ratio is perfectly consistent with thermal emission from a cluster. We do not detect a signature of point source contribution. Therefore, the identification of this X-ray source as a cluster is safe in spite of the coincidence with the AGN.

For some of the objects in this list, where the central cluster galaxy is identified with an AGN because of the observation of emission lines, the emission lines could also be associated to the cluster cooling core. Emission lines with preferentially low excitation energies are frequently observed in cooling core clusters (e.g. Crawford et al. 1999 and references therein). In these cases the dominant X-ray emission comes from the cluster and its cooling core. Therefore the observation of emission lines in the central cluster galaxies does not cast doubts on the cluster identification in general.

### 7.1. Objects removed from the present catalogue at final inspection

In the final two observing runs a number of cluster candidates were observed which had been flagged to be weak cluster candidates. A large fraction of them turned out to be clusters at the telescope and were therefore included in the catalogue. Now, during this final inspection a few of them turn out to be most probably optical clusters with a dominant X-ray AGN. In the following we list these 7 objects which were excluded from our catalogue.

**RXCJ0730.8-6602** looks like a point source. The central galaxy with a redshift of  $z = 0.1063$  could be an AGN; it has a bright core in the optical image. While the DSS image shows a trace of a promising galaxy grouping at the center of the X-ray position, a deeper R-band CCD did not confirm the presence of a rich enough cluster. The Parks 4.85 GHz survey lists a 84 mJy radio source, PMN0730-6602, (Griffith & Wright 1993) and the SUMSS survey (Mauch et al. 2003) as a 81.7 mJy source at 485 MHz. Therefore we have removed this object from the final catalogue and classify it tentatively as an X-ray AGN, possibly a BL Lac, within a galaxy group, where the X-ray emission comes preferentially from the AGN.

**RXCJ0934.4-1721** is a source with a marginal X-ray extent, but a hardness ratio consistent with thermal cluster emission within  $1\sigma$ . There is no striking galaxy overdensity in deeper optical images and no clear central BCG. A galaxy close to the center with a redshift of  $z = 0.2499$  was identified as a BL Lac candidate by Bauer et al. (2000) in the ROSAT-NVSS correlation sample. Therefore, this object is most probably not a cluster and was removed from our cluster catalogue.

**RXCJ1046.8-2535** looks like a point source in the RASS and is confirmed to be a point source in a ROSAT

HRI observation. Therefore, a cluster identification is ruled out for the dominant fraction of the X-ray emission. Nevertheless we find an optical cluster at redshift  $z = 0.2426$  with 8 coincident galaxy velocities. The source is also listed as a radio source in Condon et al. (1998) and Bauer et al. (2000). There is an indication in the HRI observation that there is a faint halo underneath the point source with a flux of at most 5% of that of the central source, which could be the emission from the cluster. The flux is, however, more than an order of magnitude below the REFLEX limit and therefore the cluster was removed from the REFLEX sample. This object falls most probably into the category of X-ray AGN in a galaxy group or cluster.

**RXCJ1213.3-2617** is coincident within 0.5 arcmin with a BL Lac identified by Fischer et al. (1998). Our spectrum of the central galaxy does not show an AGN or BLLac signature, however, and a CCD image provides some indication of a cluster. The X-ray emission is not significantly extended and the spectral hardness ratio is consistent with thermal cluster emission. A short ROSAT HRI exposure (2.7 ksec) shows only a point source, whose flux corresponds only to about 0.13 PSPC counts  $s^{-1}$  compared to 0.244 observed in the survey. There is no signature of further extended emission in the HRI image. Therefore the most likely interpretation of this X-ray source is an AGN which has shown a dimming by a factor of 1.8 between the two ROSAT observations.

**RXCJ1545.7-2339** appears as point-like in RASS, but has a reasonable hardness ratio for cluster emission. The archival HRI data show that more than 90% of the flux comes from a point source. Since the total flux of the source is only about twice above the REFLEX flux limit and since the cluster emission for this object at a redshift of 0.1205 should well be extended at the HRI resolution, we remove this source from the REFLEX sample. Bauer et al. (2000) list this as a radio source without further classification, making an AGN counterpart likely, but our ESO spectroscopic observations provided no evidence for an AGN. Two coincident galaxy redshifts found make it likely that the AGN resides in a group or cluster.

**RXCJ2040.0-7114**, tentatively identified with the cluster A3701 at redshift  $z = 0.1607$ , is an X-ray source that appears point-like in the RASS with a hardness ratio consistent with cluster emission. An archival ROSAT HRI observation shows a surface brightness distribution with a bright point source and a faint, small halo with an upper limit on the flux contribution of only a few percent. This brings this X-ray source well below the REFLEX flux limit and we removed this source from the REFLEX catalogue. An R-band CCD image shows a nice galaxy cluster with two bright central galaxies, which is no surprise as it was already classified as a cluster by Abell et al. (1989). Our spectroscopic follow-up provides 12 coincident galaxy redshifts confirming the cluster detection. Therefore, this object falls most probably into the category of X-ray luminous AGN in a galaxy cluster.

**RXCJ2041.8-3733**, tentatively identified with the cluster S892 at redshift  $z = 0.0997$  (offset  $\sim 5$  arcmin), is an X-ray source that appears point-like in the RASS with a hardness ratio which is too soft by about  $1.8\sigma$  compared to the expectation for cluster emission. An archival ROSAT HRI observation shows only a point source. Our spectroscopic follow-up observations show a Seyfert 1 spectrum for the central galaxy and provide 8 further coincident galaxy redshifts. A deep R-band image shows a cluster with an appearance consistent with the determined redshift around  $z = 0.1$  and the central galaxy appears to have a bright core. At the measured redshift this cluster should appear clearly as an extended X-ray source. in the RASS and definitely in the HRI image. Therefore we identify the main X-ray emission with the AGN and removed this object from the REFLEX catalogue.

The source is also listed in the bright RASS - NVSS correlation by Bauer et al. (2000) as an unclassified radio source and as a cluster in the ROSAT Bright Survey (Schwope et al. 2000).

## 8. Notes on double clusters

One problem in defining an X-ray cluster catalogue, as well as in comparing different cluster catalogues, is the identification of double clusters and of single clusters with substructure. This becomes obvious when we compare our results to other compilations in the next section. For the present catalogue we have taken a very pragmatic approach and made the distinction on the basis of a visual inspection as to how well the different parts can be separated. If the X-ray halos are hardly connected in the RASS images, given the short exposure, we treated them a separate units, while different maxima still engulfed by a common X-ray halo were treated as multiple-maxima clusters. This is a subjective criterion because the distinction is exposure and distance dependend. Also due to the short exposure in the RASS only a smaller fraction of the objects in this category will be found having enough source counts. Therefore a catalogue with any kind of completeness is extremely difficult to produce. A more viable approach is possibly a statistical characterization of the type used by Schuecker et al. (2001b) to describe the substructure frequency in the brighter REFLEX clusters. Therefore the present compilation is merely pointing out the most obvious examples of the two kinds, which could also be interesting targets for follow-up studies.

We distinguish between two classes of objects in the catalogue: close cluster pairs and clusters with two pronounced X-ray maxima in the surface brightness distribution which were treated as single units. In total we find 10 close cluster pairs (including one triplet and one quadruplet) at closely concordant redshifts, listed in Table 11. We have not included pairs seen only in projection where the redshift of the two components is clearly different. Table 12 lists those 14 clusters which feature two or several distinct X-ray maxima.

**Table 11.** List of cluster pairs and close groupings in the REFLEX catalogue

name	redshift	alternativename
RXCJ0229.3 – 3332	0.0779	
RXCJ0230.7 – 3305	0.0760	A3027
RXCJ0542.1 – 2607	0.0380	
RXCJ0545.4 – 2556	0.0424	A548W
RXCJ0548.6 – 2527	0.0410	A548E
RXCJ0626.3 – 5341	0.0531	3391
RXCJ0627.2 – 5428	0.0512	3395
RXCJ1254.3 – 2901	0.0553	A3528a
RXCJ1254.6 – 2913	0.0532	A3528b
RXCJ1255.5 – 3019	0.0544	A3530
RXCJ1257.2 – 3022	0.0555	A3532
RXCJ1327.9 – 3130	0.0482	A3558, Shapley center
RXCJ1329.7 – 3136	0.0495	Shapleycenter
RXCJ1331.5 – 3148	0.0429	Shapley center
RXCJ1333.6 – 3139	0.0502	A3562, Shapleycenter
RXCJ1347.2 – 3025	0.0141	A3574W, substructure
RXCJ1349.3 – 3018	0.0141	A3574E, main cluster
RXCJ2014.2 – 8038	0.1373	A3664
RXCJ2016.2 – 8047	0.1309	A3666
RXCJ2145.9 – 1006	0.0808	A2377
RXCJ2147.0 – 1019	0.0780	
RXCJ2152.2 – 1942	0.0963	A2384b
RXCJ2152.4 – 1933	0.0943	A2384a

Another complication arises in the cluster redshift determination as quite frequently several redshift groupings are found in the line-of-sight towards the cluster, indicating that several clusters and groups of galaxies are seen in projection, or narrow features of the large-scale structure (like walls and filaments) are threaded by the line-of-sight. In this case we have assigned the redshift to the cluster, which is derived from the largest number galaxies (including the bright central galaxy). In most cases the assignment is quite obvious, as illustrated by Table 13 for the combined data of our follow-up observations and the literature search. The table is ordered such that the first component refers to the chosen cluster identification while the remaining components are ordered by their redshift. The table also gives a helpful reference for those cases where discrepancies may be found in future observations. Most of the detailed information listed in the table comes from the ESO key program of the ENACS survey by Katgert et al. (1996) and Mazure et al. (1996). For each line-of-sight component we list the redshift and the number of known coincident galaxies.

## 9. Comparison to other catalogues

We have inspected the previously published catalogues of clusters detected in the RASS, to further check the completeness of our sample. Of these previous surveys the RASSB1 (De Grandi et al. 1999), the XBACS (Ebeling et



**Table 12.** List of REFLEX clusters with two or more clearly visible X-ray maxima

name	morphology	orientation
RXCJ0034.6 – 0208	two maxima	East – West
RXCJ0152.7 – 0100	two maxima	East – West
RXCJ0157.4 – 0550	two maxima	NE – SW
RXCJ0330.0 – 5235	two maxima	NE – SW
RXCJ0624.6 – 3720	two maxima	East – West
RXCJ0948.6 – 8327	two maxima	East – West
RXCJ0956.4 – 1004	three maxima	NE – W – S (diffuse)
RXCJ1305.9 – 3739	two maxima	NE – SW
RXCJ1330.8 – 0512	large elongation	towards NE
RXCJ2106.0 – 3846	two maxima	NE – SW
RXCJ2157.4 – 0747	two maxima	East – West
RXCJ2202.0 – 0949	two maxima	NE – SW
RXCJ2218.2 – 0350	two maxima	NEE – SWW
RXCJ2319.2 – 6750	two maxima	North – South

al. 1998), the SGP Survey (Cruddace et al. 2002, 2003), and HIFLUGCS (Reiprich & Böhringer 2002) surveys have made use of the material that was compiled during the ongoing REFLEX survey. Thus these samples are not independent. But since we have used a very strict automated selection criterion for the primary selection of the cluster candidates and have not included arbitrarily all we know about clusters in the REFLEX region, this is a very important completeness test and a test of the galaxy overdensity detection method applied to the COSMOS data base as described in paper I.

The XBACS catalogue lists 5 clusters that are not included in REFLEX after four clusters are removed from the correlation (A3186, A3216, A3230, A3389), because they are located in the Magellanic cloud regions that have been excised in the present sample. For these 5 objects we have a definite reason for the exclusion. A3041: the REFLEX flux is  $2.58 \cdot 10^{-12} \text{ erg s}^{-1} \text{ cm}^{-2}$  and below the current flux limit; A467: is characterized by a point source which is by about  $5\sigma$  too soft to be consistent with cluster emission; A3662: the REFLEX flux is  $1.67 \cdot 10^{-12} \text{ erg s}^{-1} \text{ cm}^{-2}$ , below the flux limit of REFLEX, but there is a  $\sim 40\%$  uncertainty in the flux due a low exposure of only 122 sec in RASS II; A3701: (RXCJ2040.0-7114) was removed from our cluster list as explained in section 7; A3716: has no exposure in RASS2 (This is implicitly accounted for in the construction of the sky coverage map). Thus no cluster has been missed in REFLEX which is included in XBACS. There are further some nomenclature problems that are encountered in this comparison: A189 in XBCAS is a misclassification since the Abell cluster is about half a degree away and the correct identification should be NGC 533 as in REFLEX, A1664 is identical with A3541, A3017 in XBACS is identified with A3016 in REFLEX. Three clusters are listed with two separate components in XBACS which are treated as one source in the present compilation: A901, A1631, and A1750.

A comparison with the SGP sample by Cruddace et al. (2002, 2003) which is based on the same X-ray source catalogue and source characterization as REFLEX but used a different optical search method, shows only two additional clusters with a recently determined flux above the REFLEX flux limit: RXCJ2356.0-0129 which is here treated as a double source where each component falls below the flux limit, and RXCJ0016.3-3121 which was for the REFLEX catalogue deblended from a soft contaminating component and therefore fell below the flux limit after this treatment. Six clusters listed in the SGP sample catalogue with a flux above the REFLEX flux limit have slightly lower fluxes in REFLEX and are scattered below the REFLEX flux limit: RXCJ2306.8-1324, RXCJ0048.6-2114, RXCJ0108.5-4021, RXCJ0212.8-4707, RXCJ0244.1-2611, RXCJ0248.2-0216. They will be included in REFLEX II. The following 9 clusters in the SGP region are only listed in the REFLEX catalogue: RXCJ0034.6-0208, RXCJ0043.4-2037, RXCJ0132.6-0804, RXCJ0250.2-2129, RXCJ0301.6+0155, RXCJ2211.7-0350, RXCJ2248.5-1606, RXCJ2251.7-3206, RXCJ2306.6-1319. Note that already four of these nine objects have a problematic identification, as discussed in section 7. Therefore the missing of these clusters is to a large part not a real incompleteness but a classification problem.

The southern RASS Bright sample, compiled from an earlier version of the ESO key program X-ray cluster identification list based on the RASS1 data set (De Grandi et al. 1999), contains two additional clusters that should be included in REFLEX. One was again found in our supplementary search for clusters among the sources found to be extended by the GCA analysis, RXCJ2129.6+0005 at  $z = 0.2347$ . This source and RXJ0600.5-4846 were not flagged by the optical correlation. Since these objects were not automatically included through the correlation with the COSMOS data we have not included them in the present list. RXCJ0528.9-3927 listed by De Grandi et al. is removed from the present list as explained in section 7. Two further objects from this catalogue have been removed from our sample in earlier steps of the identification RXJ2136.4-6224 is a point-like X-ray source coincident with a Seyfert 1 galaxy at  $z = 0.0588$  and RXJ2253.9-5812 is a point source with a soft spectrum coincident with the radio source PMNJ2253-5812. All the objects listed in the HIFLUGCS sample by Reiprich & Böhringer (2002) in the REFLEX survey area are included in the present catalogue.

## 10. Discussion and conclusions

More than 100 000 X-ray sources were identified in the ROSAT All-Sky Survey (Voges et al. 1999) and more than 10% of the X-ray sources in the sky away from the Galactic plane are expected to be galaxy clusters for the relevant range of flux limits. Thus taking into account the surely lower detection efficiency for extended cluster X-ray sources and the Galactic source population one can easily expect about 6000 - 8000 clusters among the X-ray sources

**Table 13.** Multiple redshift clustering in the line-of-sight of REFLEX clusters

Name	alt.name	redshifts						references
		Comp1	Comp2	Comp3	Comp4	Comp5	Comp6	
RXCJ0003.2 – 3555	A2717	0.0490(40)	0.0720(5)					2
RXCJ0011.3 – 2851	A2734	0.0620(83)	0.0260(5)	0.1190(4)	0.1410(6)			2
RXCJ0013.6 – 1930	A0013	0.0940(37)	0.0270(4)					<i>S</i> , 2, 140, 141
RXCJ0017.5 – 3509	A2755	0.0968(23)	0.1210(10)					<i>E</i> , 2, 3, 33, 140, 141
RXCJ0041.8 – 0918	A0085	0.0555(308)	0.0762					130, 148, 149
RXCJ0042.1 – 2832	A2811	0.1082(29)	0.0540(6)					<i>E</i> , 33, 96
RXCJ0056.3 – 0112	A0119	0.0442(104)	0.1400(4)					2
RXCJ0108.8 – 1524	A0151A	0.0533(63)	0.0410(25)	0.1000(35)				1, 2
RXCJ0110.0 – 4555	A2877	0.0238(58)	0.2470(97)					12, 130, 131, 146
RXCJ0115.2 + 0019	A0168	0.0450(76)	0.0176(4)	0.0720(4)	0.0890(7)			<i>S</i> , 2
RXCJ0137.2 – 0912		0.0409(5)	0.0700					<i>S</i> , 120
RXCJ0152.7 + 0100	A0267	0.2300(1)	0.0592(8)					55, 147, 159
RXCJ0152.9 – 1345	NGC0720	0.0050(3)	0.8348(6)					12, 160, 161
RXCJ0157.4 – 0550	A0281	0.1289(4)	0.088					<i>E</i> , 1
RXCJ0202.3 – 0107	A0295	0.0427(47)	0.1020(5)					2, 148, 162
RXCJ0231.9 + 0114	RCS145 <sup>d</sup>	0.0221(10)	0.2881					55, 64, 110
RXCJ0337.0 – 3949	A3142	0.1030(21)	0.0660(12)					2
RXCJ0338.4 – 3526	FORNAX	0.0051(32)	0.1124(48)					166, 167, 168, 170, 171
RXCJ0342.8 – 5338	A3158	0.0590(105)	0.0740(4)	0.1020(4)				2
RXCJ0408.2 – 3053	A3223	0.0600(81)	0.1100(8)	0.1370(8)				<i>E</i> , 2
RXCJ0448.2 – 2028	A0514	0.0720(90)	0.0850(4)	0.1100(8)				2
RXCJ0525.5 – 3135	A3341	0.0380(64)	0.0780(15)	0.1150(18)	0.1310(7)	0.1540(5)		2
RXCJ0525.8 – 4715	A3343	0.1913(5)	0.1626(6)					<i>E</i>
RXCJ0530.6 – 2226	A0543	0.1706(11)	0.0850(10)					<i>E</i> , 1
RXCJ0542.1 – 2607	CID36	0.0390(4)	0.0292(2)	0.0429(69)				<i>E</i> , 120
RXCJ0548.6 – 2527	A0548E	0.0420(237)	0.0310(4)	0.0630(9)	0.0870(14)	0.1010(21)	0.1380(4)	2, 3
RXCJ0637.3 – 4828	A3399	0.2026(11)	0.1180(3)	0.3796(2)				<i>E</i>
RXCJ0645.4 – 5413	A3404	0.1644(2)	0.3377(2)					<i>E</i>
RXCJ0658.5 – 5556	1ES0657 <sup>h</sup>	0.2965(78)	0.0790(3)					<i>E</i> , 73, 79
RXCJ0944.1 – 2116		0.0077(1)	0.0152(1)					<i>E</i> , 12, 84
RXCJ1039.7 – 0841	A1069	0.0650(35)	0.1140(4)					2
RXCJ1050.4 – 1250	USGCS152	0.0155(6)	0.0760(5)					<i>E</i> , 20, 31
RXCJ1141.4 – 1216	A1348	0.1195(6)	0.1392					<i>H</i> , 16
RXCJ1254.3 – 2901	A3528(A)	0.0542(69)	0.0730(9)					2
RXCJ1327.9 – 3130	A3558	0.0480(341)	0.0320(4)	0.0771(6)	0.1285(7)			1, 14, 44, 102, 141, 148
RXCJ1329.7 – 3136	A3558(B)	0.0488(57)	0.1823(4)					3, 14, 44, 63, 101, 102
RXCJ1330.8 – 0152	A1750	0.0852(46)	0.1492(3)					1, 41, 96
RXCJ1333.6 – 3139	A3562	0.0490(114)	0.0367(4)					1, 141
RXCJ1347.5 – 1144		0.4516(2)	0.2090(3)					<i>E</i>
RXCJ1401.6 – 1107	A1837	0.0698(38)	0.0372(14)					1
RXCJ1952.2 – 5503	A3651	0.0600(79)	0.1010(5)					2
RXCJ2012.5 – 5649	A3667	0.0556(162)	0.0350(2)	0.0990(5)				2, 3, 138, 140, 141
RXCJ2032.1 – 5627	A3685	0.1380(5)	0.2852(6)					<i>E</i>
RXCJ2034.3 – 3429	A3693	0.1240(6)	0.0910(16)					<i>E</i> , 3
RXCJ2034.7 – 3548	A3695	0.0894(81)	0.0934(18)	0.1310(7)				2, 140, 141
RXCJ2101.8 – 2802	A3733	0.0382(91)	0.0739(4)					13, 14, 146
RXCJ2104.3 – 4120	A3739	0.1651(2)	0.0820(16)					<i>E</i>
RXCJ2107.2 – 2526	A3744	0.0381(71)	0.0650(5)					2
RXCJ2146.3 – 5717	A3806	0.0760(99)	0.0540(9)	0.1380(4)				2
RXCJ2146.9 – 4354	A3809	0.0620(94)	0.0910(4)	0.1100(10)	0.1410(11)	0.1520(4)		2
RXCJ2154.1 – 5751	A3822	0.0760(84)	0.0390(4)	0.0520(4)	0.1020(4)			2
RXCJ2158.3 – 2006	A2401	0.0570(23)	0.0884(2)	0.0930(5)				2, 3
RXCJ2158.4 – 6023	A3825	0.0750(61)	0.1040(17)	0.1190(4)				2, 3
RXCJ2234.5 – 3744	A3888	0.1510(70)	0.2077(7)					1, 44
RXCJ2249.9 – 6425	A3921	0.0940(32)	0.1340(4)					<i>E</i> , 3
RXCJ2312.3 – 2130	A2554	0.1108(35)	0.0707(5)					38, 127
RXCJ2321.5 – 4153	A3998	0.0894(16)	0.0665(3)					<i>S</i> , 16, 31, 33, 48
RXCJ2336.2 – 3136	S1136	0.0643(2)	0.0260(3)					15, 52, 26
RXCJ2354.2 – 1024	A2670	0.0765(219)	0.1506(13)					66, 86, 105

The footnotes in the alternative name column (2) are explained in Table 10

in the bright and faint ROSAT All-Sky Survey catalogue. The REFLEX cluster sample with a flux limit of  $3 \cdot 10^{-12}$  erg s<sup>-1</sup> cm<sup>-2</sup> is therefore only the tip of the iceberg of the RASS cluster population. However, the REFLEX sample is constructed from a selection with a relatively high flux limit, in order to yield a sample of high quality. The median number of detected source photons for the REFLEX clusters is 79 photons. Relatively safe source detections, e.g. as listed in the RASS faint source catalogue, can still be obtained from a detection of only 6 photons in a detection aperture with 2 arcmin radius, which for the typical exposure of about 400 sec and a typical background in the hard band (channel 52 - 201) of about  $3 \cdot 10^{-4}$  cts s<sup>-1</sup> arcmin<sup>-2</sup> would contain about 1.5 background photons. Thus a detection of 6 photons corresponds roughly to a  $3.7\sigma$  background enhancement and roughly to a flux limit of  $3 \cdot 10^{-13}$  erg s<sup>-1</sup> cm<sup>-2</sup> - a flux limit one order of magnitude below the REFLEX cut. Thus the RASS provides the prospect of finding many more clusters than presented here, but the price is a much lower quality of the X-ray characteristics as well as a much more difficult job for the definitive source identification.<sup>1</sup>

With the relatively high flux cut the high quality of the REFLEX sample is characterized by the following most important properties: (i) a flux determination with a typical accuracy of 10 - 20%, (ii) a large fraction of the cluster X-ray sources can be characterized as extended ( $\sim 80\%$ ) which adds very much to a safe identification, (iii) we can in general obtain a meaningful spectral hardness ratio which allows further discrimination in our identification, (iv) we arrive at a selection function which is almost homogeneous across the sky. At an even higher flux limit, e.g.  $6 \cdot 10^{-12}$  erg s<sup>-1</sup> cm<sup>-2</sup>, only 9 clusters are not flagged as extended X-ray sources by our analysis. The spatially very homogeneous selection function ensures for example that, for a detection limit of 10 photons used in most of our spatial distribution analysis, the flux limit is reached in 97% of the sky and only small corrections apply for the remaining region. The selection function is also characterized by the analysis of the source photon count distribution shown in Fig. 25 of paper I, from which we conclude that only about 14 clusters might be missed if the correction for the lower sensitivity in some regions of the REFLEX survey is neglected. Therefore the cosmological results derived by us in the series of REFLEX papers could also be reproduced in good approximation if the angular modulation of the selection function given in Tables 8 and 9 were neglected.

Since the completion of the optical follow-up observations for REFLEX we have already embarked on the extension of this survey, REFLEX II which is now close to complete down to a flux limit of  $1.8 \cdot 10^{-12}$  erg s<sup>-1</sup> cm<sup>-2</sup>

including more than 800 clusters. We stress that in addition to the fact that the X-ray parameters become less accurate at these lower fluxes, the identification work becomes significantly harder: the optical counter parts are less striking on for example the optical DSS images, it is more difficult to detect and catch the signature of contamination AGN, and the spatial modulation of the selection function can no longer be neglected. Therefore the gain in the statistics by the increase of the sample size has a price and there is some optimum quality and size of the cluster sample, depending of course on the application, for which the flux limit should not be much lower than that of REFLEX I.

Further work on the identification of RASS clusters is useful if the RASS data can be combined with survey information from other wavelengths. A good example is the Sloan Digital Sky Survey. Based on the parent SDSS cluster sample from Sheldon et al. (2001) we have demonstrated that we can almost recover the REFLEX X-ray luminosity function for clusters down to a flux limit in the RASS of  $8 \cdot 10^{-13}$  erg s<sup>-1</sup> cm<sup>-2</sup>. Work in progress on the combined detection of galaxy clusters in X-rays (RASS) and the optical (SDSS) extends these detections to even lower fluxes (Schuecker et al., 2003c) recovering an arial density of about 0.5 clusters deg<sup>-2</sup>.

The high quality of the REFLEX sample makes the present catalogue a useful basis for the careful selection of targets for detailed follow-up studies at all wavelengths. A deep XMM-Newton follow-up study has been targeted at a complete sample of 13 X-ray luminous REFLEX clusters ( $L_x \geq 1 \cdot 10^{45}$  erg s<sup>-1</sup>) in the redshift interval 0.27 to 0.31 (Zhang et al. 2003) to study for example the evolution of the cluster population at the high mass end, from  $z \sim 0.3$  to the present. One first result of this study is that all 13 clusters of the sample show X-ray emission which is dominated by thermal, diffuse intracluster medium radiation and only two clusters have a point source contribution of at most 30%. This provides a very nice confirmation for the REFLEX cluster sample, since at this upper end of the redshift distribution of the REFLEX clusters it is already quite difficult to recognize the point source contamination of the cluster emission. The same clusters form also the subject of a very detailed optical study with the VLT in the frame of a Large Program to study among other objectives the galaxy dynamics, the characteristics of the galaxy population, and the supernova rate. Recently a Large XMM-Newton follow-up program has been approved, to study in detail 33 clusters from REFLEX selected in such a way that they form a volume complete sample (with a complex but known volume structure), that they cover the X-ray luminosity range almost homogeneously, and that they are optimally observed with the field-of-view of the XMM-Newton instruments. The main goal of this survey is to understand the statistics of cluster structure and the scaling relations of observable and physical parameters, like the very important X-ray luminosity-mass and temperature-mass relations. These

<sup>1</sup> Already the number of spurious sources is expected to be of the order of 1000 in the REFLEX area for the mentioned low flux limit. This is in comparison to a few Thousand clusters to be found in the same area not unreasonable. But good extra information as for example optical or other wavelength data is mandatory for an identification in this case.

relations form the backbone of the cosmological application of cluster samples like REFLEX.

Further applications of the REFLEX catalogue are in progress involving the study of radio haloes, Sunyaev-Zeldovich observations, correlations with microwave background data (e.g. WMAP), and gravitational lensing studies. The cosmological applications of the REFLEX sample demonstrates the power of using clusters of galaxies as cosmological probes in a way complementary to studies based on supernovae and on the microwave background. Therefore we hope that in a next step a new X-ray all-sky survey which goes much deeper, covers a larger X-ray band width, and provides a better angular resolution will enable us with much higher precision to test cosmological models and determine cosmological parameters. There is a constant effort in the X-ray community to make such a project and such an important progress possible.

*Acknowledgements.* We like to thank the ROSAT team at MPE for the support with the data reduction of the ROSAT All-Sky Survey and the staff of ESO La Silla for the technical support during the numerous observing runs for the ESO key programme. We also thank G. Vettolani, W.C. Seitter, K.A. Romer, U.G. Briel, H. Ebeling, R. Dümmler, T.H. Reiprich, R.A. Schwarz, S. Molendi, H. Gursky, and D. Yentis for help during the programme. We also thank the referee for very useful comments.

The production of the COSMOS digital optical data base, based on scans of the UK Schmidt southern sky survey IIIa-J plates, and the development of techniques for detecting cluster candidates in the COSMOS data, was a major project, requiring the coordinated efforts of Harvey MacGillivray (ROE), Daryl Yentis and Brad Stuart (NRL), and John Wallin (George Mason University).

This research also made use of the NASA/IPAC Extragalactic Database (NED), which is operated by the Jet Propulsion Laboratory, California Institute of Technology, under contract with NASA. P.S. acknowledges the support by the Verbundforschung under grant No. 50 OR 93065.

## References

- Abell, G.O., 1958, ApJS, 3, 211  
 Abell, G.O., Corwin, H.G. & Olowin, R.P., 1989, ApJS, 70, 1  
 Allen, S.W., Edge, A.C., Fabian, A.C., et al., 1992, MNRAS, 259, 67  
 Alonso, M.V., Valotto, C., Lambas, D.G., Muriel, H., 1999, MNRAS, 308, 618  
 Andernach, H. & Tago E., 1998, in Proceedings of the 12th Potsdam Cosmology Workshop: Large Scale Structure: Tracks and Traces, Mueller, S. Gottloeber, J.P. Muecket, J. Wambsganss (eds.), World Scientific, 1998, p. 147  
 Andernach, H. 2002 (private communication) upgrade of the compilation by Andernach & Tago, 1998  
 Anders, E. & Grevesse, N., 1989, Geochimica et Cosmochimica Acta, 53, 197  
 Arnaud, M., Hughes, J.P., Forman, W., Jones, C., Lachieze-Rey, M., Yamashita, K., Hatsukade, I., 1992, ApJ, 390, 345  
 Bade, N., Fink, H.H., Engels, D., Voges, W., Hagen, H.-J., Wisotzki, L., Reimers, D., 1995, A&A, 110, 469  
 Bardelli, S., Zucca, E., Vettolani, G., Zamorani, G., Scaramella, R., Collins, C. A., MacGillivray, H. T., 1994, MNRAS, 267, 665  
 Bardelli, S., Pisani, A., Ramella, M., Zucca, E., Zamorani, G., 1998, MNRAS, 300, 589  
 Bardelli, S., Zucca, E., Baldi, A., 2001, MNRAS, 320, 387  
 Barrena, R., Biviano, A., Ramella, M., Falco, E.E., Seitz, S., 2002, A&A, 386, 816  
 Barton, E., Geller, M.J., Ramella, M., Marzke, R.O., Da Costa, L.N., 1996, AJ, 112, 871  
 Batuski, D.J., Burns, J.O., Newberry, M.V., Hill, J.M., Deeg, H.-J., Laubscher, B.E., Elston, R.J., 1991, AJ, 101, 1983  
 Batuski, D.J., Miller, C.J., Slinglend, K.A., Balkowski, C., Maurogordato, S., Cayatte, Y., Felenbok, P., Olowin, R., 1999, ApJ, 520, 491  
 Bauer, F.E., Condon, J.J., Thuan, T.X., Broderick, J.J., 2000, ApJS, 129, 547  
 Beers, T.C., Forman, W., Huchra, J.P., Jones, C., Gebhardt, K., 1991, AJ, 102, 1581  
 Beers, T.C., Gebhardt, K., Huchra, J.P., Forman, C., Bothun, G.D., 1992, ApJ, 400, 410  
 Beers, T.C., Kriessler, J.R., Bird, C.M., Huchra, J.P., 1995, 109, 874  
 Bernardi, M., Alonso, M.V., da Costa, L.N., Willmer, C.N.A., Wegner, G., Pellegrini, P.S., Rite, C., Maia, M.A.G., 2002, AJ, 2990  
 Blakeslee, J.P. & Tonry, J., 1992, AJ, 103, 1457  
 Böhringer, H., Guzzo, L., Collins, C.A., et al., 1998, The Messenger, No. 94, 21  
 Böhringer, H., Voges, W., Huchra, J.P., McLean, B., Giacconi, R., Rosati, P., Burg, R., Mader, J., Schuecker, P., Simić, D., Komossa, S., Reiprich, T.H., Retzlaff, J., Trümper, J., 2000, ApJS, 129, 435  
 Böhringer, H., Schuecker, P., Guzzo, L., Collins, C.A., Voges, W., Schindler, S., Neumann, D.M., Cruddace, R.G., De Grandi, S., Chincarini, G., Edge, A.C., MacGillivray, H.T., Shaver, P., 2001a, A&A, 369, 826 (**Paper I**)  
 Böhringer, H., Schuecker, P., Lynam, P., Reiprich, T.H., Collins, C.A., Guzzo, L., Ikebe, Y., Molinari, E., Barone, L., Ambros, C., 2001, The Messenger, 106, 24  
 Böhringer, H., Schuecker, P., Komossa, S., Retzlaff, J., Reiprich, T.H., & Voges, 2001b, in *Mapping the Hidden Universe*, Proc of a workshop in Guanajuato, Mexico, February 2000, R.C. Kraan-Korteweg, P.A. Henning, & H. Andernach (eds.), p. 93, astro-ph/0011461  
 Böhringer, H., Collins, C.A., Schuecker, P., Guzzo, L., Voges, W., Neumann, D.M., Schindler, Cruddace, R.G., De Grandi, S., Chincarini, G., Edge, A.C., Reiprich, T.H., & Shaver, P., 2002, ApJ, 566, 93 (**Paper IV**)  
 Burns, J.O., Ledlow, M.J., Loken, C., et al., 1996, ApJ, 467, L49  
 Caccianiga, A., Maccacaro, T., Wolter, A., Della Ceca, R., Gioia, I. M., 2000, A&AS, 144, 247  
 Caldwell, N., Rose, J.A., 1997, AJ, 113, 492  
 Caretta, C.A., Maia, M.A.G., Kawasaki, W., Willmer, C.N.A., 2002, AJ, 123, 1200  
 Carter, D. & Malin, D.F., 1983, MNRAS, 203p, 49  
 Cavaliere, A. & Fusco-Femiano, R., 1976, A&A, 49, 137  
 Chen, J., Huchra, J.P., McNamara, B., & Mader, J., 1998, BAAS, 30, 1307 – data located at <http://cfa-www.harvard.edu/~huchra/clusters>  
 Christiani, S., de Souza, R., D’Odorico, S., Lund, G., Quintana, H., 1987, A&A, 179, 108

- Collins, C.A., Guzzo, L., Nichol, R.C., & Lumsden, S.L., 1995, *MNRAS*, 274, 1071
- Collins, C.A., Guzzo, L., Böhringer, H., Schuecker, P., Chincarini, G., Cruddace, R., De Grandi, S., Neumann, D., Schindler, S., & Voges, W., 2000, *MNRAS*, 319, 939, (**Paper II**)
- Colless, M., Dalton, G., Maddox, S., 2001, *MNRAS*, 328, 1039
- Collins, M., Hewett, P., 1987, *MNRAS*, 224, 453
- Condon, J.J., Cotton, W.D., Greisen, E.W., Yin, Q.F., Perley, R.A., Taylor, G.B., Broderick, J.J., 1998, *AJ*, 115, 1693
- Couch, W.J. & Sharples, R.M., *MNRAS*, 1987, 229, 423
- Couch, W.J., Barger, A.J., Smail, I., Ellis, R.S., Sharples, R.M., *ApJ*, 1998, 497, 188
- Crawford, C.S., Edge, A.C., Fabian, A.C., Allen, S.W., Böhringer, H., Ebeling, H., McMahon, R.G., Voges, W., 1993, 274, 75
- Crawford, C.S., Edge, A.C., Fabian, A.C., Allen, S.W., Böhringer, H., Ebeling, H., McMahon, R.G., Voges, W., 1995, *MNRAS*, 274, 75
- Crawford, C.S., Allen, S.W., Ebeling, H., Edge, A. C., Fabian, A.C. 1999, *MNRAS*, 306, 857
- Cruddace, R., Voges, W., Böhringer, H., Collins, C.A., Romer, K.A., MacGillivray, H.T., Yentis, D., Schuecker, P., Ebeling, H., De Grandi, S., 2002, *ApJS*, 140, 239
- Cruddace, R., Voges, W., Böhringer, H., Collins, C.A., Romer, K.A., MacGillivray, H.T., Yentis, D., Schuecker, P., Ebeling, H., De Grandi, S., 2003, *ApJS*, 144, 299
- da Costa, L.N., Willmer, C., Pellegrini, P.S., Chincarini, G., 1987, *AJ*, 93, 1338
- da Costa, L.N., Pellegrini, P.S., Davis, M. Meiksin, A., Sargent, Wallace L.W., Tonry, J.L., 1991, *ApJS*, 75, 935
- da Costa, L. N., Willmer, C.N.A., Pellegrini, P.S., et al. 1998, *AJ*, 116, 1
- Dale, D.A., Giovanelli, R., Haynes, M.P., Scodreggio, M. 1998, *AJ*, 115, 418
- Dalton, G.B., Efstathiou, G., Maddox, S.J., & Sutherland, W.J., 1994, *MNRAS*, 269, 151
- Dalton, G.B., Maddox, S.J., Sutherland, W.J., & Efstathiou, G., 1997, *MNRAS*, 289, 263
- Dantas, C.C., De Carvalho, R.R., Capelato, H.V., Mazure, A., 1997, *ApJ*, 485, 447
- Davoust, E. & Considere, S., 1995, *A&AS*, 110, 19
- De Carvalho, R.R., Ribiero, A.L.B., Capelato, H.V., Zepf, S.E., 1997, *ApJS*, 110, 1
- De Grandi, S., Molendi, S., Böhringer, H., & Voges, W., 1997, *ApJ*, 486, 738
- De Grandi, S., Böhringer, H., Guzzo, L., et al., 1999, *ApJ*, 514, 148
- den Hartog, R., Ph.D. thesis, Univ. Leiden (1995)
- den Hartog, R. & Katgert, P., 1996, *MNRAS*, 279, 349
- de Vaucouleurs, G., de Vaucouleurs, A., Corwin, H.G. Jr., Buta, R.J., Paturel, G., Fouqué, P., Third Reference Catalogue of Bright Galaxies, Springer Verlag, 1991
- Di Nella, H., Couch, W.J., Paturel, G., Parker, Q.A., 1996, *MNRAS*, 283, 367
- Dickey, J.M. & Lockman, F.J., 1990, *ARAA*, 28, 215
- Dressler, A., Shectman, S.A., 1988, *AJ*, 95, 284
- Dressler, A., Schechter, P.L., Rose, J.A., 1986, *AJ*, 91, 1058
- Drinkwater, M.J., Proust, D., Parker, Q.A., Quintana, H., Slezak, E., 1999, *PASA*, 16, 113
- Drinkwater, M.J., Gregg, M.D., Holman, B.A., Brown, M.J.I., 2001, 326, 1076
- Durret, F., Felenbork, P., Lobo, C., Slezak, E., 1998, *A&AS*, 129, 28
- Ebeling, H., Voges, W., Böhringer, H., Edge, A.C., 1993, *A&A*, 275, 360
- Ebeling, H., Maddox, S.J., 1995, *MNRAS*, 275, 1155
- Ebeling, H., Voges, W., Böhringer, H., Edge, A.C., Huchra, J.P., Briel, U.G., 1996, *MNRAS*, 281, 799
- Ebeling, H., Edge, A.C., Böhringer, H., et al., 1998, *MNRAS*, 301, 881
- Ebeling, H., Edge, A.C., Allen, S.W., Crawford, C.S., Fabian, A.C., & Huchra, J.P., 2000a, *MNRAS*, 318, 333
- Ebeling, H., Jones, L.R., Perlman, E., Scharf, C., Horner, D., Wegner, G., Malkan, M., Fairley, B.W., Mullis, C.R., 2000b, *ApJ*, 534, 133
- Ebeling, H., Edge, A.C., Henry, J.P., 2001, *ApJ*, 553, 668
- Ebeling, H., Mullis, C.R., Tully, R.B., 2002, *ApJ*, 580, 774
- Edge, A.C. & Stewart, G.C., 1991, *MNRAS*, 252, 414
- Edge, A.C., Stewart, G.C., Fabian, A.C., 1992, *MNRAS*, 258, 177
- Einasto, M., Einasto, J., Tago, E., Mueller, V., Andernach, H., 2001, *AJ*, 122, 2222
- Ellis, R.S., Gray, P.M., Carter, D., Godwin, J., 1984, *MNRAS*, 206, 285
- Ettori, S., Guzzo, L., Tarengi, M., 1995, *MNRAS*, 276, 689
- Fadda, D., Girardi, M., Giuricin, G., Mardirossian, F., Mezzetti, M., 1996, *ApJ*, 473, 670
- Fairall, A.A., 1984, *AJ*, 210, 69
- Fairall, A.P., Willmer, C.N.A., Calderon, J.H., Latham, D.W., Nicolaci da Costa, L., Pellegrini, P.S., Nunes, M.A., Focardi, P., Vettolani, G., 1992, *AJ*, 103, 11
- Falco, E.E., Kurtz, M.J., Geller, M.J., Huchra, J.P., Peters, J. Berlind, P., Mink, D.J., Tokarz, S.P., Elwell, B., 1999, *PASP*, 111, 438
- Fetisova, T.S., Kuznetsov, D.Yu., Lipovetskii, V., Starobinsky, A.A., Olowin, R.P., 1993, *Astron. Lett.*, 19, 198
- Fischer, J.-U., Hasinger, G., Schwobe, A.D., Brunner, H., Boller, T., Trumper, J., Voges, W., Neizvestny, S., 1998, *AN*, 319, 347
- Garilli, B., Maccagni, D., Vettolani, G., 1991, *AJ*, 101, 795
- Garilli, B., Maccagni, D., Tarengi, M., 1993, *A&AS*, 100, 33
- Gioia, I.M., Maccacaro, T. Morris, S.L., Schild, R.E., Stocke, J.T., Wolter, A., & Henry, J.P., 1990, *ApJS*, 72, 567.
- Gioia, I.M., Henry, J.P., Mullis, C.R., et al. 2003, *ApJS*, 149, 29
- Goto, T., Sekiguchi, M., Nichol, R.C., Bahcall, N.A., Kim, R.S.J., Annis, J., Ivezić, Z., Brinkmann, J., Hennessy, G.S., Szokoly, G.P., Tucker, D.L., 2002, *AJ*, 123, 1807
- Grazian, A., Omizzolo, A., Corbally, C., Cristiani, S., Heanelt, M.G., Vanzella, E., 2002, *AJ*, 124, 2955
- Green, M.R., Godwin, J.G., Peach, J.V., 1988, *MNRAS*, 234, 1051
- Green, M. R., Godwin, J.G., Peach, J.V., 1990, *MNRAS*, 243, 159
- Green, M. R., Godwin, J.G., Peach, J.V., 1999, *AJ*, 118, 1468
- Griffith, M.R. & Wright, A.E., 1993, *AJ*, 105, 1666
- Guzzo, L., Böhringer, H., Schuecker, P., et al., 1999, *The Messenger*, No. 95, 27
- Heckman, T.M., O'Dea, C.P., Baum, S.A., Laurikainen, E., 1994, *ApJ*, 428, 65
- Henry, J. P., Gioia, I. M., Huchra, J. P., et al., 1995, *ApJ*, 449, 422 not yet quoted
- Henry, J. P., Mullis, C.R., 1997 (priv. com.)
- Henry, J.P., Gioia, I.M., Mullis, C.R., et al., 2001, *ApJ*, 553, L109
- Hewitt, A. & Burbidge, G., 1991, *ApJS*, 75, 297

- Heydon-Dumbleton, N.H., Collins, C.A., & MacGillivray, H.T., 1989, *MNRAS*, 238, 379
- Hickson, P., Mendes de Oliveira, C., Huchra, J.P., Palumbo, G.G., 1992, *ApJ*, 399, 353
- Hilker, M., Infante, L., Vieira, G., Kissler-Patig, M., Richtler, T., 1999, *A&A*, 134, 75
- Huchra, J.P., Postman, M., Geary, J., Geller, M.J., 1991 preprint (cited in Postman, Huchra & Geller 1992)
- Huchra, J., Latham, D.W., Da Costa, L.N., Pellegrini, P.S., Willmer, C.N.A., 1993, *AJ*, 105, 1637
- Huchra, J.P., Vogeley, M.S., Geller, M.J., 1999, *ApJS*, 121, 287
- Huchtmeier, W. K., 1994, *A&A*, 286, 389
- Jones, C. & Forman, W., 1999, *ApJ*, 511, 65
- Jorgensen, I., Franx, M., Kjaergaard, P., 1995, *MNRAS*, 276, 1341
- Kaldare, R., Colless, M., Raychaudhury, S., Peterson, B.A., 2003, *MNRAS*, 339, 652
- Kapahi, V.K., Athreya, R.M., van Bruegel, W., McCarthy, P.J., Subrahmanya, C.R., 1998, *ApJS*, 118, 275
- Katgert P., Mazure, A., Perea, J., den Hartog, R., Moles, M., et al., 1996, *A&A*, 310, 8
- Katgert, P., Mazure, A., den Hartog, R., Adami, C., Biviano, A., Perea, J. 1998, *A&AS*, 129, 399
- Kerscher, M., Mecke, K., Schuecker, P., Böhringer, H., Guzzo, L., Collins, C. A., Schindler, S., De Grandi, S., Cruddace, R., 2001, *A&A*, 377, 1
- Koranyi, D.M., Geller, M.J., 2002, *AJ*, 123, 100
- Kristian, J., Sandage, A., Westphal, J.A., 1978, *ApJ*, 221, 383
- Lauberts, A. & Valentijn, E.A., 1989, The surface photometry catalogue of the ESO-Uppsala galaxies, ESO, Garching, Germany
- Lauer, T.R. & Postman, M., 1994, *ApJ*, 425, 418
- Lebedev, V.S. & Lebedeva, I.A., 1992, A Compilation of Redshifts of Clusters of Galaxies (Special Astrophys. Obs. unpublished)
- Ledlow, M. J. & Owen, F.N., 1995, *AJ*, 110, 1959
- Ledlow, M. J., Loken, C., Burns, J. O., Owen, F.N., Voges, W., 1999, *ApJ*, 516, L53
- Lemonon, L., Pierre, M., Hunstead, R., Reid, A., Mellier, Y., Böhringer, H., 1997, *A&A*, 326, 34
- Liang, H., Lemonon, L., Valtchanov, I., Pierre, M., Soucail, G., 2000, *A&A*, 363, 440
- Loveday, J., Peterson, B.A., Maddox, S.J., Efstathiou, G., 1996, *ApJS*, 107, 201
- Lumsden, S.L., Nichol, R.C., Collins, C.A., & Guzzo, L., 1992, *MNRAS*, 258, 1
- Lucey, J.R., Dickens, R.J., Mitchell, R.J., Dawe, J.A., 1983, 203, 545
- MacGillivray, H.T. & Stobie, R.S., 1984, *Vistas Astr.*, 27, 433
- MacGillivray, H.T., Law, S.D., Cruddace, R.G., Collins, C.A., Gursky, H., & Yentis, D.J., 1994, in *Cosmological Aspects of X-ray Clusters of Galaxies*, W.C. Seitter (ed.), Kluwer Academic Publ., Netherlands, p. 339
- Machalski, J. & Condon, J.J., 1999, *ApJS*, 123, 41
- Mahdavi, A., Böhringer, H., Geller, M. J., Ramella, M., 2000, *ApJ*, 534, 114
- Malamuth, E.M., Kriss, G.A., Dixon, V.D., Ferguson, H.C., Richie, C., 1992, *AJ*, 104, 495
- Mamon, G.A., Parker, Q.A., Proust, D., 2001, *PASA*, 18, 232
- Markevitch, M., 1998, *ApJ*, 504, 27
- Marzke, R.O., Huchra, J.P., Geller, M.J., 1996, *AJ*, 112, 1803
- Matsumoto, H., Pierre, M., Tsuru, T.G., Davis, D.S., 2001, *A&A*, 374, 28
- Matthews, L.D. & van Driel, W., 2000, 143, 421
- Mathewson, D.S., Ford, V.L., Buchhorn, M., 1992, *ApJS*, 81, 413
- Mathewson, D.S. & Ford, V.L., 1996, *ApJS*, 107, 97
- Mauch, T., Murphy, T., Buttery, H.J., Curran, J., Hunstead, R.W., Piestrzynski, B., Robertson, J. G., Sadler, E. M., 2003, *MNRAS*, 342, 1117
- Maurogordato, S., Proust, D., Cappi, A., Slezak, E., Martin, J.M., 1997, *A&AS*, 123, 411
- Maurogordato, S., Proust, D., Beers, T.C., Arnaud, M., Pello, R., Cappi, A., Slezak, E., Kriessler, J.R., 2000, *A&A*, 355, 848
- Mazure, A., Katgert, P., den Hartog, R., Biviano, A., Dubath, P., Escalera, E., Focardi, P., Gerbal, D., Giuricin, G., Jones, B., et al. 1996, *A&A*, 310, 31
- McCarthy, P.J., Kapahi, V.K., van Bruegel, W., Persson, S.E., Athreya, R.M., Subrahmanya, C.R., 1996, *ApJS*, 107, 19
- Melnick, J. & Quintana, H., 1981, *AJ*, 86, 1567
- Merrifield, M.R., Kent, S.M., 1991, *AJ*, 1001, 783
- Metcalfe, N., Fong, R., Shanks, T., Kilkenny, D., 1989, *MNRAS*, 236, 207
- Mieske, S., Hilker, M., Infante, L., 2002, *A&A*, 383, 823
- Minniti, D., Kissler-Patig, M., Goudfrooij, P., Meylan, G., 1998, *AJ*, 115, 121
- Mohr, J.J., Geller, M.J., Wegner, G., 1996, *AJ*, 112, 1816
- Mould, J.R., Staveley-Smith, L., Schommer, R.A., Bothun, G.D., Hall, P.J., Ming, S.H., Huchra, J.P., Roth, J., Walsh, W., Wright, A.E., 1991, *ApJ*, 383, 467
- Mulchaey, J.S., Davis, D.S., Mushotzky, R.F., Burstein, D., 1996, *ApJ*, 456, 80
- Müller, K., Wegner, G., Raychaudhury, S., Freudling, W. 1999, *A&AS*, 140, 327
- Muriel, H., Nicotra, M., Lambas, D.G., 1991, *AJ*, 101, 1997
- Muriel, H., Nicotra, M.A., Lambas, D.G., 1995, *AJ*, 110, 1032
- Oegerle, W.,R. & Hill, J.M., 2001, *AJ*, 122, 2858
- Olowin, R., De Souza, R.E., Chincarini, G., 1988, *A&AS*, 73, 125
- Ortiz-Gil, A., Guzzo, L., P. Schuecker, H. Böhringer, C.A. Collins, 2003, *MNRAS*, submitted
- Owen, F.N., Ledlow, M.J., Keel, W.C., 1995, 109, 14
- Owen, F.N., Ledlow, M.J., Keel, W.C., Morrison, G.E., 1999, *AJ*, 118, 633
- Patten, D.R., Carlberg, R.G., Marzke, R.O., Pritchett, C.J., Da Costa, L.N., 2000, *ApJ*, 536, 153
- Peacock, J.A. & West, M., 1992, *MNRAS*, 259, 494
- Pena, M., Ruiz, M.T., Maza, J., 1991, *A&A*, 251, 417
- Peterson, B.A., Wright, A.E., Jauncey, D.L., Condon, J.J., 1997, 232, 400
- Piccinotti, G., Mushotzky, R.F., Boldt, E.A., et al., 1982, *ApJ*, 253, 485
- Pierre, M., Böhringer, H., Ebeling, H., et al., 1994, *A&A*, 290, 725
- Pierre, M., Oukbir, J., Dubreuil, D., Soucail, G., Sauvageot, J.-L., Mellier, Y., 1997, *A&AS*, 124, 283
- Pismis, P., Mampaso, A., Manteiga, M., Recillas, E., Cruz Gonzales, G., 1995, *AJ*, 109, 140
- Postman, M., Huchra, J.P., Geller, M.J., 1992, *ApJ*, 384, 404
- Postman, M. & Lauer, T.R., 1995, *ApJ*, 440, 28
- Quintana, H. & Ramirez, A., 1990, *AJ*, 1424
- Quintana, H. & de Souza, R., 1993, *A&AS*, 101, 475
- Quintana, H. & Ramirez, A., 1994, *ApJS*, 96, 343
- Quintana, H., Fouque, P., Way, M.J., 1994, *A&A*, 283, 722
- Quintana, H., Ramirez, A., Melnick, J., Raychaudhury, S., Slezak, E., 1995, *AJ*, 110, 463

- Quintana, H., Ramirez, A., Way, M.J., 1996, *AJ*, 111, 603
- Quintana, H., Ramirez, A., Way, M.J., 1996, *AJ*, 112, 36
- Ramella, M., Focardi, P., Geller, M.J., 1996, *A&A*, 312, 745
- Ramella, M., Geller, M.J., Pisani, A., da Costa, L.N., 2002, *AJ*, 123, 2976
- Ramirez, R.C., de Souza, R.E., 1998, *ApJ*, 496, 693
- Ratcliffe, A., Shanks, T., Parker, Q.A., Broadbent, A., Watson, F.G., Oates, A.P., Collins, C.A., Fong, R., 1998, *MNRAS*, 300, 417
- Raymond, J.C. & Smith, B.W., 1977, *ApJS*, 35, 419
- Reimers, D., Köhler, T., Wisotzki, L., 1996, *A&AS*, 115, 235
- Reiprich T.H. & Böhringer, H., 2002, *ApJ*, 567, 716
- Retzlaff, J., Borgani, S., Gottlöber, S., Klypin, A., & Müller, V., 1998, *New Astronomy*, 3, 631
- Richter, O.-G., 1987, *A&AS*, 67, 261
- Rizza, E., Burns, J.O., Ledlow, M.J., Owen, F.N., Voges, W., Bliton, M., 1998, *MNRAS*, 301, 328
- Romer, A.K., Ph.D. thesis (Liverpool Univ.)
- Romer, A.K., Collins, C.A., Böhringer, H., Cruddace, R.G., Ebeling, H., MacGillivray, H.T., & Voges, W., 1994, *Nat*, 372, 75
- Rose, J.A., Gaba, A.E., Christiansen, W.A., Davis, D.S., Caldwell, N., Hunstead, R.W., Johnston-Hollitt, M., 2002, *AJ*, 123, 1216
- Schindler, S., 2000, *A&AS*, 142, 433
- Schuecker, P., Böhringer, H., Guzzo, L., Collins, C.A., Neumann, D.M., Schindler, S., Voges, W., Chincarini, G., Cruddace, R.G., De Grandi, S., Edge, A.C., Müller, V., Reiprich, T.H., Retzlaff, J., & Shaver, P., 2001a, *A&A*, 368, 86 (**Paper III**)
- Schuecker, P., Böhringer, H., Reiprich, T. H., Feretti, L., 2001b, *A&A*, 378, 408
- Schuecker, P., Guzzo, L., Collins, C.A., Böhringer, H., 2002, *MNRAS*, 335, 807 (**Paper VI**)
- Schuecker, P., Böhringer, H., Collins, C.A., Guzzo, L., 2003a, *A&A*, 398, 867, (**Paper VII**)
- Schuecker, P., Caldwell, R.R., Böhringer, H., Collins, C.A., Guzzo, L., Weinberg, N.N., 2003b, *A&A*, 402, 53,
- Schuecker, P., Böhringer, H., Voges, W. , 2003c, *A&A*, in press - astro-ph/0403116
- Schwope, A., Hasinger, G., Lehmann, I., Schwarz, R., Brunner, H., Neizvestny, S., Ugryumov, A., Balega, Y., Trümper, J., Voges, W., 2000, *AN*, 321, 1
- Sharples, R.M., Ellis, R.S., Gray, P.M., 1998, *MNRAS*, 231, 479
- Shetman, S.A., Landy, S.D., Oemler, A., Tucker, D.L., Lin, H., Kirshner, R.P., Schechter, P.L., 1996, *ApJ*, 470, 172
- Sheldon, E.S., Annis, J., Böhringer, H., et al., 2001, *ApJ*, 554, 881
- Slinglend, K., Batuski, D., Miller, C., Michaud, K., Hill, J.M. 1998, *ApJS*, 115, 1
- Smith, R.J., Lucey, J.R., Hudson, M.J., Schlegel, D.J., Davies, R.L. 2000, *MNRAS*, 313, 469
- Sodre, L. Jr., Capelato, H.V., Steiner, J.E., Proust, D., Mazure, A., 1992, *MNRAS*, 259, 233
- Sodre, L., Jr., Proust, D., Capelato, H.V., Lima Neto, G.B., Cuevas, H., Quintana, H., Fouque, P., 2001, *A&A*, 377, 428
- Solanes, J.M. & Stein, P. 1998, *A&AS*, 131, 221
- Stark, A.A., Gammie, C.F., Wilson, R.W., et al., 1992, *ApJS*, 79, 77
- Stein, P. 1996, *A&AS*, 116, 203
- Stocke, J.T., Morris, S.L., Gioia, I.M., Maccacaro, T., Schild, R., Wolter, A., Fleming, T.A., and Henry, J.P., 1991, *ApJS*, 76, 813
- Strauss, M.A., Huchra, J.P., Davis, M., Yahil, A., Fisher, K.B., Tonry, J., 1992, *ApJS*, 83, 29
- Struble, M.F. & Rood, H.J. 1999, *ApJS*, 125, 35
- Teague, P.F., Carter, D., Gray, P.M., 1990, *ApJS*, 72, 715
- Thompson, D.J., Djorgovski, S., Vigotti, M., Gruett, G., 1992, *ApJS*, 81, 1
- Tittley, E.R., Henriksen, M., 2001, *ApJ*, 563, 673
- Tonry, J.L., 1985, *AJ*, 90, 2431
- Trager, S.C., Faber, S.M., Worthey, G., Gonzalez, J.J., 2000, *AJ*, 119, 1645
- Trasarti-Battistoni, R. 1998, *A&AS*, 130, 341
- Tritton, K.P., 1972, *MNRAS*, 158, 277
- Trümper, J., 1992, *Royal Astron. Soc. Quart. J.*, 33, 165
- Trümper, J., 1993, *Science*, 260, 1769
- Tucker, D.L., Oemler A. Jr., Hashimoto, Y., Shetman, S.A., Kirshner, R.P., Lin, H., Landy, S.D., Schechter, P.L., Allam, S.S., 2000, *ApJS*, 130, 237
- Tucker, W., Blanco, P., Rappoport, S., David, L., Fabricant, D., Falco, E.E., Forman, W., Dressler, A., Ramella, M., 1998, *ApJ*, 496L, 5
- Veron-Cetty, M.-P. & Veron, P., 2001, *A&A*, 374, 92
- Vettolani, G., Cappi, A., Chincarini, G., Focardi, P., Garilli, B., Gregorini, L., Maccagni, D., 1989, *A&AS*, 79, 147
- Vettolani, G., Chincarini, G., Scaramella, R., Zamorani, G., 1990, *AJ*, 99, 1709
- Vettolani, G., Zucca, E., Merighi, R., Mignoli, M., et al. 1998, *A&AS*, 130, 323
- Voges, W., Boller, T., Dennerl, K., et al., 1996,
- Voges, W., Aschenbach, B., Boller, T., Bräuninger, H., Briel, U., Burkert, W., Dennerl, K., Englhauser, K., Gruber, R., Haberl, F., Hasinger, G., Kürster, M., Pfeffermann, E., Pietsch, W., Predehl, P., Rosso, C., Schmitt, J.H.M.M., Trümper, J., & Zimmermann, H.U., 1999, *A&A*, 349, 389
- Way, M.J., Flores, R.A., Quintana, H., 1998, 502, 134
- Wegner, G. Colless, M., Baggley, G., Davies, R.L., Bertschinger, E. Burstein, D., McMahan, R.K., Saglia, R.P., 1996, *ApJS*, 106, 1
- Wegner, G. Colless, M., Saglia, R.P., McMahan, R.K., Davies, R.L., Burstein, D., Baggley, G., 1999, *MNRAS*, 305, 259
- West, R.M., Frandsen, S., 1981, *A&AS*, 44, 329
- Whiteoak, J.B., 1972, *AuJPh*, 25, 233
- Willmer, C.N.A., Focardi, P., Chan, R., Pellegrini, P.S., da Costa, N.L., 1991, *AJ*, 101, 57
- Willmer, C.N.A., Maia, M.A.G., Mendes, S.O., Alonso, M.V., Rios, L.A., Chaves, O.L., de Mello, D.F., 1999, *AJ*, 118, 1131
- York, D.G., Adelman, J., Anderson, J.E., et al., 2000, *AJ*, 120, 1579
- Zabludoff, A.I., Huchra, J.P., Geller, M.J., 1990, *ApJS*, 74, 1
- Zabludoff, A., Geller, M., Huchra, J.P., Vogeley, M.S., 1993, *AJ*, 106, 1273
- Zabludoff, A., Mulchaey, J.S., 1998, *ApJ*, 496, 39
- Zhang, Y.-Y., Finoguenov, A., Böhringer, H., Ikebe, Y., Matsushita, K., Schuecker, P., 2003, *A&A*, 413, 49
- Zimmermann, H.U., Becker, W., Belloni, T., Döbereiner, S., Izzo, C., Kahabka, P., & Schwentker, O., 1994, *EXSAS User's Guide*, MPE Report No. 257